FACULDADE DE ENGENHARIA DA UNIVERSIDADE DO PORTO

Desenvolvimento de um sistema de controlo e monitorização para uma caixa de transporte de equipamento médico-hospitalar, a ser utilizada por Drones

Nuno Manuel Vaz Ferreira Figueiredo



Mestrado em Engenharia Mecânica
- Automação -

Supervisor: Prof. António Ramos Silva

Supervisor at CEiiA: António Figueiredo dos Reis

October 16, 2023

© Nuno Manuel Vaz Ferreira Figueiredo, 2023

Desenvolvimento de um sistema de controlo e monitorização para uma caixa de transporte de equipamento médico-hospitalar, a ser utilizada por Drones

Nuno Manuel Vaz Ferreira Figueiredo

Mestrado em Engenharia Mecânica
- Automação -

October 16, 2023

Resumo

Os veículos aéreos não tripulados (VANT) surgiram como uma solução promissora para o transporte rápido e eficiente de mercadorias, particularmente em áreas remotas e inacessíveis. Com a crescente utilização dos utilização dos VANT para o transporte de qualquer tipo de mercadoria, surge também a possibilidade de transportar mercadorias de natureza mais sensível. E assim se cria a necessidade de caixas de carga útil que impeçam a deterioração destes bens, por exemplo, artigos médicos, como sangue, vacinas ou mesmo medicamentos.

O estudo inicia-se com uma revisão promenorizada sobre o transporte de sangue, medicamentos e vacinas começando pelas normas relacionadas com estes componentes, seguindo-se os diferentes métodos de transporte mais precisamente a utilização de VANTs. E termina com as tecnologias envolvidas neste tipo de transporte,desde a utilização de métodos passivos de refrigeração aos métodos activos de refrigeração.

O estudo começa com uma revisão abrangente dos sistemas de carga útil de VANTs existentes e suas limitações no transporte de produtos médicos, enfatizando a necessidade crucial de controle preciso de temperatura durante o trânsito. Diferentes métodos de refrigeração, incluindo sistemas ativos, como compressores de vapor e dispositivos Peltier, bem como soluções passivas, como Materiais de Mudança de Fase (PCMs), foram minuciosamente investigados. A análise revelou que o sistema passivo de PCM era a escolha mais adequada para viagens de VANT, dadas suas compatibilidade com restrições de peso, eficiência energética e a capacidade de manter a faixa de temperatura necessária para carga médica.

Na fase subsequente, a tese elabora como a integração da tecnologia PCM no design da caixa de carga útil permite a realização de uma solução sustentável e eficiente. Com o uso estratégico de PCMs, torna-se viável criar uma caixa de carga útil capaz de manter a faixa de temperatura desejada por até 4 horas, alinhando-se com os requisitos específicos de transporte de VANT para produtos médicos. A solução baseada em PCM oferece uma abordagem inovadora para a regulação de temperatura, aprimorando a confiabilidade e eficácia de UAVs nesta aplicação crítica.

Os resultados desta tese fornecem informações significativas sobre os factores-chave do planeamento e da criação de uma caixa de carga útil para artigos médicos transportados por VANT. A investigação faz avançar a tecnologia dos VANT no sector da saúde, permitindo a entrega segura e eficiente de material médico que salva vidas.

Abstract

Unmanned Aerial Vehicles (UAVs) have emerged as a viable method for delivering products quickly and efficiently, particularly in remote and inaccessible places. As the usage of UAVs for transporting various commodities expands, so does the necessity to transfer delicate goods without jeopardising their integrity. As a result, there is a need for customised payload boxes to keep these products from degrading, which includes medical supplies like as blood, vaccinations, and medications.

The study begins with a comprehensive review on the transport of blood, drugs and vaccines starting by the norms related to these components, followed by the different methods of transport more precisely the use of UAVs. And finishing it with the technologies involved with this kind of transportation. From the use of refrigeration passive methods to active cooling methods.

The study begins with a comprehensive review of existing UAV payload systems and their limitations in transporting medical goods, emphasizing the crucial need for precise temperature control during transit. Different refrigeration methods, including active systems such as vapor compressor and Peltier devices, as well as passive solutions like Phase Change Materials (PCMs), were thoroughly investigated. The analysis revealed that the passive PCM system was the most suitable choice for UAV travel, given its compatibility with weight constraints, energy efficiency, and the ability to maintain the required temperature range for medical cargo.

In the subsequent phase, the thesis elaborates on how the integration of PCM technology into the payload box design allows for the realization of a sustainable and efficient solution. With the strategic use of PCMs, it becomes feasible to create a payload box capable of maintaining the desired temperature range for up to four hours, aligning with the specific requirements of UAV transport for medical goods. The PCM-based solution provides an innovative approach to temperature regulation, enhancing the reliability and effectiveness of UAVs in this critical application.

The findings of this thesis give significant insights into the key factors of planning and creating a payload box for UAV-transported medical items. The research advances UAV technology in the healthcare sector, allowing for the safe and efficient delivery of life-saving medical supplies.

Acknowledgments

I would like to express my sincere gratitude to Professor Antonio Ramos Silva, whose guidance, expertise, and unwavering support played a pivotal role in the successful completion of this thesis. Your mentorship has been invaluable, and I am truly fortunate to have had the opportunity to learn under your tutelage.

I extend my heartfelt thanks to the entire team of the Department of Advanced Air Mobility at CEIIA. Your collective patience, assistance, and willingness to help whenever I needed it have been instrumental in my research journey. Special appreciation goes to Ines Furtado and Renato Machado for not only granting me this invaluable opportunity but also for their continuous support throughout this endeavor. I am also grateful to Antonio Reis for his meticulous proofreading and editing, without which my work would have been less readable.

To my family, I owe a debt of gratitude that words cannot fully express. Thank you for your unwavering support, from the countless dinners at the working table to patiently correcting numerous orthographic errors. Your encouragement and belief in me have been my driving force.

I reserve a special place in my heart for Maria Ana, who has been my rock throughout this academic journey. Your unwavering support, motivation, and refusal to let me give up have pushed me beyond my limits and kept me on this path.

Thank you all for being an integral part of this journey and for contributing to the realization of this thesis.

Nuno Figueiredo

Contents

1 Introduction **1**
- 1.1 CEiiA - Centre of Engineering and Product Development . . . 2
- 1.2 Motivation . . . 3
- 1.3 Objectives . . . 4
- 1.4 Structure . . . 4

2 State of the art **5**
- 2.1 Introduction . . . 5
- 2.2 Blood, Drugs and Vaccines Transportation . . . 7
  - 2.2.1 Regulations and Good Practices . . . 8
  - 2.2.2 Means of transport . . . 10
- 2.3 Drone Applications for Blood Transport . . . 12
- 2.4 Technologies Used During Transport . . . 13
  - 2.4.1 Cooling Methods . . . 13
  - 2.4.2 Control and Monitoring . . . 15

3 Cargo box conceptual design **17**
- 3.1 Development of the Cargo Box . . . 17
  - 3.1.1 Dimensional and Material Analysis of the Transport Box . . . 17
  - 3.1.2 Components . . . 21
- 3.2 Thermal Management System . . . 24
  - 3.2.1 Heat Transfer . . . 24
  - 3.2.2 Active Cooling . . . 31
- 3.3 Comparison of cooling systems . . . 35
  - 3.3.1 Passive Temperature Maintenance . . . 37
  - 3.3.2 Passive vs Active Cooling . . . 41
- 3.4 Development of the Test Process . . . 47

4 Results and Discussion **51**
- 4.1 Tests Analyses . . . 51
  - 4.1.1 Sensor Validation . . . 51
  - 4.1.2 Model Validation . . . 55
- 4.2 Payload Box Conceptual Design . . . 63

5 Conclusions and Future Works **66**
- 5.1 Conclusions . . . 66
- 5.2 Future Works . . . 67

References **69**

A EPS box **76**

B Sensors **78**

C Solidworks simulation **88**

List of Figures

1.1 CEiiA Logo . . . 3

2.1 Examples of blood transport containers . . . 6
2.2 The ambient temperature and air temperature inside the container without PCM [1]. 15
2.3 Graphs of temperature of the boxed developed . . . 15

3.1 Arrangement of boxes inside of the cargo space . . . 19
3.2 Sensor placement . . . 22
3.3 Connection diagram between ESP32 and sensors . . . 24
3.4 Model for convective and conductive heat transfer [2] . . . 26
3.5 Equivalent thermal circuit for a series composite wall [3]. . . . 27
3.6 Vapor compression refrigeration diagram [4]. . . . 32
3.7 Vapor Compression Refrigeration Cycle P-V Diagram [5]. . . . 32
3.8 Cooling COP of a thermoelectric module under optimum electrical current with fixed hot side temperature of 300 K, Zhao and Tan [6]. . . . 35
3.9 Peltier current vs Heat diagram . . . 37
3.10 Photos of different PCM samples Nie et al. [7]. . . . 39
3.11 DSC curves of different PCMs Nie et al. [7] . . . 39
3.12 3d model for thermal simulation . . . 43
3.13 3D model for thermal simulation with outside surfaces subjected to a convective thermal load . . . 43
3.14 3D model for thermal simulation with outside surfaces subjected to a convective thermal load . . . 44
3.15 Simulink block scheme for thermal balance of air contained in the box. . . . 46
3.16 Simulink block scheme for thermal balance of the blood. . . . 46
3.17 Simulink block scheme for thermal balance of PCM. . . . 46
3.18 Simulink block scheme for thermal balance of PCM. . . . 47
3.19 Connections between ESP 32 and the SD module through the use of a protoboard 48
3.20 Sensors position for validation tests. . . . 49
3.21 Thermal chamber, left 1000L right 500L. . . . 50

4.1 First sensor verification test . . . 52
4.2 Second sensor verification test . . . 53
4.3 Test 3 at room temperature for sensor verification, but with cold water bottles inside the box. . . . 54
4.4 Difference on measured temperature by comparing two sensors for test 3. . . . 54
4.5 First test done in the chamber without PCM. . . . 56
4.6 Simulation of the model at a start temperature of 7ºC without PCM. . . . 56
4.7 Second test done in the chamber without PCM. . . . 57

4.8 First test done in the chamber with PCM. 58
4.9 Second test done in the chamber with PCM. 59
4.10 Simulation of the model at a start temperature of 7ºC. 60
4.11 Humidity development through the four different tests. 61
4.12 Conceptual design of the box with the different components. 64
4.13 Exploded view of 3d model. 64

List of Tables

2.1 Current Medications Carried by the Neonatal/Pediatric Critical Care Transport Team That Have an Associated Cold Temperature Storage Recommendation [8] . 9
2.2 Transport temperature manufacturer's requirements [9] 10

3.1 Summary of Mission Parameters for Logistical Resupply and Emergency Deliveries [10] 18
3.2 Dimensions for plastics containers, label areas and nominal capacity in mm [11] . 20
3.3 EPS Box Dimensions 30
3.4 EPS Box Areas 30
3.5 Parameters to calculate heat transfer coefficient 31
3.6 Parameters to calculate quantity of PCM needed 42
3.7 Parameters of the mash 44
3.8 Parameters of the climate chambers 49
3.9 Parameters of the Tests 50

4.1 Cost of the different components 65

Abbreviations and symbols

AAM	Advanced Air Mobility
AC	Alternating current
AED	Automated external defibrillators
COP	Coefficient of Performance
DSC	Differential Scanning Calorimetry
DC	Direct current
PCM	Phase Changing Material
RBC	Red Blood Cells
TEC	Thermoelectric Cooler
UAV	Unmanned Aerial Vehicles
CEiiA	Centre of Engineering and Product Development
EPS	Expanded Polystyrene
NTC	Negative Temperature Coefficient
RTD	Resistance Temperature Detectors
IPST	Instituto Português do Sangue e da Transplantação
IATA	International Air Transport Association
DGR	Dangerous Goods Regulations
BU	Business Unit
Qa	Heat absorbed at the cooling side of a peltier module
Qd	Heat dissipated at the heat sink of a peltier module
Q_{pcm}	Total energy absorbed by the PCM
R_{cond}	Conduction Thermal Resistance
R_{conv}	Convection Thermal Resistance

Chapter 1

Introduction

In the recent years, unmanned aerial vehicles (UAVs), more commonly known as drones, have been used more often for multiple for practices like goods delivery, disaster management, or even for military use. Companies like Amazon, Flytrex, among others, have been developing UAVs of their own, because these offer a fast and efficient way to transport goods, from packages to medical support, as many researches show [12]. In the medical area, UAVs could be used for the swift transportation of crucial life-saving items like blood bags, organ transplants, health products and medical equipment and also be used to overcome transportation challenges caused by traffic congestion. Another solution, that UAVs would answer, is the possibility of delivering goods to hard-to-reach areas that may be difficult to access by traditional means, such as ambulances or helicopters. The organization "Doctors Without Borders" utilized UAVs to deliver dummy test samples from a rural settlement to a major metropolis[13]. Another organization that is using UAVs to deliver medical goods is Zipline. With only 2 warehouses, they are able to supply Rwanda hospitals [14].

Considering deliveries of goods in the healthcare sector, one of the most important issues is the transport of blood, since it is essential for various medical procedures, treatments and emergency situations. The process more commonly used for transferring blood from one person to another, is blood donation. Normally the sampled blood will have to be transported from its sampling location to the place it is intended to be used. In order to make this transportation swiftly, a land-based vehicle with a qualified driver or a helicopter with a pilot is needed. This has various drawbacks, including the fact that they are inefficient, when compared to modern technology, susceptible to human error, influenced by pollution and affected by traffic conditions. The whole request, preparation and delivery procedure may increase wait times and put patients' lives in danger, while also adding significant expenses to both the public and private healthcare systems for each minute that is delayed. When it is required to quickly deliver to remote places, like far-off mountain regions or islands, the issues are worsened.[15]

1.1 CEiiA - Centre of Engineering and Product Development

With the objective to envision, create and commercialize inovative technologies, products and services, that will improve society's sustainability, CEiiA, a Portuguese Engineering and Product Development center, first opened its doors in 1999. It links public sector, business and universities in high-tech sectors including automotive and mobility, as well as aerospace and nautical sectors. It is one of Portugal's top R&D instituions. In order to facilitate the development of new services and business models in the direction of a carbon-zero future, a Smart & Sustainable Living strategy is used. This strategy focus on developing emerging technologies and products, particularly in aerospace and mobility sectors in order to take advantage of the resources and technology developed[16].

One of the most important projects in the aeronautics sector, is the KC-390, the largest aircraft built by Embraer. CEiiA had notable part in the creation of this aircraft, by working on the development and design of the central fuselage, the elevator and the sponson[17]. Others projects that can be affiliated with this sector, are for example the UAS30, which is an Autonomous Unmanned Aerial Vehicle with a maximum takeoff weight of 30kg and flight characteristics that make it unique when compared to competitors in the same class. It is a highly versatile aircraft, as it allows the integration of various payloads. During 2020, test flights were carried out in autonomous mode, which was then used for the Troante project which has as objective to obtain topographic-hydrographic, oceanographic and direct observation surveys by utilizing the sensors of the aircraft UAS30 in a more economically advantageous and effective manner compared to traditional methods [18].

Another notable project is the MAGELLAN Research and Development project, led by RFA Portugal in collaboration with CEiiA. It constitutes a unique opportunity for Portugal to enter the market of small launchers, whose strategic importance is recognized and which is currently expanding. This project aims to develop structures for small launchers in Portugal, namely Kick-Stage, Separation Interface Flanges and Payload Fairing, capable of demonstrating the national potential to develop complex, low-cost, lightweight and customized aerospace solutions from concept to manufacturing[19]. The project AdAM, invisioned for the automation sector, which is an R&D project under innovation iniative PT2020 which aims to define industrial requirements for the adoption of advanced automation in industry. The role of CEiiA focuses on the development of quality inspection applications based on computer vision and non-destructive testing[20]. The team supporting this thesis is a multidisciplinary team with strong background in aircraft development and smart mobility and working in Advanced Air Mobility (AAM). The main goal of this business Unit (BU) is to push the safe implementation of AAM, working in collaboration with strategic partners and authorities.



Figure 1.1: CEiiA Logo

1.2 Motivation

The CEiiA BU-AAM is developing an UAV to be used as a delivery vehicle in logistics and healthcare. The development of UAVs designed for these two distinct purposes is another contributing factor to the growing utilization of UAVs. Consequently, there is currently an increasing interest to develop a specialized UAVs for transporting medical supplies to remote or hard-to-reach areas. For this purpose it is also of great interest to develop a specialized box for medical goods delivery, since it creates an opportunity to increase the efficiency, safety and reliability of this healthcare service. A box tailored for this purpose can solve specific issues and so improve the delivery process. Another aspect, that increases the importance of creating a customized container, is the fact, that dangerous goods, can only be transported by air transport, provided certain principles are strictly followed according to IATA [21].

The transportation of blood typically involves the presence of a qualified individual who can intervene in case of any problem. However, in the case of blood transport via UAVs, this human intervention aspect is absent, necessitating the implementation of systems to ensure the continuous quality of the blood. In conventional transport, temperature maintenance is a standard requirement and for UAV transport, it becomes imperative to incorporate sensors for continuous temperature monitoring during the delivery process. This is essential as the temperature-sensitive nature of blood products must be upheld throughout the journey. Moreover, the specially designed transport box for UAVs must establish communication channels to relay temperature data to the ground-based logistical team. This real-time data exchange enables proactive measures in case of unexpected events.

Considering that the UAV delivery box operates without direct human surveillance, it becomes paramount to incorporate additional safety and security precautions for the blood cargo. Thus, it is advisable to implement a robust locking system and a comprehensive tracking system. This dual-layered security approach ensures that unauthorised access to the box does not allow to access to its contents, safeguarding the integrity of the blood supply during UAV transport.

1.3 Objectives

The primary objective of this research is to study a new concept of a carrier box designed for medical emergencies, specifically intended for transportation via UAVs. Initially, the study explores the various methods of UAV implementation and pursues their potential applications within the healthcare sector. Subsequently, an examination of the existing norms and protocols for blood transportation is conducted, aiming to identify the specific areas where UAV-based transport could have a significant impact.

As a deeper understanding of the concept is cultivated, the research will progress to simulate methods of refrigerating the carrier box. This simulation aims to determine the most efficient practices for implementing temperature control within the carrier box while minimizing any adverse effects on the cargo capacity of the UAV. The envisioned carrier box should be designed for easy transport and seamless integration with the UAV, which is currently under development by the Advanced Air Mobility team at CEiiA.

1.4 Structure

This document is composed of a total of 5 chapters, including the introduction. This first chapter shows the motivation behind this work and its main goals.

Chapter 2 provides a comprehensive review of the state of the art and offers summaries of related works. Chapter 3 introduces and explains key concepts essential for the development of the final solution. These concepts establish a foundational knowledge base for the subsequent chapter. It also elucidates the methods employed in crafting the final solution. Chapter 4 conducts an in-depth analysis of the results obtained, serving as a platform for presenting a conceptual design of the payload box and all its constituent components. Finally, in Chapter 5, the primary conclusions drawn from the preceding chapters are consolidated.

Chapter 2

State of the art

This chapter details the literature revision of current blood transportation norms and its best practices. This focus on the current practices and challenges associated with blood transportation, along with the potential integration of UAV technologies to enhance this crucial process. The chapter begins by examining various approaches to utilizing UAVs for the transportation of medical goods and explores their potential applications and benefits in improving blood transportation logistics. Afterward, it is looked into various methods of implementing a cooling system to maintain the appropriate temperature during blood transportation.

2.1 Introduction

Blood bags require specialized containers designed to maintain the proper temperature, and prevent damage or contamination during transportation. Depending on the volume of blood being transported, these containers are of various sizes and configurations. Typically, they are constructed from insulated materials, as illustrated in Figure 2.1. which provides examples of currently available container types.

The majority of blood bag shipments are carried out using refrigerated vehicles such as vans or ambulances equipped with refrigeration units capable of sustaining the required temperature range of 2-8ºC. This temperature range is critical for preserving the viability of blood cells and reducing the risk of hemolysis[22, 23]. During transportation, blood bags are often secured within racks or crates to minimize movement and the potential for damage. To ensure the accurate administration of blood to the intended recipient, these containers are labeled with essential information, including blood type, donor details and other pertinent data. The transportation of blood bags is a highly regulated process that demands specialized equipment and stringent procedures to ensure the safety and integrity of the transported blood products[24].



(a) Transport box proposed by Teams and centres [25]



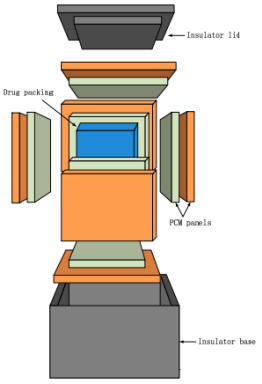
(b) Transport box proposed by Scalea et al. [26]



(c) Transport box proposed by Amicone et al. [27]



(d) Transport box proposed by Selleng et al. [28]



(e) Transport box proposed by Huang and Piontek [1]



(f) Transport box proposed by Yakushiji et al. [22]

Figure 2.1: Examples of blood transport containers

2.2 Blood, Drugs and Vaccines Transportation

Blood, drugs, and vaccines are essentials in the healthcare sector, each playing a pivotal role in the prevention and treatment of diseases. Typically, these vital components are stored at centralized locations and will then be shipped to other locations. Given their significance in healthcare, the transportation of these materials is subject to careful consideration to prevent deterioration during transit. The utilization of drones for their transport presents numerous advantages in terms of speed, accessibility, and cost-effectiveness.

Drugs are fundamental to medical treatment and human prosperity. Ensuring the storage and transport of drugs under optimal conditions is crucial to their efficient administration. The pharmaceutical supply chain must effectively manage all distribution stages, from drug manufacturing in laboratories to their final destination at pharmacies. The importance of monitoring drugs, both during storage and transport, cannot be overstated. While developing a system for pharmaceutical transport, traceability is essential to verify whether the goods have encountered adverse conditions that could compromise their effectiveness or damage the packaging. The transport box being developed aims to maintain storage specifications, minimizing ambient temperature variations during transit. Temperature monitoring is the primary consideration, followed by humidity. Although high relative humidity has little impact on pharmaceutical stability, humid conditions can weaken secondary cardboard packaging, potentially leading to physical damage[29, 30].

Vaccines are another component that should be prioritized since they guarantee the timely delivery of life-saving immunization to communities all over the world. In vaccine shipment keeping the inside at the specific temperature is a must as temperatures below or above the recommended ranges may result in vaccine deterioration. Controlling the temperature and humidity of the container along the supply chain is necessary to ensure that their efficacy is not lost. Temperature excursion is described as an unintended incidence in which a vaccine or other biological product is exposed to temperatures outside of the authorized thermal selection during storage or transit. Temperatures below the recommended range can be equally as harmful as keeping them above it. As a result, an effective method of transporting vaccinations within their specified temperature range should be explored and developed [31].

Blood is a vital component of the healthcare system, particularly during emergencies. Ensuring efficient access to blood is essential for improving human health. Rapid delivery of blood donations from banks or donation centres to hospitals and medical facilities is crucial. Effective and safe transportation is essential to prevent waste, especially in regions with scarce blood supplies. Because blood donations are in short supply in some areas, it is critical that there exist effective methods of storing and transporting them so that none are wasted. In Portugal, for example, it was demonstrated in early 2023 that Lisbon had a shortfall of blood donations and hence had to get them from other regions of the country, such as the northern region [32]. Collaborative efforts among blood banks, medical facilities and transportation companies are essential for optimising

blood transportation. Proper scheduling, routing and logistics coordination help ensure efficient resource utilisation and a steady supply of blood products. There's even the possibility with the usage of UAVs to centralise the blood and non-essential medicine storage and creating a swift access point to other location in need, like Zipline did in Rwanda, which will further explored in chapter 2.3.

Accurate tracking and documentation systems are vital for efficient blood transport. Each blood unit must be correctly identified, documented and monitored throughout its journey to maintain traceability, accountability and transparency in the supply chain. To achieve this, Sarkar et al. [33] have developed a low-cost cold supply chain and cold storage environment monitoring device. This device is used in warehouses or cold storage containers during transportation, where it monitors and maintains temperature and humidity settings. If any monitored parameters, such as temperature, humidity, light intensity, or gas levels, exceeds predefined thresholds, the system triggers an alert and sends an email notification to ensure timely corrective actions, thus preventing loss or damage of the stored items.

Another parameter studied, when addressing the impact of UAV flights on the quality of blood, is the vibrations provoked by the aircraft. The transport of dummy blood products and vials with human insulin solution for injection was tested with various packaging types in a series of real-world drone test flights to determine how much vibration caused by the drone was transferred to the cargoes.[34]. As the study shows, that the vibration levels during the UAV flight were higher then for the road transport. Nevertheless the impact of these wasn't visible after the flight. A different study on subject, where it was simulated the impact of 1- and 2-hour UAV flights using random vibration and turbulence on various blood sample, from healthy volunteers to patient with different diseases[35]. It could be concluded that the blood samples could tolerate the impact of vibrations and turbulence up to two hours.

2.2.1 Regulations and Good Practices

While designing a new container for transporting medical equipment and perishable goods such as blood, drugs, or vaccines, it is essential to consider the existing regulations and best practices related to temperature control and storage. These regulations and practices help ensure the safety and effectiveness of the transported goods. The safe transport of blood and medical products in Portugal involves compliance with guidelines and regulations provided by entities like the Instituto Português do Sangue e da Transplantação (IPST), the Portuguese institute of blood and transfusion, and Infarmed, the national authority of medicines and health products [36, 37]. The International Air Transport Association (IATA) is an international globally recognised organisation, which sets the Dangerous Goods Regulations (DGR) guidelines and requirements for the transportation of hazardous materials, chemicals and substances by air [21]. The regulations set by these entities cover aspects like temperature control, packaging, labelling and documentation to ensure the integrity and safety of these essential medical supplies during transit. Adherence to these guidelines is crucial to safeguard public health and maintain the effectiveness of medical products.

For drugs and vaccines, maintaining the recommended temperature range during transportation is crucial to preserve their efficacy. While the different drugs and vaccines have their own standard values of storage compliance, it is possible to identify temperature ranges that align with the storage requirements of many drugs and vaccines. For example, a study by Clancy et al. [8] analysed various medications and found that five out of seven cartridges needed to be stored between 2ºC and 8ºC, with two requiring storage between 2ºC and 25ºC. The recommendations for the individual cartridges are displayed in table 2.1. It is important to note that once drugs or vaccines exceed their recommended temperature range, they may become ineffective and cannot be returned to their original state. Therefore, the payload box should be designed to maintain these temperature ranges during transit.

Table 2.1: Current Medications Carried by the Neonatal/Pediatric Critical Care Transport Team That Have an Associated Cold Temperature Storage Recommendation [8]

Drug Name	**Recommended Storage Temperature**	**Room Temperature Expiration**	**Can Be Returned to refrigerator**
Racemic epinephrine	2ºC-25ºC	Not specified	Yes
Poractant alfa	2ºC-25ºC	24 hours	Once
Succinylcholine	2ºC-8ºC	14 days	No
Rocuronium bromide	2ºC-8ºC	60 days	No
Alprostadil	2ºC-8ºC	24 hours	No
Lorazepam	2ºC-8ºC	60 days	No data
iSTAT cartridge	2ºC-8ºC	2 months	No

In the context of vaccines, there are also studies indicating that it is possible to narrow down the storage temperature range, making it similar to that of temperature-sensitive drugs. When discussing vaccines, Ng et al. [31] categorise them into two temperature groups. Frozen vaccines are stored at a temperature of -15ºC, whereas refrigerated vaccines are kept within the range of 2-8ºC. It's worth noting that once a vaccine has been exposed to temperature variations that compromise its thermal stability, its potency cannot be restored. Additionally, UNICEF Supply Division [38] have published an article concerning the cold chain supply and vaccine containers, in which they provide insights into crucial guidelines for vaccine carriers. This article delineates two distinct time frames within the cold compartment. The first one is referred to as the "cold life," during which the empty container is filled with ice packs and brought to stability at +43°C ambient temperature. Under constant ambient conditions of +43°C, the cold life is calculated from the moment the container lid is closed until the warmest point within the vaccine storage compartment reaches +10°C. The second time frame is termed the "cool life," where coolant packs are placed inside the empty container, which has been stabilised at +43°C and maintained at +5°C for a minimum of 24 hours. The cool life is calculated from the point of container closure until the warmest location within the vaccine storage compartment exceeds +20°C, with the ambient temperature remaining constant at +43°C.

For blood products, such as red blood cells (RBC), frozen plasma and platelets, specific temperature requirements exist. According to the the Australian government and the Indian government, frozen plasma should be kept under -25ºC or -30ºC,respectively [9, 39]. Furthermore, it's important to note that fresh frozen plasma has a shelf life of 24 hours, when stored within a temperature range of 1ºC to 6ºC.
For platelets, there is a more consistent and uniform temperature range requirement. Platelets should be maintained at room temperature, typically falling within the range of 20ºC to 24ºC. This temperature range is also supported by other entities concerned with platelet storage [36, 24].
RBC transportation may involve different temperature ranges, but they consistently require a minimum of 2ºC. The maximum temperature for RBC transportation may vary between 6ºC, 8ºC and 10ºC, depending on specific guidelines. For example, the Portuguese Health Ministry defends a more strict threshold of 6ºC for the storage of RBC, while not expressing any concrete values for the transport. As for the Indian Health Ministry and British Blood Transfusion committee, both present same temperature selection for the storage of RBC, but present at the same time a maximum temperature of 10ºC during transport. Compliance with these temperature ranges is essential to maintain the integrity of blood products during transportation[9, 36, 24, 40, 28, 41].
Table 2.2 presents the transport temperature ranges according to the Australian government, since most don't present values for transport, only for storage.

Table 2.2: Transport temperature manufacturer's requirements [9]

Product	**Transport Temperature**	**Comments**
Red blood cells	2-10ºC	All blood refrigerators, including theatre and other holding refrigerators, must comply with current AS3864
Fresh frozen plasma, cryoprecipitate, cryodepleted plasma	At or below -25ºC	Plasma freezers must comply with current AS3864
Platelets	20-24ºC	Discontinuation of agitation of platelets during transportation should not exceed 24 hours

2.2.2 Means of transport

In the contemporary healthcare landscape, the primary modes of medical product transportation include ground-based options such as ambulance services and aerial transport via helicopters. Extensive research has been conducted to compare the effects of helicopter versus ground transportation on blood products, as it is presented in the following chapter.

One notable initiative sought to establish a system for supplying blood products, specifically RBC concentrates and thawed plasma, through helicopter emergency services for pre-hospital

transfusions in regions with limited hospital access and extended patient transport duration. To ensure the integrity of blood products during air transport, a comprehensive risk analysis was conducted, accompanied by the development of a validation strategy. This strategy involved testing and identifying a specialised blood product delivery container capable of maintaining temperatures between 2ºC and 6ºC for up to 36 hours, even in conditions as challenging as 35ºC ambient temperature. The study rigorously assessed blood product quality before and after air transport via helicopter, focusing on factors such as haemoglobin, hematocrit, hemolysis rate for RBCs and the activities of single clotting factors in frozen plasma. The conclusion drawn from this research is that supplying helicopter emergency medical services with RBCs and plasma is a viable approach that enhances patient care during pre-hospital treatment, with no detrimental impact on blood product quality [28].

Additionally, Wallace [23] conducted a study examining the delivery of temperature-sensitive medicines in an air medical context while ensuring that medications remained within acceptable temperature ranges. This investigation revealed frequent temperature excursions above the accepted maximum of 8ºC during transport. To address this challenge, the researchers devised an experimental methodology employing a commercially available shipping container and established a rapid conditioning regimen to maintain the desired temperature range of 2ºC to 8ºC. The study underscores the critical importance of maintaining precise temperature control during the transportation of temperature-sensitive medications in the air medical setting. The proposed system demonstrates promise in effectively achieving this objective.

The transportation of medical components holds immense significance as it can often be a critical factor in saving lives. The previously mentioned studies illustrate that even with conventional transportation methods, there are opportunities for improvement. As a result, a growing body of research is focusing on the transportation of medical products, with an increasing emphasis on the use of UAVs in the healthcare sector. UAVs have the ability to access areas with limited accessibility, making them particularly valuable in situations where helicopters or ambulances face challenges. Additionally, UAVs' vertical take-off capability eliminates the need for large take-off and landing areas.

In an effort to evaluate the potential of UAVs as an alternative to ambulances for blood transport, Homier et al. [42] conducted a study. The primary objective was to determine whether UAVs could transport simulated blood products to an urban trauma centre more rapidly than ground transportation. A secondary goal was to ascertain if the UAVs could maintain simulated blood product temperatures within a specified range. The study employed a payload carrier designed to keep the payload within the temperature range of 1ºC to 6ºC during a 90-minute period, as the primary aim was to meet crisis-related demands. The research findings demonstrated that the transport of simulated blood products by unmanned aerial vehicles significantly outpaced ground delivery, in a margin of 9 min to 21min, and the temperatures of these simulated blood products remained within the permissible range throughout the transportation process. Further research is needed to evaluate the feasibility of using UAVs for the transportation of actual blood products in

densely populated areas.

Another study in this domain investigated the impact of drone flight on blood products. The study involved six units each of RBCs, apheresis platelets and unthawed plasma, all frozen within 24 hours of collection. Over a two-day period, these experimental units were placed in a cooler, attached to a small multirotor aircraft ("S900" fromDJI), and flown for up to 26.5 minutes, with temperature logging throughout the flight. Following flight, various examinations were conducted to assess the impact on the blood products. Multiple tests were carried out to determine the effects of drone transportation on the blood products. According to the study's findings, drone transport had no adverse effects on the units. Consequently, the study concludes that employing drone delivery systems for shipping blood products is a practical and viable possibility [43].

2.3 Drone Applications for Blood Transport

In the present day, UAV technology is experiencing a rapid development, leading to its increasing integration into various domains. Roberts et al. [44] conducted a study that examined the financial and time-saving impacts of employing drones for the transportation of medical goods. They initially compared the costs associated with three distinct UAV models and concluded that, in all cases, significant cost savings were attainable. Additionally, the study assessed the time-saving efficacy in comparison to traditional ground transportation and even public-access Automated External Defibrillators (AEDs).
One notable study conducted in Sweden demonstrated that the use of drones for medical delivery resulted in a average reduction of 16 minutes in delivery time compared to the emergency medical services. Subsequently, other studies analysed by Roberts et al. [44] consistently indicated that UAV-based deliveries were consistently faster than ground-based alternatives. Moreover, deploying a drone for the delivery of an AED was found to be quicker than relying on bystanders to locate and use publicly accessible AEDs.

To comprehensively compare time and cost measures between drone and ground transport, it is essential to evaluate time savings relative to the distance being covered. Johannessen [45] developed two models for this purpose, focusing on relatively short transportation routes, which aligns with the typical range capabilities of drones. The longest flight route in their study covered 183 km and was completed in less than 2 hours by a UAV travelling at a speed of 100 kilometres per hour, whereas the ground-based delivery took around 3 hours and 40 minutes and the route it had to take was of 262 km. This study demonstrated that air transport significantly enhances time efficiency, especially when drones are capable of high-speed travel and the ground distance is substantial. However, it is important to note that weight and payload capacity constraints on drones can limit the feasibility of this approach for larger routes. Nevertheless, for shorter routes, drones can still offer considerable time savings, as evidenced in the previously mentioned article, which consistently highlighted the advantages of using drones for transportation. The amount of items transported by drone is frequently less than that of goods carried by ground. In that sense, utilising UAVs to deliver smaller quantity of products is more efficient. However, one limitation

of UAVs during medical emergencies is that they can only transport items and have no medical staff on board.

One particular application where drones can revolutionise logistics is in the medical sector, specifically in the transportation of critical medical supplies such as blood bags and vaccines. Several companies have recognised the potential advantages of employing drones for delivering blood products. In regions like Africa, where blood shortages are common and infrastructure challenges exist, drone delivery can be a game-changer. Companies like Zipline, initiated medical deliveries by drone in Rwanda, operating of two warehouse centres covering a radius of 80 kilometres. Their deliveries often take less than an hour, significantly reducing delivery times compared to traditional methods, which could take around four hours. By 2019, Zipline had already delivered over 13,000 units of blood and was responsible for supplying 20% of the donated blood outside the capital. Zipline designed its own aircraft, which is easy to assemble and it takes around 7 minutes from receiving an order to having the drone ready for departure. They can deliver payloads of up to 1.8 kilograms, primarily to rural areas, where the payload is dropped from a height of around 30 feet (9.14m) and falls into an insulated cardboard box attached to a parachute[15, 14].

Another company, Matternet is a drone company that has already completed over 1800 flights between the Swiss cities of Lugano and Bern transporting blood and pathology specimens and they have even expanded their operation to Zurich. Outside of Europe, they have transported medication to Haiti, the Dominican Republic and New Guinea, to name a few. The group has collaborated with organisations like UNICEF and "Doctors Without Borders". [15].

This chapter underscores the significant benefits of using drones for blood delivery and suggests that further research in this field holds great promise for improving healthcare logistics.

2.4 Technologies Used During Transport

This section explores various technologies used for the transportation of medical products, focusing on cooling methods and payload monitoring.

2.4.1 Cooling Methods

Currently, the predominant cooling method involves the use of ice packs or ice in dedicated blood distribution rooms. However, there is a growing interest in technologies that can actively control temperatures during transport, ensuring ideal conditions for medical products. Two of such technologies are thermoelectric coolers and compressor-based cooling systems.

One study examined the feasibility of using a thermoelectric cooler as a blood carrier box due to its compact size and compatibility with a 12-volt DC power source. The thermoelectric cooler, measuring 306 mm x 256 mm x 163 mm, utilised Peltier elements of type TEC1-12706 and its box was constructed from composites made from oil palm empty fruit bunches, possessing a thermal conductivity of 0.13 W/mK. The study achieved a coefficient of performance (COP) of 0.168, where COP is the ratio between the energy removed from the air and the electric power supplied to

the system, with successful testing involving seven 350 ml blood bags subjected to 9-volt voltage variations. The results demonstrated that the thermoelectric cooler maintained a blood temperature of 2.65ºC throughout the entire test. Overall, this study highlights the potential of a space-saving and effective blood transportation box that utilises a thermoelectric cooler and composites made from oil palm empty fruit bunches, eliminating the need for a specialised cooling chamber while keeping blood within the desired temperature range [46].
Another study explored the design and development of a temperature-controlled blood bank transport cooler utilising a thermoelectric Peltier cooler and a microcontroller with a Proportional-Integral-Derivative (PID) controller. This system aimed to maintain blood properties within the specified range of 2 to 8 degrees Celsius during transit within a hospital. The cooler continuously monitored and displayed the internal temperature on an LCD panel, with alerts in the form of light and sound triggered if the temperature deviated from the desired range. The cooler's effectiveness was validated through testing, with temperature measurements taken every minute from five locations within the box over 60 minutes. Measurement errors were found to be within 10.984%, falling within the permissible range set by the World Health Organization (WHO) guidelines [47].

Another innovative cooling method involves the use of Phase Changing Materials (PCMs). PCMs undergo a phase transition at a specific temperature, transitioning from one physical state to another (e.g., solid to liquid or liquid to gas). They are highly effective in storing and controlling thermal energy due to their ability to absorb and release substantial thermal energy during phase changes, while maintaining a constant temperature.
A study by Huang and Piontek [1] discussed the development of a cold-chain insulated container incorporating different PCM, one with a melting/freezing point of 5 ºC and water, for temperature-controlled transportation in the 2 to 8°C range. This container was designed and tested with under various temperature conditions, including extreme highs of 35 ± 2ºC, extreme lows of -20 ± 2ºC and alternating within these selected temperatures, starting at a high temperature and then changing to the lower level. The study's findings revealed that the cold-chain insulated container with the PCM with a melting/freezing point of 5 ºC was more effective at maintaining the acceptable temperature range during transportation for an extended duration, ensuring the quality and safety of the transported items. The container's internal dimensions were 420 × 300 × 360 mm and multiple measuring points were incorporated for temperature monitoring in multiple point as seen in figure 2.2.

For the test it was tested firstly without any PCM (Figure 2.3a) and then two other test were made, one with water as PCM (Figure 2.3b) and the other with a water and alkane mixture called OP5E (Figure 2.3c). Comparing the 3 graphs it can be accessed, that the temperature-controlled time was extended from 1 h to more than 80 h and the internal temperature maintained at 4 to 5 ºC by using a PCM with a melting/freezing point of 5ºC, while the container presented a sub cooling effect in a range of -1 to 2ºC when using water as PCM.

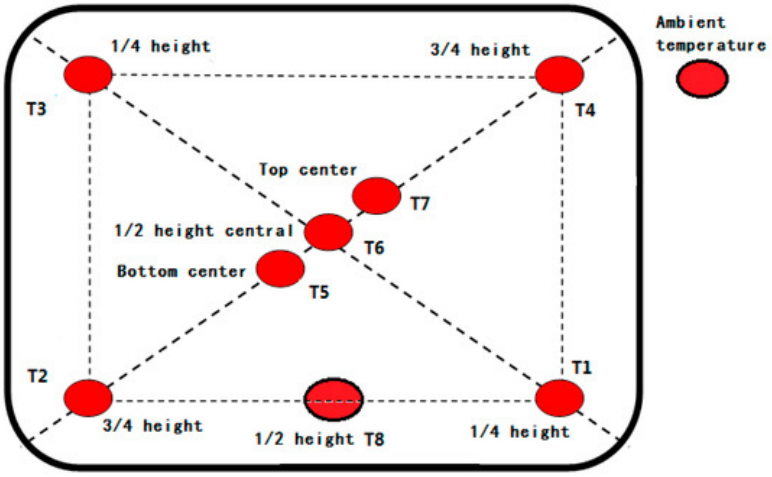
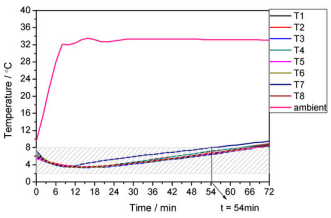


Figure 2.2: The ambient temperature and air temperature inside the container without PCM [1].

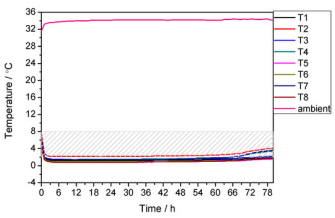
2.4.2 Control and Monitoring

Ensuring the safe and efficient transportation of medical products, especially when using unmanned systems like drones, requires advanced monitoring systems to perform the functions normally done by humans over sighting the transport. These systems must allow real-time tracking and control of the payload's condition and location. Several studies have proposed innovative solutions in this regard.

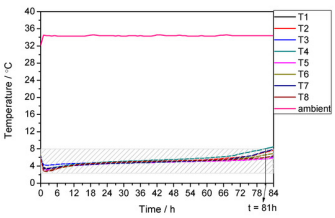
One approach proposed by Damiani et al. [40] is the development of a smart blood transport box with a temperature control system that utilises eutectic materials stored in a separate compartment. A partition wall equipped with blowers circulates cold air, facilitating heat exchange with blood bags. When the temperature inside the box exceeds a predefined limit, the blowers activate, extending the cooling effect of the eutectic material. This system integrates with a cloud-based intelligent container that maintains a continuous connection to a central server. Through this link, real-time monitoring, recording and rapid access to information regarding potential problems and alerts related to essential operational elements are possible. This includes monitoring ambient and



(a) The ambient temperature and air temperature inside the container without PCM.



(b) The ambient temperature and air temperature inside the container with water as PCM.



(c) The ambient temperature and air temperature inside the container with OP5E as PCM.

Figure 2.3: Graphs of temperature of the boxed developed
Transport box proposed by: [1]

internal temperatures, humidity levels, location, acceleration, speed, tilt angle, box integrity and a comprehensive log of all operations. The integration of smart box technology with temperature control and dynamic simulation aims to enhance the safety and efficiency of blood product transportation, ensuring their quality and usability upon arrival [40].

In a different approach, Amicone et al. [27] address the challenges of monitoring temperature during drone transportation of medical products. They propose a Smart Capsule equipped with artificial intelligence, offering a fully autonomous drone delivery service for perishable and high-value medical items while integrating real-time quality monitoring and control. The Smart Capsule is designed to guide autonomous aerial vehicles attached to it, specifically catering to the transportation of critical medical items such as blood, organs, tissues, test samples and drugs. The Smart Capsule continuously monitors the temperature, agitation and humidity of the medical items, adjusting these parameters as needed to maintain product integrity. For example, it can employ vibrations to ensure the necessary degree of agitation. This system represents a cutting-edge solution for real-time monitoring and control in drone-based medical product transport [27].

Chapter 3

Cargo box conceptual design

This chapter encompasses the initial assumptions underlying the development of the transport box, along with the groundwork for producing a functional prototype. It is divided into three main sections. The first section outlines considerations regarding the prototype as a whole, including the dimensions of the box, which is an integral component of the UAV currently under development. The second section explores the various methods of thermal management, elucidating their theoretical foundations and exploring their potential application within the container. It also details the comprehensive process of selecting the most suitable refrigeration methods, supported by simulations. The third section introduces the testing phase, which serves as a validation method for the simulations. It covers the steps involved in creating a prototype for testing purposes, as well as the different parameters to be assessed during testing.

3.1 Development of the Cargo Box

3.1.1 Dimensional and Material Analysis of the Transport Box

In the first steps of the creation of the transport box, it was first searched for its external dimensions. These dimensions should accommodate the different points, for example, the adaptability of the whole system inside of the cargo bay, the convenience of being transported by personnel to and from the aircraft, or its thermal characteristics. Firstly, it was compared to the different existing boxes, in order to gain a preliminary view on the volume needed for the transport of blood bags in an aircraft mission. The missions involving the healthcare department are of two different natures: either logistical resupply or emergency delivery. Gilmore et al. [10] have summarized both types of missions categorizing them in two different parameters, as it can be seen in table 3.1

Table 3.1: Summary of Mission Parameters for Logistical Resupply and Emergency Deliveries [10]

Parameter	**Logistical Resupply**	**Emergency Delivery**
Range	∼100 miles	∼10 miles
Time	1 hour	15 minutes
Payload	10+ blood units	1 to 3 units

In the case of the UAV under development developed, it is considered it is going to be used for logistical resupply, therefore, the compartment must accommodate the presented 10 or more blood bags. Homier et al. [42] tested the use of transported goods via drone versus ground delivery. For this test, they used RBC bags with 313 ml, or in other cases like Yakushiji et al. [22] present a value for whole blood of 400 ml and for RBC of 250 ml. Assuming the average value is to be established as the basis for the creation of the transport box, the minimal volume from a logistical resupply point of view should be around 3.13 L.

The second parameter to establish the final dimensions of the product to be created is the available cargo space in the drone. Most of the articles testing the transport of blood products or medical equipment are normally done with off-the-shelf drones. And so it can't be created a comparison between the aircraft being developed by the team at CEiiA against other drones. Since the box to be used in this UAV is to be transported in the fuselage, this also limits the box dimensions. In order to achieve the established requirements of the partners in the project, the aircraft should be able to transport a box with the external dimensions of 420x360x370 mm^3, length, width, and height respectively. This represents a total volume of around 56 liters, and so, being able to easily surpass the intended values of 10 blood bags, even if are considered the bigger bags of 400 ml. As also specification for the payload, it should be no more than 15kg, for the possibility of being transported by human personnel.
Considering the need to transport critical components that require careful handling, a decision was made to divide the larger container into smaller ones to facilitate transportation to and from the aircraft. Given that the surface areas are rectangular, it was determined that there should be a total of four boxes. The dimensions chosen for these boxes are 210x360x185 mm^3, with the only dimension not divided by two is the width of the cargo space. Figure 3.1 provides a schematic representation of how these boxes would be arranged inside the cargo bay when viewed from the side. Another improvement of utilizing a smaller box is that the heat transfer area of the box is smaller and so creates a smaller intake of the rate of heat transfer.

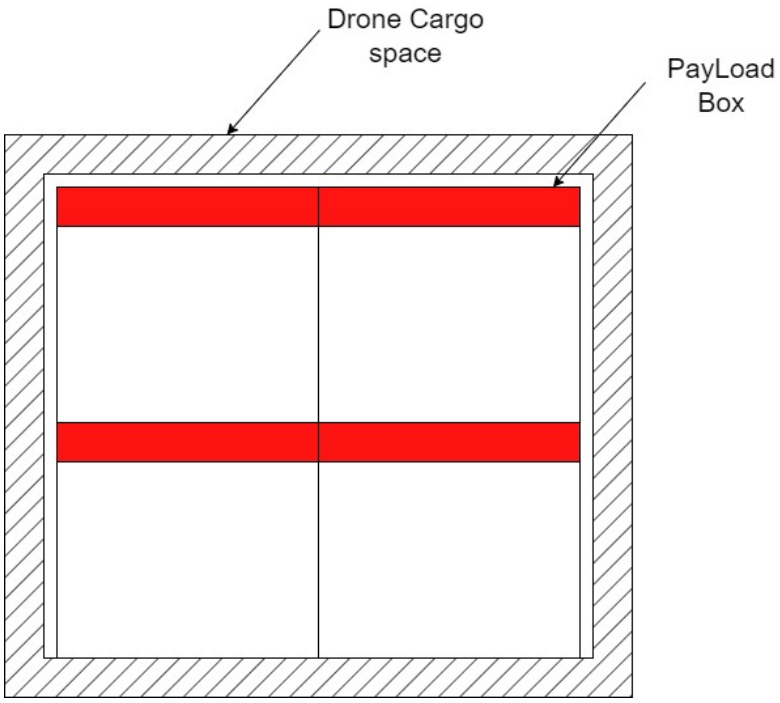


Figure 3.1: Arrangement of boxes inside of the cargo space

After establishing the external dimensions, there were searches for different existing boxes, that are with similar dimensions so that they could be afterward tested without diverging significantly from the end product. The materials considered initially for the box, were expanded polystyrene (EPS) and polyurethane, since they both have a very low thermal conductivity, which for this part in question was its most important characteristic. The insulation box's primary function is to be able to maintain during the whole mission the blood bags in the intended temperature range of 2-8 ºC. This box however serves more as a guideline for the upcoming prototype.

The first step is to assess the amount of insulation required to keep the blood bags in the specified range for the whole trip without using any of the cooling methods. For this it is used the equation 3.22 and is obtained a value of e=178mm, which would make it impossible to transport anything. The goal of conducting tests with an off-the-shelf box is to efficiently validate the heat transfer models under study, all while minimizing significant alterations to the dimensions. This approach allows for the validation of these models before embarking on a more detailed custom development phase. So it was chosen to go with an EPS box of 4.7L and the outer dimensions of 300x200X185 mm^3.(Appendix A) For these dimensions is important to check if the blood bags fit inside of the box. The internal dimensions for blood are presented in the table 3.2 and the internal dimensions of the box are 270x140x125 mm^3.

As is seen, the 400 ml blood bags fit inside the box, but because of its format, it is not possible to put 10 blood bags inside of each of the boxes, since each bag, when full has a thickness (e) of 19.608 mm, as it is shown in the equation 3.1.

Table 3.2: Dimensions for plastics containers, label areas and nominal capacity in mm [11]

Nominal capacity	**Inside width**	**Inside height**	**Size of label area**	
ml	w_1	h_1	$w_2 \pm 5$	$h_2 \pm 5$
100	75	120	60	85
250	120	130	90	85
400	120	170	105	105
500/600	120	185	105	105

$$e = \frac{V}{h \cdot w} \cdot 10^3 = \frac{400}{170 \cdot 120} \cdot 10^3 = 19.608[mm] \tag{3.1}$$

As such, it is possible to transport up to 6 bags in each box, which makes a total of 24 bags per mission. Interestingly, each box exhibits additional space when filled with six 400 ml bags, which amounts to a surplus of 100 mm in length, 20 mm in width, and 40 mm in height.

After choosing the component, that is responsible for the insulation, it is important to create an outer skin, with the aim to protect the insulation boxes, and the electronic parts. This should also provide structural integrity to the whole system. The box's hardness ensures that it can endure impacts, vibrations, and even severe handling during shipping. It protects the fragile contents from outside influences that could otherwise jeopardize the integrity of the blood products. Although the use of the EPS box does not a primary function the support impacts for a product being transported, it does also offer this extra characteristic. This is also used in most of the bicycle helmets. These use EPS to distribute the energy of an impact [48].

The material used for the exterior layer must take into account a number of characteristics, including weight, strength, thermal qualities, cost, and usability. There are some possibilities for example the use of Carbon or aramid, also known as Kevlar, fiber composites. Carbon fiber composites have a high strength-to-weight ratio. They are lightweight while remaining extremely robust and stiff, thus offering great protection for fragile cargo. They possess high tensile strength (ranging from 3 to 7 GPa). This property makes them particularly useful for situations, where structural integrity is critical. Their stiffness, which stems from their high modulus(ranging from 200 to 500 GPa), improves their applicability for scenarios requiring rigidity. In terms of tensile strength the fibers excel, displaying the ability to sustain pulling forces without surrendering quickly. Furthermore, their high fatigue resistance allows them to withstand repeated stress cycles. While their electrical conductivity is advantageous in some situations, it can also be a disadvantage depending on the application's needs. Carbon fiber composites are generally more expensive due to the sophisticated production processes needed [49].

Kevlar, on the other hand, is known for its high tensile strength of about 3,620 Mega-Pascal. Its exceptional impact resistance makes it a perfect alternative for applications requiring collision

or impact protection. Notably, Kevlar has greater flexibility than carbon fiber, making it useful in circumstances where some bending or deformation is expected. Kevlar is lightweight, but its strength is slightly lower than that of carbon fiber. However, it makes up for this with good abrasion resistance, making it suited for settings with friction or wear. Furthermore, Kevlar has a lower thermal conductivity, which is useful in situations where temperature insulation is required. Furthermore, Kevlar is sometimes less expensive than carbon fiber, making it an enticing option where cost is a factor.[50]

For this project the choice was Kevlar as material for the skin. Since both have very good mechanical properties, being that carbon has better results, it is important to see, if the choice of selecting a not stronger material, is the adequate one. The first point is that when compared to the 200 W/(mK) thermal conductivity of the carbon fiber[51], Kevlar has a much lower thermal conductivity with only 0.04W/(mK)[52]. Although the major support of heat resistance comes from the EPS box, the bigger this resistance is, the better can the box maintain the temperature of its contents in the expected range. Secondly, it comes to the price, which elevates furthermore the choice of going on with Kevlar for the outer wall. [53, 54]

3.1.2 Components

Once the structural aspects of the payload box have been selected, the next step involves categorizing the additional components and assessing their implications when integrated. In the context of creating a transport box for blood products, the initial focus naturally gravitates towards refrigeration. However, the components required for this purpose will not be listed in this subsection, as it is imperative to first conduct research to determine the most effective method of maintaining blood within the desired temperature range.

Beyond the structural foundation and cooling system, the additional components should encompass functionalities such as temperature and humidity monitoring, locking mechanisms, communication and tracking systems, as well as battery and power management. Other functions, like shock absorption and attachment mechanisms to the drone, are addressed through the choice of materials for the box. Attachment mechanisms are unnecessary in this specific context, as the system is intended to be transported within the aircraft's cargo bay and does not require attachment to the drone's body.

The initial component for analysis is the monitoring system. During flight, the most crucial parameters to observe and record are the temperature and humidity inside the box. Concerning temperature, it has been determined that two different measuring points within the box are essential. It's also vital to ensure that the sensors exhibit some resistance to humidity since humidity levels tend to rise when handling low temperatures and fluid-containing bags.

The first sensor should measure the general ambient temperature inside the box, providing an overview of the environment. To achieve this, the temperature sensor is placed within the payload box's airspace. Given that this sensor does not directly contact the blood bags, it is advantageous for it to also have the capability to measure humidity within the environment. The second sensor is intended to be positioned between the blood bags, providing a direct reading of the temperature of the blood products, which is critical for maintaining their integrity. When considering the sensors for both cases, it is pertinent to note that the sensor placed between the bags should not only be resistant to high humidity levels, but also be waterproof in case of potential blood bag rupture. Figure 3.2 presents a schematic representation of how the sensors are arranged within the EPS box.

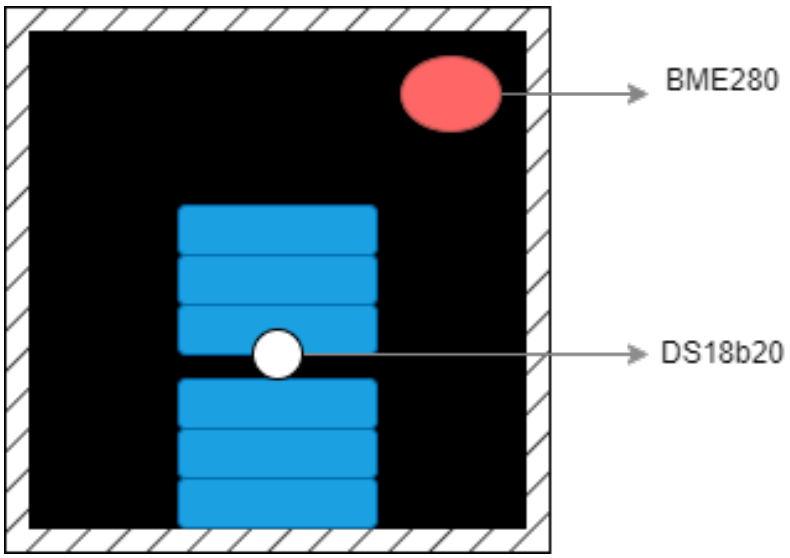


Figure 3.2: Sensor placement

For the first sensor, the BME280 sensor has been selected, due to its affordability and ready availability at the institution. The existing sensor suffices for all required tasks, eliminating the need to acquire another one. This sensor also allows the monitoring of the pressure inside of the box, which wasn't one of the absolute requirements. Another thing to be remarked is that the BME280 cannot be completely air and water-tight, since this would diminish its capability to measure the humidity and pressure. Because of this it is planned that this sensor is placed as seen in figure 3.2 and having an enclosure. This still allows the measurement of every parameter but gives some support and protection to the sensor in cases of direct impact or exposure to water.

In the second position the most important characteristics that the temperature sensor should have, are rapid sensing capabilities for slight temperature deviations and being waterproof. For this, two different sensors were selected in order to afterward test and create a better understanding of the measuring system.
The first is a Negative Temperature Coefficient (NTC) thermistor, which is the most common type of thermistor, and it is very easy to use. They are known for their extreme sensitivity to

temperature changes, which makes them ideal for applications requiring precise temperature measurements. Because thermocouples are small and compact, they are appropriate for applications with limited space, which in this case is important. Thermistors are often more cost-effective compared to other temperature sensing technologies, such as resistance temperature detectors (RTDs) or analog temperature sensors. While thermistors are non-linear sensors, their response may frequently be well-characterized using calibration curves or mathematical equations, allowing for reliable temperature measurements with proper adjustment.

Thermocouples often respond quickly to temperature changes. Because of its simple circuitry and compact size, thermistors can be employed in low-power applications, hence prolonging device battery life.[55] (Appendix B The second option is a digital temperature sensor, like the DS18b20. The DS18B20 uses the 1-Wire protocol to communicate, which allows numerous sensors to be connected to a single digital pin on a microcontroller. This makes interacting with the sensor simple, especially if you have numerous temperature sensors in your setup. The DS18B20 measures temperature with great precision and resolution up to 12 bits, corresponding to a 0.0625 ºC resolvable temperature, enabling high-precision temperature measurement. This precision qualifies it for applications requiring precise temperature control or monitoring. Because each DS18B20 sensor is factory-calibrated, you won't need to execute any additional calibration or characterization steps in most circumstances. This simplifies their setup while also ensuring consistent accuracy. The DS18B20 sensor is available in a variety of models with varying temperature measurement ranges, allowing you to select a sensor that corresponds to the temperature range of your application.[56]

For processing all the different signals of the sensor a micro-controller was implemented. The chosen micro-controller was ESP32, since it was already available in the laboratory. Supporting why this micro-controller can be the one selected for this project, we recognize that wireless connectivity to the IoT using Wi-Fi or Bluetooth has been made relatively simple using ESP32 modules and kits. In this case, all of the three sensors have different communication protocols, like the I2C for the BME280, the one-wire protocol for the DS18b20, that works similarly to the I2C, and for the thermistor, although it isn't a communication protocol, the signal must be converted from an analog value to digital one, and the ESP32 can process all these signals. Another reason to choose the ESP32 is because modules are relatively affordable. Figure 3.3 it is presented a schematic configuration of the connection between the sensors and micro-controller.

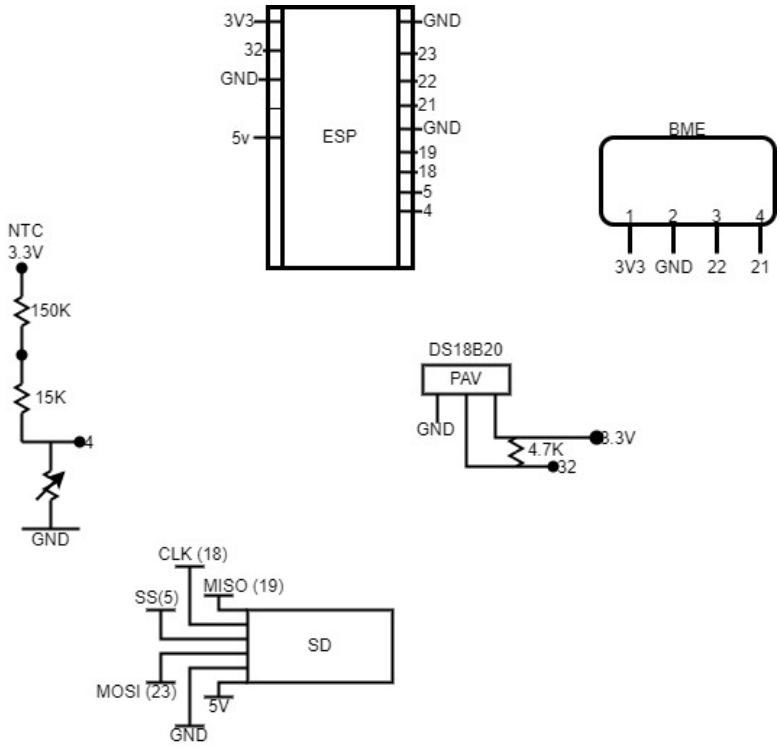


Figure 3.3: Connection diagram between ESP32 and sensors

3.2 Thermal Management System

In this subsection, we will analyze various methods for controlling the temperature inside the payload box. We will begin by discussing the fundamental theoretical concepts behind these methods and conclude with simulations that will help us decide on the most suitable control system to be tested later.

3.2.1 Heat Transfer

Heat transfer is a fundamental concept in physics and engineering that plays a crucial role in understanding various natural and technological processes that govern temperature and its changes. A solid grasp of heat transfer principles enables the development of innovative solutions, energy optimization, and the assurance of effectiveness and safety in countless applications. The three primary modes of heat transfer are conduction, convection, and radiation, each possessing distinct characteristics and applicability in different situations[3].
In the context of the discussed case, it is only regarded that heat transfer occurs through conduction and convection as the payload interacts with the surrounding air. Also, the temperature differences expected should be low enough for the heat transfer by radiation could be discarded.

Conduction is the transfer of heat within a solid or between two contacting solids due to molecular collisions. It involves the transmission of thermal energy from hotter regions to cooler

ones within materials. The rate of conduction depends on factors such as the material's thermal conductivity, temperature gradient, and cross-sectional area. In the case being analyzed, heat is transferred from the payload (e.g., blood bags) to the box walls if they are at different temperatures, with the rate of conduction influenced by the temperature difference and the materials' thermal conductivity [3].

Convection is the transfer of heat through the movement of fluids. It involves the motion of the fluid itself, leading to the transfer of thermal energy. Both natural and forced convection can occur. Natural convection arises when there is a temperature difference between the mass and the air within the box. As the surrounding air warms, it becomes less dense and rises, creating a convective flow. Cooler air from different parts of the box replaces the rising heated air, resulting in a continuous circulation pattern [3].

To evaluate the evolution of the system's parameters due to the heat transmission phenomena presented above, its dynamic model can be created by solving the differential equations governing the system. Concerning the heat transfer between the air surrounding the box and the payload box surface, our analysis exclusively took into account convective heat transfer as the primary mechanism, as the same assumptions were made in other studies [40, 57, 1]. The equation for heat transfer by convection can be expressed as: [3]

$$q_{\text{conv}} = \overline{h} \cdot A_{\text{box}} \cdot (T_{\text{s}} - T_{\text{ambient}}) \tag{3.2}$$

where:

- q_{conv} is the rate of heat transfer by convection (W),
- $\overline{h}$ is the convective heat transfer coefficient (W/(m$^2\cdot$ K)),
- A_{box} is the surface area of the box (m^2),
- T_s is the temperature of the surface of the box(K),
- $T_{ambient}$ is the temperature of the ambient air (K).

From the outside surface of the EPS box to its inside wall heat is transferred by conduction. The heat transfer from the external surface of the box to the interior can be calculated using the following equation: [3]

$$q_{\text{cond}} = k \cdot A \cdot \frac{\Delta T}{L} \tag{3.3}$$

where:

- q_{cond} is the rate of heat transfer through conduction (W),
- k is the thermal conductivity (W/(m· K)),
- A is the cross-sectional area (m^2),
- ΔT is the temperature difference (K),
- L is the wall thickness (m).

Building upon this foundation, we can employ the convective heat transfer equation once more to establish the temperature of the air inside the box. Subsequently, a similar approach can be applied to create a connection between the external temperature and the temperature of the blood mass, thereby completing the thermal analysis.

While it is indeed possible to calculate the internal temperature using the detailed approach described, many articles opt for a simplified method. This method involves computing the total heat transfer, derived from the entire process as previously elucidated and as depicted in the following Figure 3.4 [40, 1, 58, 57]. This streamlined approach provides a more convenient way to assess heat loss through the box's walls and can be elucidated by Equation 3.4.

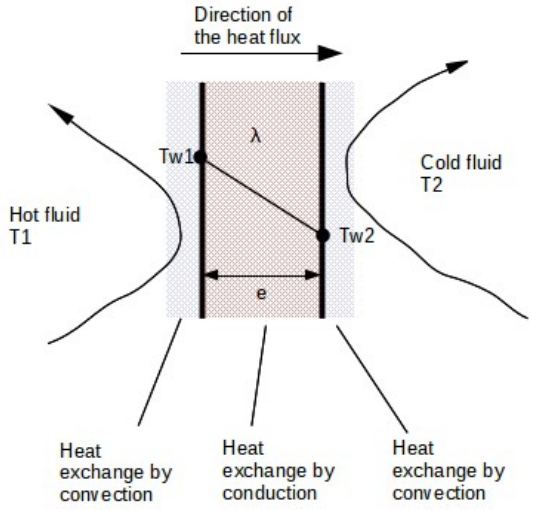


Figure 3.4: Model for convective and conductive heat transfer [2]

$$q = K_{\text{box}} \cdot A_{\text{box}} \cdot (T_{\text{mass}} - T_{\text{ambient}}) \tag{3.4}$$

where:

- q is the rate of heat transfer(W),
- K_{box} is the total heat transfer coefficient (W/(m^2· K)),

- A_{box} is the surface area of the box (m^2),
- T_s is the temperature of the surface of the box(K),
- $T_{ambient}$ is the temperature of the ambient air (K).

In particular, there exists an analogy between the diffusion of heat and electrical charge. Just as electrical resistance is associated with the conduction of electricity, thermal resistance is associated with the conduction of heat[3]. For a composite wall, as seen in figure 3.5, the different thermal resistances for section i in terms of conduction and convection can be expressed as:

$$R_{cond} = \frac{L_i}{k_i \cdot A_i} \tag{3.5}$$

$$R_{conv} = \frac{1}{h_{\text{amb}} \cdot A_i} \tag{3.6}$$

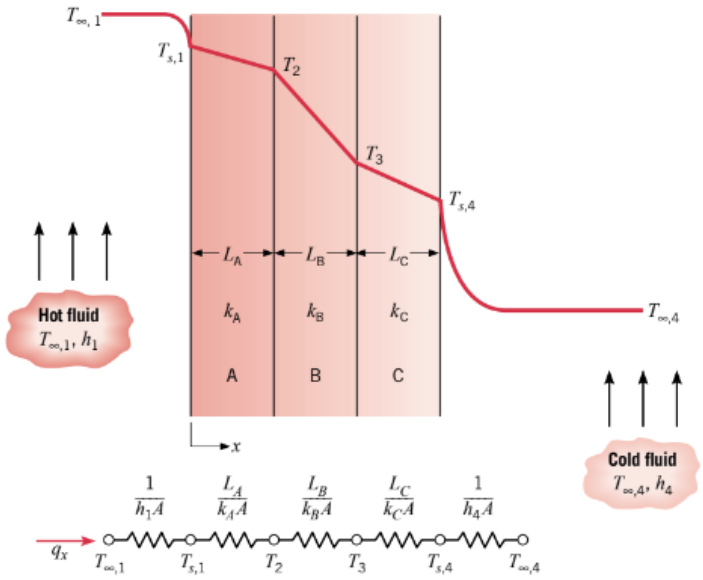


Figure 3.5: Equivalent thermal circuit for a series composite wall [3].

The total thermal resistance comes from the sum of the individual resistances. Assuming that the area is constant, it could be written as:

$$K = \frac{1}{R_{total} \cdot A} \tag{3.7}$$

For this specific case, the heat transfer coefficient can then be calculated with:[1]

$$K = \frac{1}{\frac{1}{h_{\text{amb}}} + \frac{L}{k} + \frac{1}{h_{\text{in}}}} \tag{3.8}$$

- h_{amb} and h_{in} are the heat transfer coefficients of air outside and inside the container, respectively,
- k is the thermal conductivity of the material of the box,
- L is the thicknesses of the insulation.

Additional layers of insulation should be added, the part representing the conductive resistance of that specified material, which consists of the thickness as also its thermal conductivity, $\frac{L_i}{k_i}$, as is presented in figure 3.5 The entire system can be elucidated using equation 3.9, which delineates the thermal equilibrium of the air enclosed within the payload box, as it interacts with the blood and the enclosure walls.

$$q_{\text{tot}} + q_{\text{bl}} = M_{\text{air}} \cdot C_{p_{\text{air}}} \cdot \frac{dT_{\text{air}}(t)}{dt} \tag{3.9}$$

Where:

- q_{tot} is the rate of heat transfer from the outside ambient into the box (W).
- q_{bl} is the rate of heat transfer between air and blood (W).
- $M_{\text{air}}$is the mass of the air stored inside of the box.
- $C_{p_{\text{air}}}$is the air stored inside of the box specific heat capacity.
- $T_{\text{air}}(t)$: Air temperature over time t.

The rate of heat transfer $\dot{q}_{\text{tot}}$ between the air and blood can be calculated using the equation 3.10:[40]

$$q_{bl} = h_{bl} \cdot S_{bl} \left(T_{air}(t) - T_{bl}(t)\right) = M_{bl} C_{p_bl} \frac{dT_{bl}(t)}{dt} \tag{3.10}$$

Where:

- $T_{\text{bl}}(t)$: Blood temperature over time t.
- M_{bl}: Mass of the stored blood.
- C_{p_bl}: Blood specific heat capacity.
- h_{bl}: Thermal exchange coefficient between air and blood bags.
- S_{bl}: total heat exchange surface of blood bags.

The air flows inside and outside the container are considered as natural convection. However, in cases where the box is transported outside the cargo space of the UAV, it's essential to note that the heat transfer coefficient should be calculated considering forced convection rather than natural convection. In this analysis, natural convection is assumed, as the project aims to be applied within

a UAV's designated cargo bay. To determine the value of the conductive heat transfer coefficient, denoted as h, the following expression 3.11 can be used:[3]

$$Nu = \frac{\overline{h} \cdot L}{k} \tag{3.11}$$

Where:

- Nu, is the Nusselt number (dimensionless),
- $\overline{h}$ is the convective heat transfer coefficient (W/(m^2· K))),
- L is the characteristic length (m),
- k is the thermal conductivity (W/(m· K))

Before obtaining the value of the Nusselt number, which represents the ratio between conductive and convective heat transfer, it can be used the equation 3.12 presented by Damiani et al. [40] for a similar box:

$$Nu = \left(\frac{144}{Ra^2} + \frac{2.873}{Ra^{0.5}} \right)^{-0.5} \tag{3.12}$$

And the Rayleigh number Ra is a dimensionless number that represents the ratio of buoyancy and thermal diffusivity and can calculated through equation 3.13.

- The Rayleigh number (Ra) is defined as:

$$Ra = \frac{g \cdot \beta \cdot \Delta T \cdot H^3}{\nu \cdot \alpha} \tag{3.13}$$

- Where:
- Ra is the Rayleigh number.
- g is the acceleration due to gravity.
- β is the coefficient of thermal expansion.
- ΔT is the temperature difference between the top and bottom boundaries of the fluid.
- H is thickness of the fluid layer.
- ν is the kinematic viscosity of the fluid.
- α is the thermal diffusivity of the fluid.

In order to compare both of the systems, it is first calculated the heat loss of the box to the outside world and more specifically the heat loss of the blood bags. Afterward, it is analyzed how both of the cooling types, could prevent the blood bag would coming outside of the intended

range of 2ºC and 8ºC. Another important part is to see how both of the coolings handle the whole duration of the mission. The mission duration was estimated by the team of CEiiA, should have a maximum of 4 hours, but being, that the normal flight time will be under this 4 hours. Testing for its maximum capacity of voyage is a given fact, to be sure that it can achieve its final objective.

The ambient temperature is set at 35ºC and the initial temperature of the blood bags at 4ªC. These values have been obtained through other tests that were done[1], as also from the median values of the storage values according to Portuguese's legislation [36].

Following the temperature, the total area of heat transfer and using the values presented in the table 3.3 is used the equation 3.2.1 to obtain the outside and inside area and then is used the equation 3.2.1 to assess the average heat transfer area $\overline{A}$.

Table 3.3: EPS Box Dimensions

	length	**width**	**height**
Outside	330	200	185
Inside	270	140	125

$$A = 2(h \cdot l + h \cdot w + l \cdot w) \tag{3.14}$$

$$\overline{A} = \sqrt{A_{out} \cdot A_{in}} \tag{3.15}$$

And so obtaining the following values:

Table 3.4: EPS Box Areas

Parameter	**Value**
A_{out}	0.3281 m^2
A_{in}	0.1781 m^2
$\overline{A}$	0.2417 m^2

The last parameter missing is the heat transfer coefficient K_{box}, which is calculated through equation 3.8 and uses the values listed on the table 3.5. The heat transfer coefficient of air is calculated through the equations 3.11, 3.12 and 3.13. And the thermal conductivity of EPS is obtained in the literature [59].

With these values, it is then possible to obtain a heat transfer coefficient of 0.975 W/($m^2 \cdot$ K) for the whole system. And so it can be followed by the calculations of the total amount of heat transferred from the blood bags to the outside of the payload box, which results in a total of 9.7943 W.

Table 3.5: Parameters to calculate heat transfer coefficient

Parameter	Value
h_{amb}	9.163 W/(m^2· K)
L	0.030 m
k	0.035 W/(m · K)
h_{in}	10.415 W/(m^2· K)

3.2.2 Active Cooling

Active cooling is a technique employed to dissipate or remove excess heat from a system or device, ensuring it remains within safe operating temperatures. This approach utilizes mechanical components such as fans or pumps to enhance the heat transfer process. An active cooling system employs mechanical components to dissipate heat, maintaining a lower temperature inside the container. In active cooling systems, a refrigeration mechanism is integrated to actively extract heat from the interior. This refrigeration system typically operates using a thermoelectric module or a small compressor-based system.

Smaller, portable coolers often employ a thermoelectric cooling system, also known as a Peltier cooler. This system consists of two semiconductor plates connected to a direct current (DC) power source. When an electric current flows through the module, one side becomes cold while the other becomes hot. In this setup, the cold side is positioned inside the cooler, where it absorbs heat from the contents, effectively lowering their temperature [60].
On the other hand, larger and more powerful coolers typically feature a compressor-based cooling mechanism, similar to those found in conventional household refrigerators. The compressor operates by raising the pressure and temperature of a refrigerant gas through compression. The resulting hot gas is then circulated through condenser coils located on the exterior of the cooler, where it releases heat into the surrounding environment. Subsequently, the refrigerant condenses into a liquid, flows through an expansion valve, and undergoes evaporation, cooling down in the process. This cold gas then passes through the evaporator coils within the cooler, where it absorbs heat from the contents, efficiently cooling them [61].

Active cooling systems frequently offer temperature control options, enabling users to adjust the cooling intensity or select a specific temperature to maintain the contents at the desired level of temperature. In both cases, a power source is required for operation. For thermoelectric cooling systems, a DC power supply from a 12V DC adapter or portable battery may suffice. Compressor-based cooling systems can also use an alternating current (AC) power supply, available from a standard wall outlet or from a portable power generator or inverter for outdoor use.
The choice between thermoelectric and compressor-based cooling systems is influenced by factors such as cooling capacity, available power, size, and intended application of the cooler.

Compressor-based cooling systems, also known as vapor compression refrigeration, are commonly employed in larger coolers and refrigerators. These systems utilize a refrigerant to expedite the cooling process, functioning based on thermodynamic principles. This process consists of four distinct stages, as illustrated in figure 3.6 and figure 3.7 shows the cycle P-V Diagram.

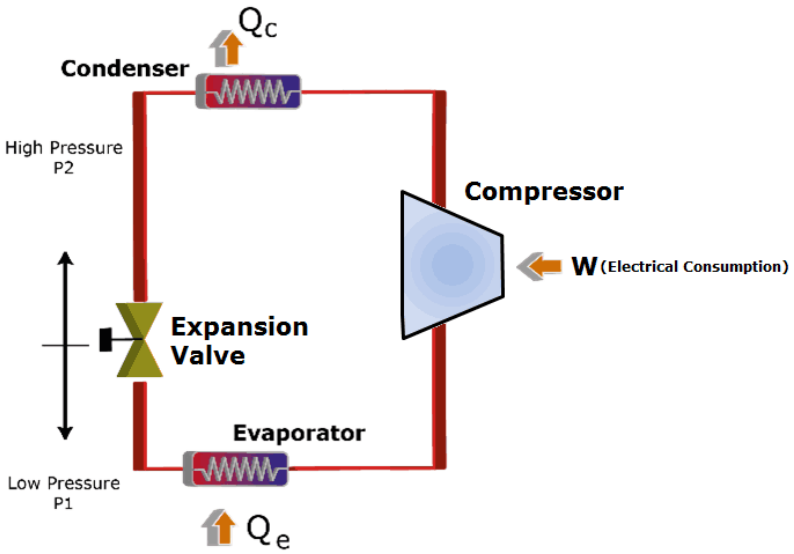


Figure 3.6: Vapor compression refrigeration diagram [4].

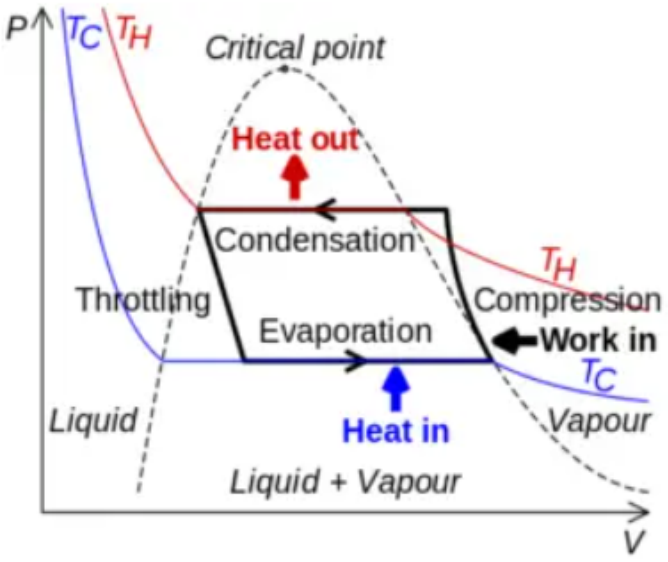


Figure 3.7: Vapor Compression Refrigeration Cycle P-V Diagram [5].

The compressor initiates the process by compressing the gaseous refrigerant, elevating its temperature and pressure. Subsequently, the refrigerant enters the condenser, where it transitions to a hot, liquid state. Since this process requires work, an electric motor could be employed. The actual compressors themselves might be of the reciprocating, centrifugal, scroll, or screw varieties. The

high-pressure refrigerant then passes through condenser coils on the exterior of the cooler, shedding heat to the surrounding air. This results in the refrigerant condensing into a liquid form, it is also in a constant pressure. The pressure of the liquid refrigerant decreases as it traverses through an expansion valve, significantly lowering its temperature. Expansion valves play a crucial role in the vapor compression cycle by maintaining a pressure difference and regulating the flow of liquid refrigerant into the evaporator. The now cold, liquid refrigerant enters the cooler's internal evaporator coils, where it undergoes evaporation, absorbing the latent heat of vaporization. The low pressure is maintained by the compressor's suction, facilitating the return of refrigerant for another cycle[4].

Thermoelectric cooling operates on the principle of the Peltier effect, discovered by Jean Peltier in 1834. It involves passing an electric current through the junction of two dissimilar conductive materials, generating a temperature difference across the junction. This results in either the absorption or release of heat, depending on the direction of the current flow. Modern Peltier devices, also known as thermoelectric coolers (TECs), use semiconductors instead of dissimilar metals. A Peltier module comprises two dissimilar semiconductor materials connected in series [62]. The Peltier effect is commonly observed in action through a Peltier module, also known as a thermoelectric cooler (TEC). This device serves as a solid-state heat pump capable of transferring heat from one side of the module to the other when an electric current is applied. Unlike traditional implementations using dissimilar metals, modern Peltier devices leverage semiconductors for their operation.

The Peltier module comprises two dissimilar semiconductor materials connected in series. It consists of two sides – a hot side (referred to as the source side) and a cold side (known as the sink side). Each side features a junction formed by connecting a p-type semiconductor material (with positive charge carriers) to an n-type semiconductor material (with negative charge carriers). These junctions are the sites where the Peltier effect occurs. In this process, the cold junction plays a vital role in transferring electrons from a low-energy region within the p-type thermocouple to a high-energy region inside the n-type thermocouple. Simultaneously, the electrons transport the heat absorbed from the cold junction to the hot junction. When the heat is dissipated into the heat sink, the electrons in the p-type thermocouple return to a lower energy state. The junction of the p-n semiconductors in a TEC encompasses several effects, including the Fourier effect, which states that the rate of heat transfer depends on the negative temperature gradient, the Joule effect and the Thomson effect. The Joule effect describes the evolution or absorption of heat when an electric current flows through a circuit made of a single material due to a temperature gradient along its length. Considerations for the total heat absorbed at the cooling side (Qa) and the total heat dissipated at the heat sink (Qd) can be made as through the equation 3.16 and 3.17. [63, 62]

$$Q_a = \underbrace{(\alpha_p - \alpha_n)T_c I}_{\text{Peltier cooling capacity}} + \underbrace{\frac{1}{2}\tau_c I(T_h - T_c)}_{\text{Thomson effect}} - \underbrace{\frac{1}{2}I^2(\frac{p_p L_P}{A_P} + \frac{p_n L_n}{A_n})}_{\text{Jouleeffect}} - \underbrace{(\frac{K_p A_P}{L_P} + \frac{K_n A_n}{L_n})(T_h - T_c)}_{\text{Fouriereffect}} \tag{3.16}$$

$$Q_d = (\alpha_p - \alpha_n)T_c I - \frac{1}{2}\tau_c I(T_h - T_c) - \frac{1}{2}I^2(\frac{\rho_p + L_P}{A_P} + \frac{\rho_n + L_n}{A_n}) - (\frac{k_p + A_P}{L_P} + \frac{k_n + A_n}{L_n})(T_h - T_c) \tag{3.17}$$

- α_p and α_n are the Seebeck coefficients of the P-type and N-type thermoelectric materials, respectively. They measure the voltage generated per degree temperature difference (V/K(,
- T_h is the hot junction temperature and T_c is the cold junction temperature (K(,
- I is the electric current passing through the thermoelectric materials (A),
- τ_c is the Thomson coefficient, which measures the temperature gradient produced by a current ((V/(m $\cdot$ K)) ,
- ρ_p, ρ_n is the electrical resistance of the p-type, n-type thermocouple correspondingly (Ω),
- L_p,L_n is the length of the p-type, n-type thermocouple (m),
- A_p, A_n is the cross-sectional area of the p-type, n-type thermocouple (m^2),
- κ_p, κ_n is the thermal conductivity of the p-type, n-type thermocouple (W/(m $\cdot$ K)).

The Coefficient of Performance (COP), which represents the ratio of heat transferred from the cold side to the electrical power input, is a common metric for assessing the efficiency of a Peltier module. While the COP of a Peltier module is often lower than that of compressor-based refrigeration systems. Peltier modules hold an advantage in certain applications due to their solid-state construction and compact size. To enhance heat transmission and system performance, two heat sinks are typically mounted on the hot and cold sides of a thermoelectric module. There exists an ideal current for achieving the highest COP for a given module with fixed hot and cold side temperatures, as demonstrated in equation 3.18. The cooling COP variation of a thermoelectric module operating at its best current under a fixed hot side temperature of 300 K is shown in figure 3.8 [6].

$$(COP)_c, max = \frac{T_c}{T_h - T_c}\frac{\sqrt{1 + ZT_m} - \frac{T_h}{T_c}}{\sqrt{1 + ZT_m} + 1} \tag{3.18}$$

where, ZT_m is the thermoelectric material figure-of-merit at average hot/cold side temperature T_m

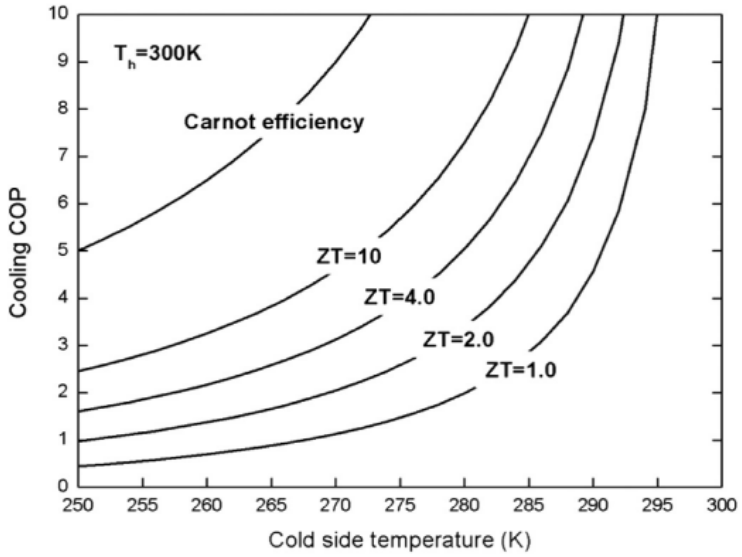


Figure 3.8: Cooling COP of a thermoelectric module under optimum electrical current with fixed hot side temperature of 300 K, Zhao and Tan [6].

An additional benefit of Peltier modules is their reversibility. By reversing the direction of the electric current, the Peltier module can function as a heater, providing greater versatility in transporting items at different temperatures. Peltier modules find widespread use in various applications, including thermoelectric coolers, temperature control systems, and electronic devices requiring precise and localized cooling or heating. They are particularly valuable in situations where the absence of moving parts, simplicity and reliability are crucial considerations. However, their cooling capacity is limited, and for large-scale cooling applications, they are generally less efficient than compressor-based refrigeration systems.

3.3 Comparison of cooling systems

This section provides a concise comparison between vapour compression and the use of a Peltier module, shining light on their distinct mechanisms, benefits and drawbacks. It's dissected the intricacies of these two dynamic techniques in the pursuit of effective cooling solutions.

Vapor compression cooling is a well-established technology widely employed in household refrigerators, air conditioning systems, and industrial cooling applications. Its prominent role in these domains can be attributed to its high cooling capacity and adaptability to various temperature ranges, making it an efficient solution to meet increased cooling demands. However, it's essential to acknowledge that this technique has its disadvantages. The primary drawback is its mechanical complexity, requiring multiple components like a compressor, condenser, and evaporator. Additionally, the use of refrigerants, some of which are environmentally hazardous, poses

an environmental concern. While research into smaller vapor compression systems is progressing, compact vapor compression systems remain relatively uncommon.

One of the key advantages of employing a Peltier module is the creation of a cooling system with no moving parts and a compact design. This results in minimal maintenance requirements and an extended operational lifespan. Furthermore, due to their reversible operation, Peltier modules can serve both cooling and heating purposes. Lastly, they offer precise temperature control, allowing for the maintenance of precise temperature differentials between the cool and hot ends. Despite these advantages, Peltier modules have limitations. Their primary drawback is their lower efficiency when compared to traditional methods. They exhibit lower cooling capacity than other active cooling technologies, making them better suited for smaller-scale cooling tasks. Prolonged operation with a significant temperature differential between both sides can affect their performance. Additionally, Peltier modules tend to have a higher cost per unit of cooling power, primarily due to their lower efficiency compared to conventional methods.

In conclusion, the choice between the most efficient and adaptable cooling system for the payload box becomes clearer after presenting both sides of the argument. In terms of sheer thermal system efficiency, a vapor compression system appears to be the ideal choice, since it displays a COP of around 9, whereas normal values of a Peltier module are around 2 and 0.5 [61, 64]. However, the inclination to explore the Peltier module as the solution stems from the constraints related to the compartment's size and weight. Even when using smaller micro-compressors, a vapor compression module remains at least 180 mm long in its shortest dimension[61, 65]. Ultimately, the optimal choice for the active cooling system in this scenario is the Peltier module. Its compact design allows for incorporation within the previously established box, making it a practical and efficient solution for the payload box.

With the value of the total heat transferred, we can also obtain the essential parameters required to select an active cooling system, in this case, a Peltier module. We need the required heat cooling capacity (Q_c) and the desired temperature difference (ΔT), which depends on the temperature of the hot side. Using supplier diagrams, we can choose a Peltier module that is most suitable for each specific situation. From the graph shown in Figure 3.9, we can extract values for voltage and current, enabling us to calculate the amount of energy required to utilize the active cooling system in the payload box. As displayed in the figure the hot side of the Peltier is at 50ºC, which means that the temperature difference between both sides should be around 45ºC. It is also known from previous calculations, that a total of 9 W of heat needs to be taken out of the system. Therefore the Peltier must be supplied with a current of around 7A and a voltage of 5V, giving a total of 35W of electrical power 140 Wh for the whole 4h of transport. A possible battery would be a Swit MINO-S140, which weighs 0.713kg [66].

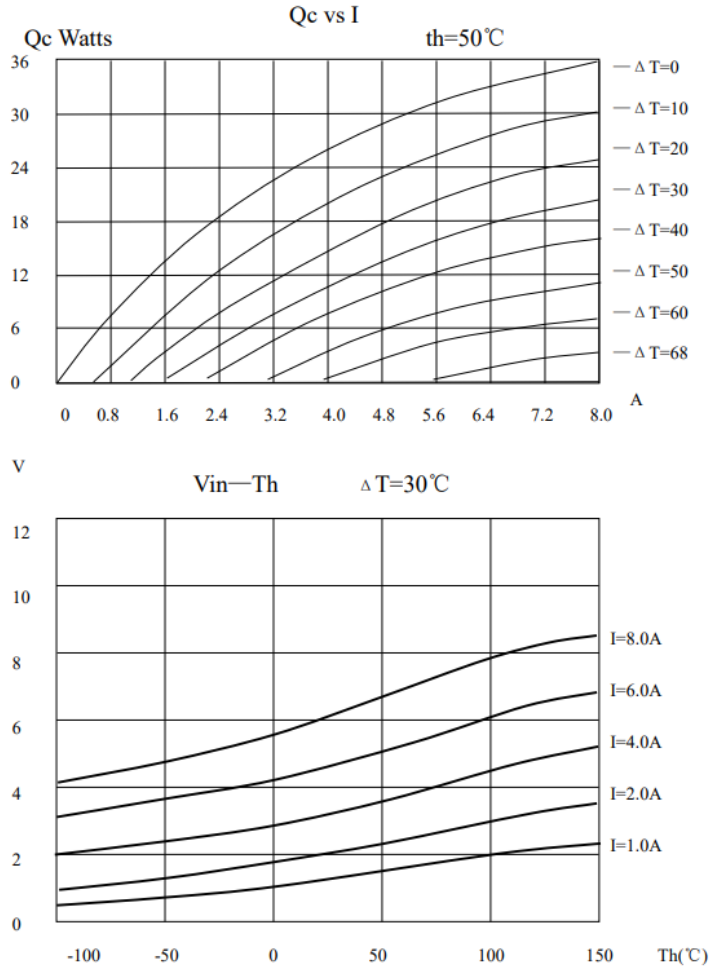


Figure 3.9: Peltier current vs Heat diagram

3.3.1 Passive Temperature Maintenance

Passive Temperature maintenance is a method that relies on natural heat dissipation mechanisms, foregoing the need for mechanical components like fans or compressors. Instead, it leverages the intrinsic physical properties of materials and the principles of heat transfer to maintain a system's temperature within safe limits. Passive Temperature maintenance systems, often found in basic conventional coolers, aim to keep the contents cold through passive heat transfer mechanisms. They are suitable for scenarios requiring simplicity, reliability, and energy efficiency. The primary objective of passive temperature maintenance is the same as active cooling: to maintain the intended temperature range, ensuring the preservation of sensitive cargo like blood during transport.

Passive temperature maintenance techniques are efficient for keeping temperatures low for shorter periods or under moderate climatic conditions. They are suitable for situations where cooling needs are not as stringent and power sources are either unavailable or unwanted. Additionally, ice packs or cold packs can be placed inside the container to enhance its cooling capacity.

These packs contain chemicals capable of absorbing and storing a significant amount of heat as they transition from a solid to a liquid state, providing extra cooling power.

Effective Passive Temperature maintenance requires careful design considerations. The size, shape, and surface area of the heat sink are critical factors influencing its ability to dissipate heat efficiently. The choice of materials and their thermal conductivity properties also play a crucial role in determining the effectiveness of the passive temperature maintenance system. While passive Temperature maintenance systems are simpler and more energy-efficient, they may not be as effective as active cooling systems in extremely hot or humid environments or for extended duration. The cooling performance largely depends on the quality of the insulation and the initial temperature of the contents placed inside the cooler.

In summary, passive temperature maintenance systems harness natural heat dissipation processes to maintain cold temperatures within a container. They are practical and reliable options for situations where a mechanical cooling system is unnecessary or unavailable.

A material that can enhance the capacity of the payload box maintaining its contents at a proper temperature without the need for an active cooling system, are Phase-changing materials (PCMs). Through the use of the latent heat characteristics of these materials, it is possible to devise solutions for energy conservation, temperature stability, and enhanced thermal performance. At the core of PCMs lies the concept of latent heat. During a phase transition (e.g., from solid to liquid), a material either absorbs or releases heat energy without changing its temperature. This heat energy, whether absorbed or released, is referred to as latent heat. PCMs are engineered with phase transition temperatures tailored to specific applications. The PCM absorbs thermal energy and undergoes a transition from a solid to a liquid state. In this scenario, it absorbs heat from the air inside the container, effectively preventing the temperature from rising further. This phenomenon is crucial for maintaining a controlled temperature environment. PCMs regulate temperature by storing and releasing heat energy during phase transitions. They absorb excess heat when the surroundings become too warm and release it when conditions cool down, thereby maintaining a stable and consistent temperature in proximity to the PCM [7].

Differential Scanning Calorimetry (DSC) stands as a robust analytical method employed for examining the thermal attributes and behavior of Phase Change Materials (PCMs) during their phase transitions. This technique operates by measuring the flow of heat into or out of a sample while subjecting it to controlled temperature variations. The sample is positioned within a specialized DSC apparatus, with a reference material possessing a known heat capacity placed in a separate compartment. The instrument concurrently adjusts the temperature of both the sample and the reference material at a consistent rate[67].

In a study conducted by Nie et al. (2021), various PCM configurations were assessed to gauge their efficiency. The investigation commenced with a paraffin-based PCM, specifically RT5 (Ru-

bitherm). Thus, silica was introduced to create three distinct PCM variants with concentrations of 2 wt.%, 4 wt.% and 6 wt.%. The images in Figure 3.10 illustrate these different PCM samples[7].

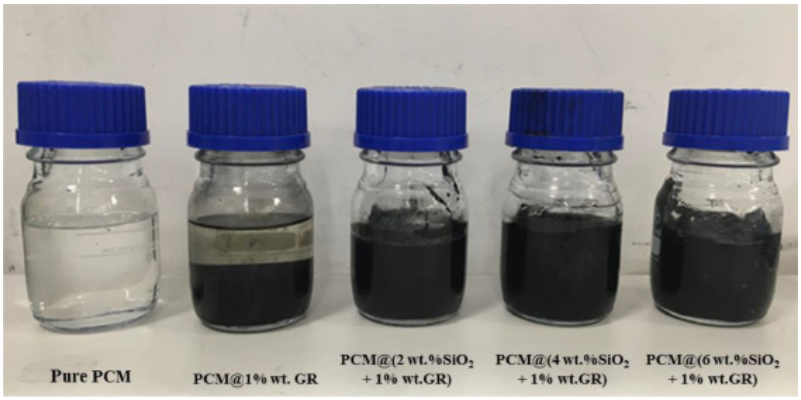


Figure 3.10: Photos of different PCM samples Nie et al. [7].

Figure 3.11 illustrates the Differential Scanning Calorimetry (DSC) curves for both pure and composite PCMs. Notably, the initiation points of melting and congealing for composite PCMs closely align with those of pure PCM. This indicates that the composite's inclusion of fumed silica and graphene has a minimal effect on the phase transition temperature.

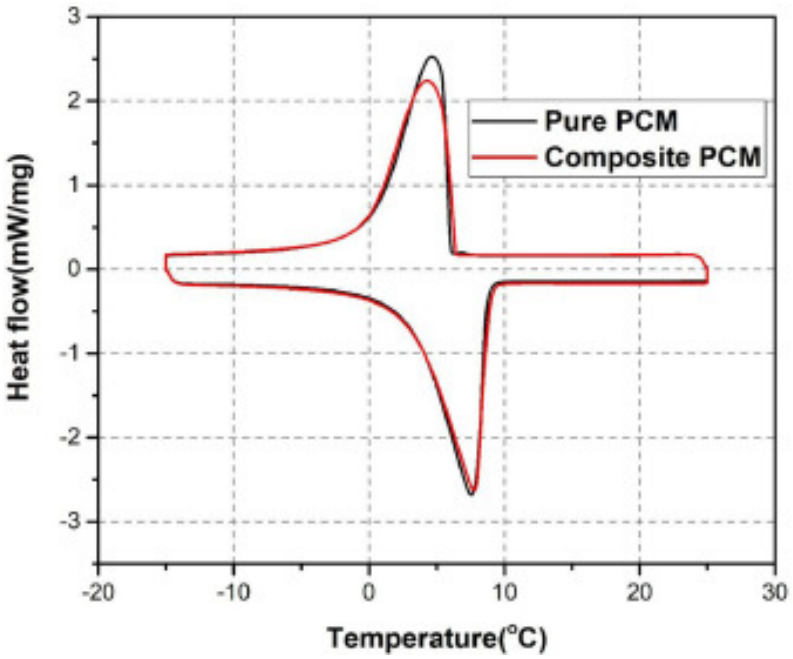


Figure 3.11: DSC curves of different PCMs Nie et al. [7]

To calculate the total energy absorbed by the PCM, Q_{pcm}, within containers placed inside the portable box during the charging process, the following equation 3.19 is employed:

$$Q_{pcm} = m_{pcm}\left[c_p\left(T_e - T_i\right) + \Delta H_{pcm}\right] \tag{3.19}$$

- m_{pcm} and ΔH_{pcm} are the mass and latent heat of the PCM, respectively.
- c_p is the specific heat capacity of the PCM.
- T_e and T_i are the end temperature and initial temperature of the PCM charging process, respectively.

.

Furthermore, the charging efficiency, $\mu_c h$, can be determined using Equation 3.20:

$$\eta_{ch} = \left| \frac{Q_{pcm}}{Q_{fr}} \right| * 100\% \tag{3.20}$$

Lastly, the quantity of PCM required for the cold plate in a cold storage heat preservation box can be estimated using the following formula presented by Xiaofeng and Xuelai [68]:

$$X = \frac{T \times K \times A \times (t_2 - t_1) \times n}{H} \tag{3.21}$$

- X: Quantity of coolant, i.e., PCM (kg).
- H: Phase change of latent heat of PCM (kJ/kg).
- T: Cooling time (h).
- K: Coefficient of heat transfer (W/(m$^2\cdot$ K)).
- A: Heat transfer area (m^2).
- t_2: Temperature outside of the box (K).
- t_1: Heat preservation temperature in the box (K).
- n: Number of open doors of the box (n = 1, i.e., top).

Alternatively, d'intérêt Economique – Economic Interest Group) [59] provides two approaches for utilizing EPS boxes to transport perishable goods while maintaining them at their specified temperatures. Both approaches aim to estimate the duration for which the EPS box can sustain the contents within the defined temperature range. For scenarios where no cooling component is employed, Equation 3.22 is employed. This equation not only calculates the time the EPS box can uphold the contents but can also be rearranged to determine the required insulation thickness for the entire transportation duration. On the other hand, when a cooling component, such as PCM, is utilized, Equation 3.23 comes into play. In this scenario, it is assumed that as long as the PCM has not completely undergone its phase change, the air inside the EPS box remains at a consistent temperature.

$$\Delta t = m_p \cdot c_p \cdot \left(\frac{\frac{1}{a} + \frac{\theta}{\lambda}}{s \cdot 3,6} \ln \frac{\theta_o - \theta_0}{\theta_o - \theta_1} \right) \tag{3.22}$$

$$e = \lambda \left(\frac{\Delta t \cdot s \cdot 3,6}{m_p \cdot c_p \cdot \ln \frac{\theta_c - \theta_0}{\theta_e - \theta_c}} - \frac{1}{\alpha} \right)$$

$$\Delta t = m_{\mathrm{u}} \cdot c_{\mathrm{g}} \cdot \left(\frac{\frac{1}{\alpha} + \frac{e}{\lambda}}{\mathrm{s} \cdot 3,6} \frac{1}{0_{\mathrm{e}} - 0_i} \right) \tag{3.23}$$

Where:

- Δt: Thermal insulation period (h) between θ_0 and θ_1.
- m_g and m_P: Cooling element weight and Packaged product weight, respectively(kg).
- c_g: Cooling element heat of fusion (kJ/kg).
- c_P: Packaged product specific heat capacity (kJ/(kg·K)).
- α: Heat transfer resistance (W/(m²·K)).
- e: EPS packaging wall thickness (m).
- λ: Packaging material thermal conductivity (W/(m·K)).
- S: EPS packaging internal surface (m²).
- θ_e: Room temperature (°C).
- θ_0: Product's initial temperature (°C)
- θ_1: EPS packaging internal temperature when filled with cooling element (°C).

After calculating the amount of heat transferred, let's proceed with a more technical comparison between the two cooling methods. To begin with, we will determine how much PCM is needed to maintain the desired temperature range for the entire mission duration using Equation 3.21. The parameters required for this calculation are presented in Table 3.6, and they result in a required quantity of PCM, denoted as X, which equals 0.318 kg. Next, using Equation 3.23 and the previously obtained mass of PCM needed, we can estimate that it would maintain the temperature for approximately 4 hours and 5 minutes. Interestingly, both cooling methods, PCM and Peltier modules, show a similar estimated time of around 4 hours for maintaining the temperature within the specified range.

3.3.2 Passive vs Active Cooling

With the choice of an active cooling system being completed, it is important to compare it to a passive system. In order to compare both, the advantages and disadvantages of the PCM cooling system should be analyzed, as it was previously done for the Peltier module, when comparing it to vapor compression cooling. However, the specified PCMs' stipulated temperature ranges limit

Table 3.6: Parameters to calculate quantity of PCM needed

Parameter	**Value**
H	260 kJ/kg
T	4 h
K	0.036 W/(m^2· K)
A	0.3281 m^2
t_2	308.15 K
t_1	274.15 K
n	1

the use of this procedure. Additionally, compared to active cooling techniques, the reaction time for obtaining the required cooling effect is typically longer, as also in case of unforeseen change in temperature it can't act on it and so preventing the degradation of the content inside the payload box. A crucial step in the design process is choosing the proper PCMs for each situation. To guarantee efficient cooling performance, the materials must match the specified temperature range and have the necessary thermal characteristics. Applications needing constant and regulated temperatures in relatively small, confined places are where PCM cooling finds its niche.

While comparing both types of cooling to each other, there are some points that elevate one of the two, while lowering the other. One of these is the fact, that the Peltier cooling system depends on electricity to work. This means that, with a small and compact design, loses a bit of its relevance since afterward it is still needed to add a power supply. This doesn't mean that when compared to vapor compression cooling has the role because both need a power supply to work On the other hand, the fact that PCM is a passive cooling component means that it won't be able to respond to unforeseen events as a Peltier module could.
Nevertheless, the amount of PCM theoretically needed to transport the safely within the range of 2-8ºC is much smaller than any option with a Peltier module. As it was calculated for the Peltier a need of a 0.713kg battery in the subsection 3.2.2 against a weight of 0.318kg of PCM needed, as seen in the subsection 3.3.1.

Since the use of PCMs shows a great possibility of maintaining the temperature as intended, two simulations were done.
The first simulation was done in Solidworks, with the purpose of obtaining an evolution of the temperature on the payload box during the estimated time of mission. This simulation can also be used as a support for the choice of the refrigeration method, since it is of a more simple method of elaboration. It was selected transient thermal analysis, whose primary focus is to understand how the model's temperature evolves over time. When performing transient thermal analysis, it's essential to define specific material properties, including thermal conductivity, density and specific heat. Additionally, it must be specified initial temperatures, the total solution time, and the time increment for accurate results. These parameters collectively enable the simulation and analysis of how the temperature within the system changes throughout the entire duration of the process,

rather than just focusing on the final steady-state condition.

The box consists of the outer shell, then the insulation of the EPS-box, afterward a shell of air, and in the center a block representing the blood bags. Figure 3.12 shows a picture of the model used for the simulation.

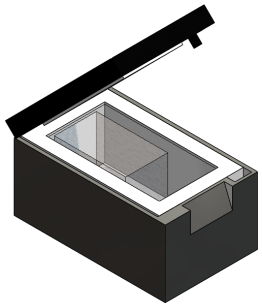


Figure 3.12: 3d model for thermal simulation

The mesh details for this simulation are presented in table 3.6. The outside faces of the box were submitted to a convective load, with a convection coefficient of h = 20W/(m · m^2) and the temperature of ambient involving the box is at 35ºC with no variations during the time of the simulation, this is presented in figure 3.13. The other thermal load, that was assumed, is in the center of the block, representing the blood bags, it is added an initial temperature of 4ºC.

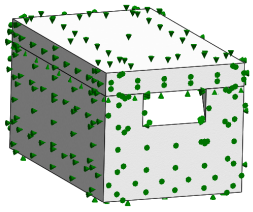


Figure 3.13: 3D model for thermal simulation with outside surfaces subjected to a convective thermal load

After running the simulation it is possible to notice, that the center blocks' temperature doesn't have a big evolution and maintains in the acceptable ranges for a system with no cooling system. Being that after the 4 hours some of the more outer zones of the block, reach temperatures of

Table 3.7: Parameters of the mash

Mesh type	**Solid Mesh**
Mesher Used:	Blended curvature-based mesh
Jacobian points for High quality mesh	16 Points
Maximum element size	51.0 mm
Minimum element size	2,55 mm
Mesh Quality	High
Remesh failed parts independently	Off

around 10 ºC, as it can be evaluated in figure 3.14.

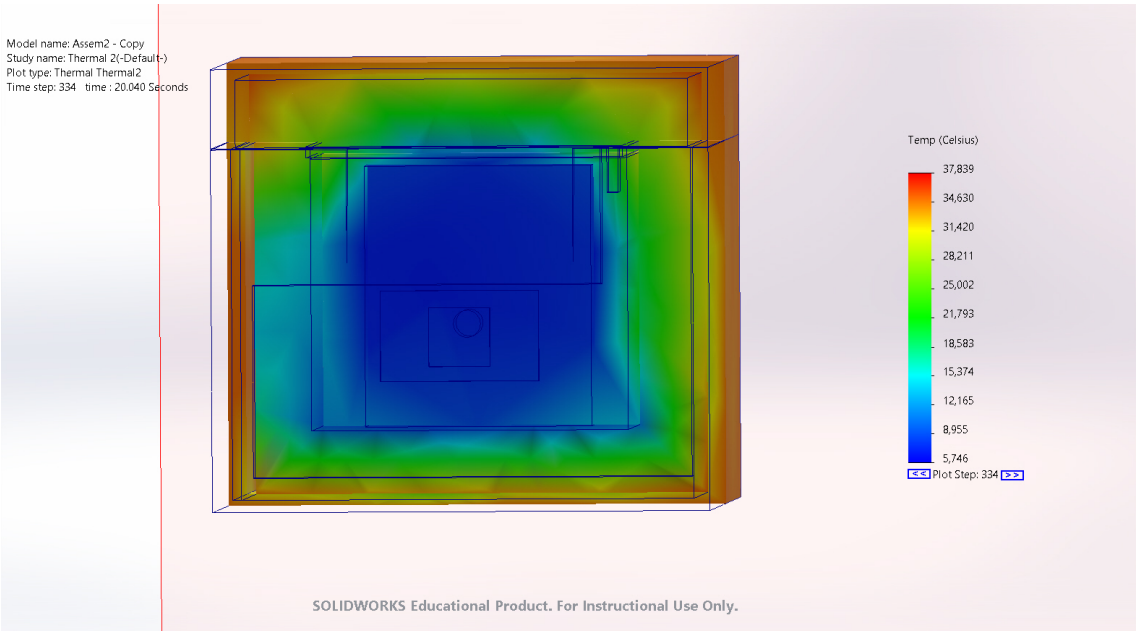


Figure 3.14: 3D model for thermal simulation with outside surfaces subjected to a convective thermal load

The second simulation was conducted using Matlab Simulink, which involved implementing most of the equations outlined in this chapter. The primary goal was to achieve the best possible approximation of the model. Additionally, this simulation aimed to assess the efficiency of both cooling methods and ultimately make an informed decision regarding which one should be used for testing. Matlab Simulink provides a block diagram environment that is well-suited for designing system models and visualizing the results using various scopes and graphical displays. It supports the simulation of continuous, discrete, and mixed-signal systems and offers a choice of fixed-step and variable-step solvers. These solvers are algorithms responsible for computing system dynamics over time. In this case, Simulink allowed for the integration of the dynamic model developed throughout this chapter, enabling thorough testing and the acquisition of valuable results.

The model created was divided in three different parts, the first where it is analyzed solely the transfer between the outside of the box and the inside, seen in figure 3.15. Secondly, there is the blood component, which interacts with the air inside the box, as it can be seen in figure 3.16 Finally, is the part where the PCM is simulated, as presented in the figure 3.17. The center part relates the air and its transfer of heat with the outside of the box, the blood, and also the PCM. For this, the equation used to test it was:

$$q_{\text{tot}} + q_{\text{bl}} + q_{\text{pcm}} = M_{\text{air}} \cdot C_{p_{\text{air}}} \cdot \frac{dT_{\text{air}}(t)}{dt}$$

Each block in Figure 3.15, represents a value on the equation above. The two gray blocks represent the other two parts, one being the blood and the other one the PCM.

The Blood block has a total of two inputs and two outputs. The two inputs are the temperature of the air and of the PCM. The two signals coming out of the block are the temperature of blood to be then compared displayed in the same graph as the other two temperatures and the other signal is the rate of heat transferred from the blood. The equation represented by the block is:[40]

$$q_{bl} = h_{bl} \cdot S_{bl_{air}} \left(T_{air}(t) - T_{bl}(t)\right) - k_{pcm} \cdot S_{bl_{pcm}} \left(T_{pcm}(t) - T_{bl}(t)\right) = M_{bl} C_{p_bl} \frac{dT_{bl}(t)}{dt}$$

Additionally to the equation for convective heat transfer applied to the PCM, some other equations are needed. Equation 3.24 and Equation 3.25 reproduce the thermal balance of the PCM. The first equation describes the behavior of the PCM during melting and is used in normal operation when the PCM has not yet entirely melted. The time-varying liquid mass fraction $X_{PCM}(t)$. This variable varies from 0 to 1 while the temperature stays constant. The second equation takes temperature into account increasing the amount of molten PCM that is exposed to the entering thermal movement.

$$\dot{q}_{PCM,OP} = h_{PCM} \cdot S_{PCM} \left(T_{PCM}(0) - T_{air}(t)\right) = m_{PCM} \cdot r_{PCM} \cdot \frac{dX_{PCM}(t)}{dt} \tag{3.24}$$

$$\dot{q}_{PCM,EX} = h_{PCM} \cdot S_{PCM} \left(T_{PCM}(t) - T_{air}(t)\right) = m_{PCM} \cdot C_{p,PCM} \cdot \frac{dT_{PCM}(t)}{dt} \tag{3.25}$$

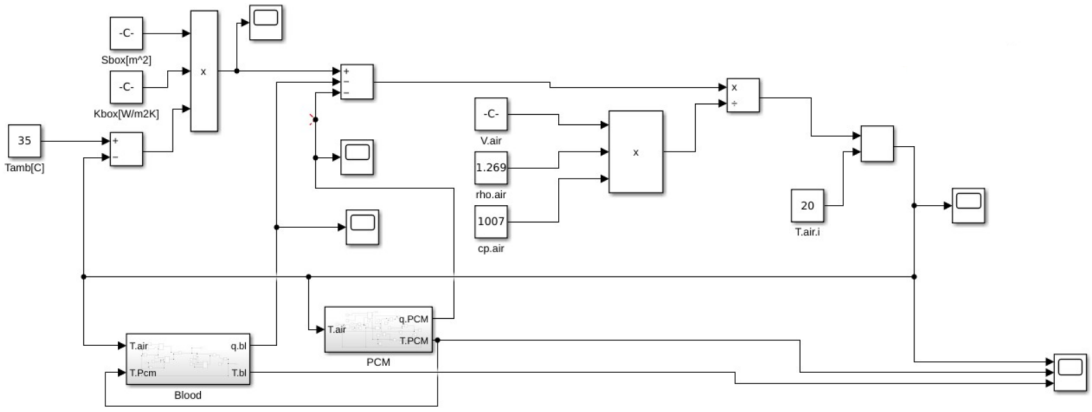


Figure 3.15: Simulink block scheme for thermal balance of air contained in the box.

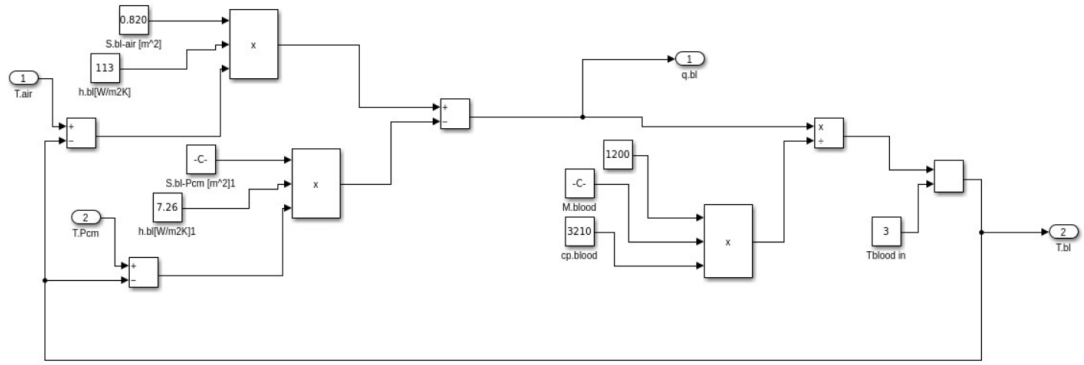


Figure 3.16: Simulink block scheme for thermal balance of the blood.

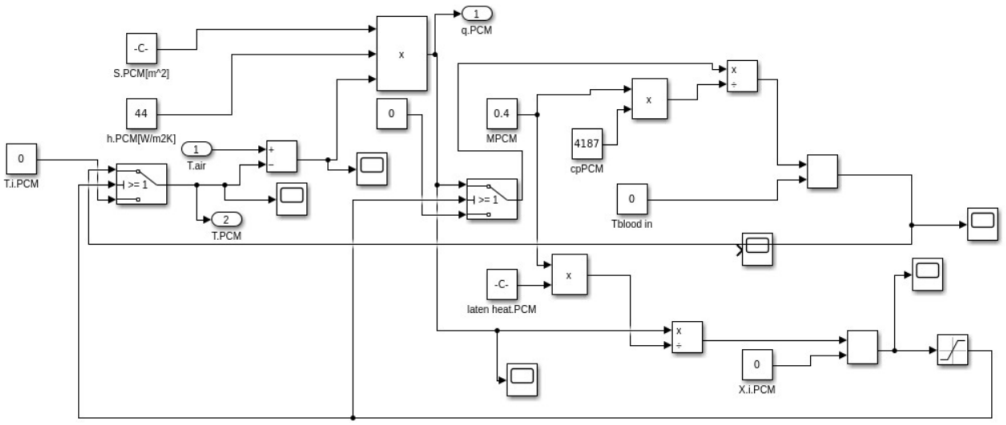


Figure 3.17: Simulink block scheme for thermal balance of PCM.

Figure 3.18 shows that with the presented model the temperature of blood stays within the pre-established range of 2-8ºC until the 5h mark. After simulating this model is possible to the

conclude, that there is no need to create a system with active cooling, since this would be heavier and would take up more space in the box. In Figure 3.18, although the Peltier device is pretty small in size and weight, in order to fully take advantage of its cooling capabilities, it needs to use a heat sink, as well as a small fan. Another part that brings a lot of weight is the need for power capacity, since a Peltier module has a very low COP.

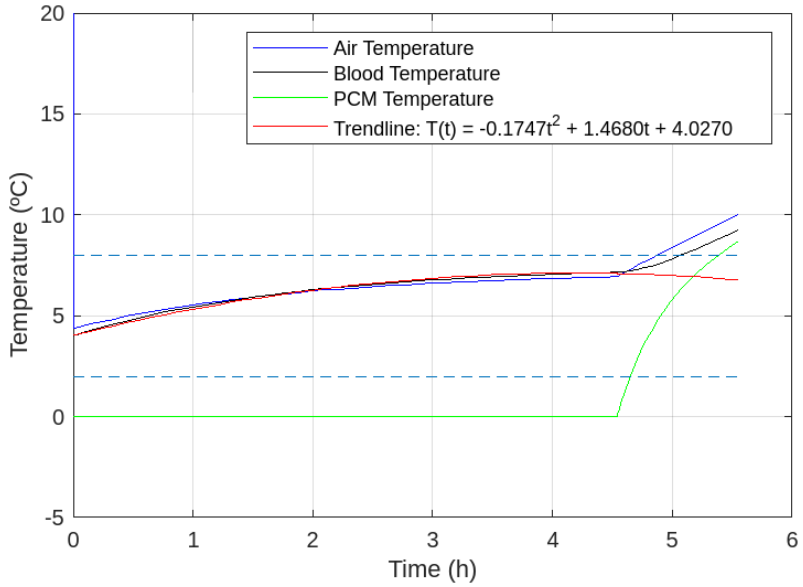


Figure 3.18: Simulink block scheme for thermal balance of PCM.

3.4 Development of the Test Process

This section explains the process of tests that were made. The parameters previously analyzed and the machines that were used are presented, in order that afterward the results are easily understood.

Before the test, the EPS box had to be prepared. For this, it is important first to combine the measuring system to the box, in a way that there's no risk of a component disconnecting itself. With this purpose in mind, there are some components needed beyond the ones presented in figure 3.3. The components not previously introduced are:

- Protoboard,
- Cables, connectors and female headers,
- a SD-Card module with a SD-Card,
- battery LI-ION 18650 3,7V 3350MAH with a charger. [69, 70]

After welding the components the header, cables, and resistances to the protoboard, as seen in figure 3.19, it is possible to start the test from a hardware point of view.

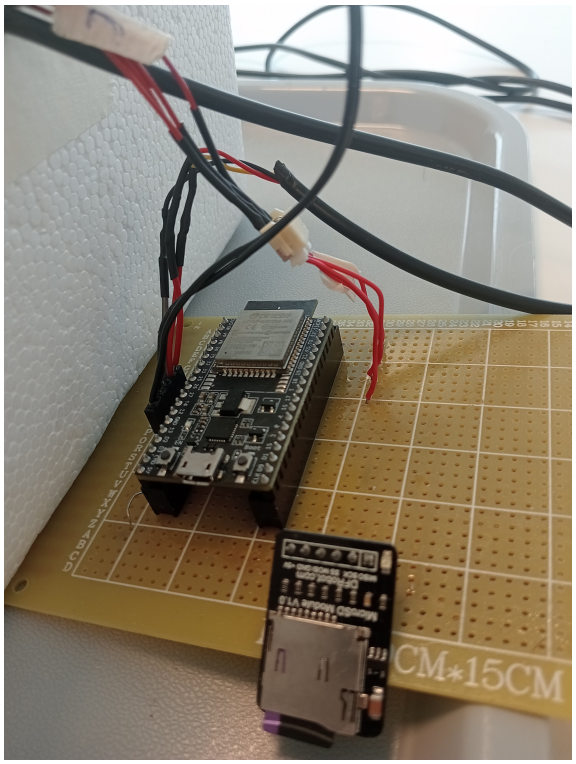


Figure 3.19: Connections between ESP 32 and the SD module through the use of a protoboard

This test consists of two parts, the first part is at room temperature with nothing inside the box. The second is with a cold component inside of the box with the lid closed and the outside temperature at normal ambient temperature. Both of these tests are to examine and compare the different sensors in matters of precision, reaction time, and errors. In order to better compare the sensors, they were placed in a manner, in which the difference in temperature wasn't problematic, even when their final placement isn't exactly as shown in the picture 3.20.



Figure 3.20: Sensors position for validation tests.

After concluding the test of the sensors, different tests are planned. Firstly, these tests have the intuition of clarifying the decision of taking a route with a Passive Temperature maintenance system, proving the choice taken. So it can afterward present a possible design of the final box.

After a thorough examination, it was concluded, that the box should be submitted to a high ambient temperature for this test. In order to test at a specified, and relative humidity, the tests were conducted in a climate chamber. Because of the availability of the chambers, the test couldn't be conducted always in the same chamber, but both are from the same manufacturer, Aralab. The specifications for each of the chambers are presented in the table 3.8 and can be seen photograph in figure 3.21.

Table 3.8: Parameters of the climate chambers

Parameter	**500L**	**1000L**
Humidity	0;98%	0;98%
Temperature	-20 to 180ºC	-75 to 180ºC
Heating rate	2.5 to 4.5ºC	
Cooling rate	2.5 to 4.5ºC	



Figure 3.21: Thermal chamber, left 1000L right 500L.

In sum, two different types of tests should be elaborated and should be executed at least twice each, to overrule the possibility of a singular occurrence. The outside for both types of temperatures should be the same, only altering the contents of the insides of the EPS box. The test should have a duration of 4h, which represents the maximum duration of a mission, the selected temperature is of 35ºC and it was considered a relative humidity of around 55%. Inside the box it should be placed simulated blood bags at the intended temperature and a total of 6 saline solution bags. In order not to waste any useful blood during the trials, the plastic bags were filled with water at a saline concentration of 0.9% accordingly with Homier et al. [42]. The differentiating factor between both tests is the use of PCM inside the box. The different parameters of each test are presented in the table 3.9.

Table 3.9: Parameters of the Tests

Parameter	**Test without PCM**	**Test with PCM**
Quantity of PCM	0	1
Weight of PCM	0	0.315 kg
Blood bag Temperature	4ºC	
Blood bag Amount	6	
Duration	4h	
Ambient Humidity	55%	
Ambient Temperature	35ºC	

The tests should both have the same order of events. The initial step is to turn on the ESP32 and therefore the sensors. After completing this step, the simulated blood bags should be retrieved from the refrigerator and then placed in the box, ending this phase by closing the lid. And then being transported to the climatic chamber, where the EPS box should spend the next 4 hours.

Chapter 4

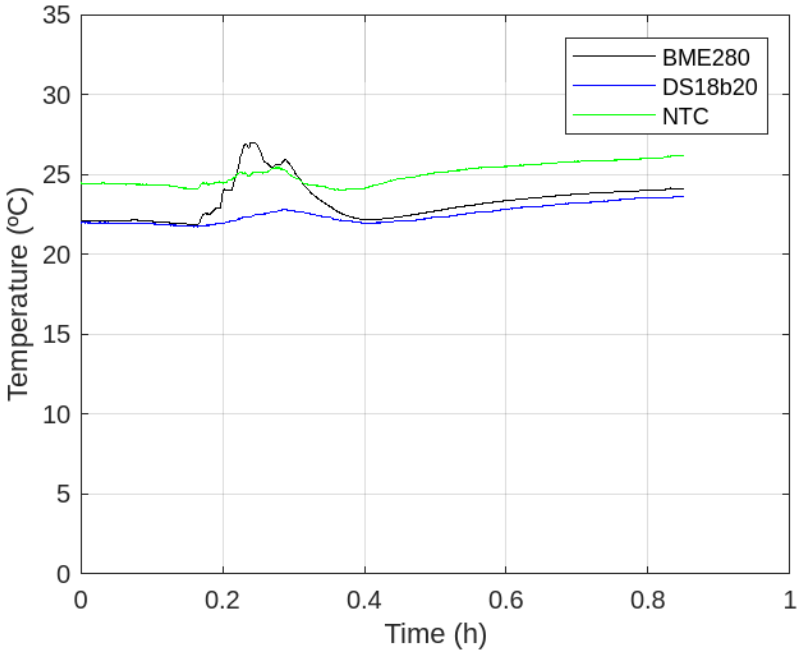
Results and Discussion

4.1 Tests Analyses

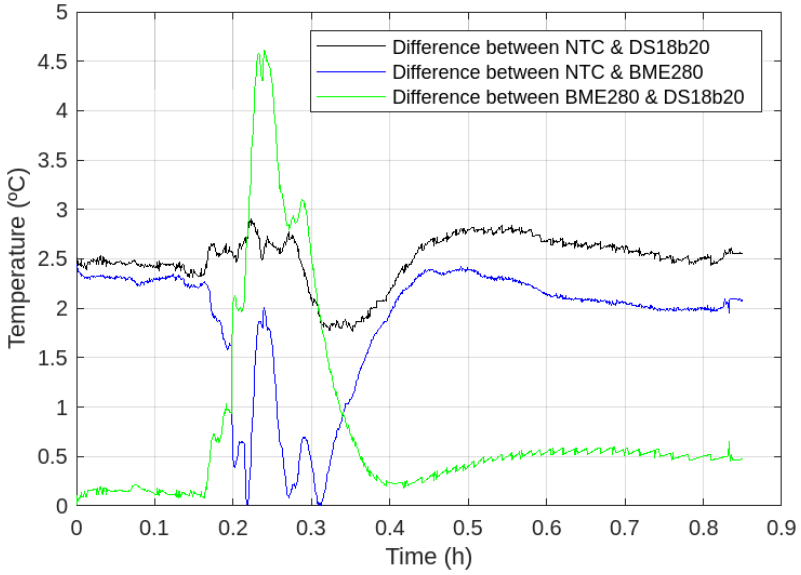
4.1.1 Sensor Validation

It is important to test the sensors to be certain of the response of each and to assess if there are any irregularities when it comes to the readings. Firstly it is analyzed how the sensors answer to being at room temperature. The graph 4.1a shows that, between both the sensors used for measuring the blood bags, DS18b20, and the thermistor, there's a small offset. The offset may be explained by an error in the characterization of the thermistor, another possibility is due to the ESP32 Analogic to Digital Converter (ADC) sensitivity to noise leading to large discrepancies in ADC readings. This offset can be more clear in the graph 4.1b, where it is possible to see that the difference between both maintains constant around a $\Delta T = 2$ ºC, except when there is a small change of temperature, where there is a faster response of the thermistor when compared to the DS18b20. Since the value of the DS18b20 is a digital one, we have a more precise value, although it is slower than the thermistor. Another aspect that should be taken into account is that around the 0.2h mark there is a change in temperature detected in all the three sensors. However the BME280 reacts differently than the others, and this could have an impact, when it comes to measuring the temperature changes.

Figure 4.2a and figure 4.2b present the measured temperatures during the second test and the difference measured between the different sensors, respectively. A total of a liter of refrigerated water, whose temperature wasn't directly measured, was put inside the box and the lid was closed. It can be seen, that the temperature doesn't change directly, because what is measured is air inside the box, which doesn't change instantly, and not the water. Firstly we can see that DS18b20 has a bigger reaction time than the others. So it takes more time to stabilize around the temperature of the air inside the box. Both the BME 280 and the thermistor reacted quickly to the change of temperature, but as it happened before, the thermistor had an offset of 3ºC after stabilizing compared to the DS18b20.

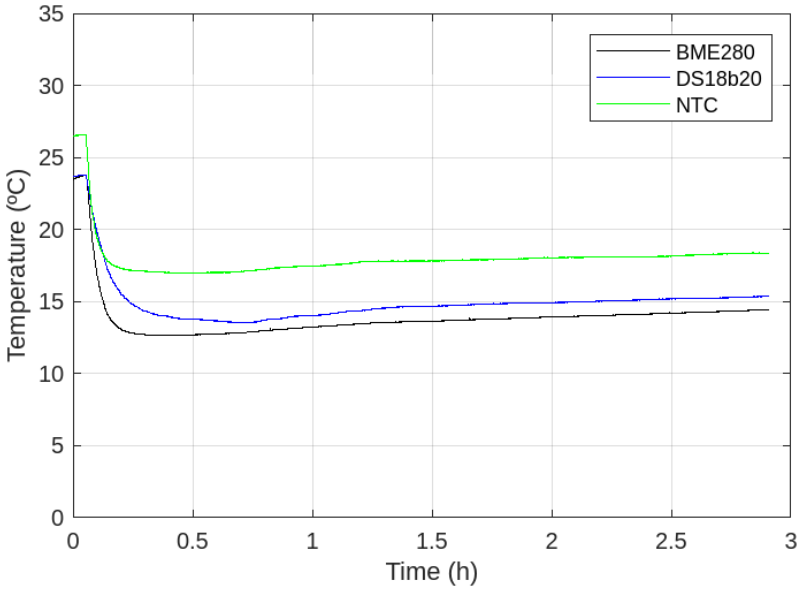


(a) Test at room temperature for sensor verification.

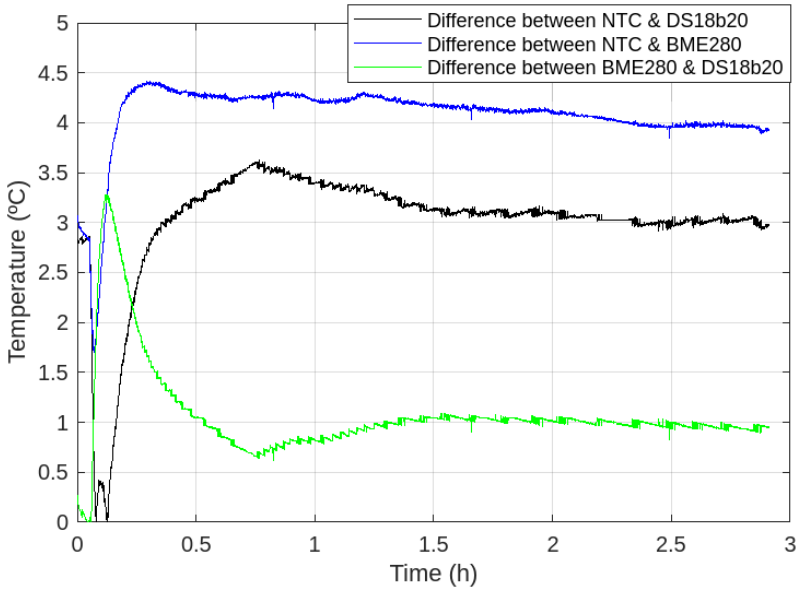


(b) Difference on measured temperature by comparing two sensors.

Figure 4.1: First sensor verification test



(a) Test 2 at room temperature for sensor verification, but with cold water bottles inside the box.



(b) Difference on measured temperature by comparing two sensors for test 2.

Figure 4.2: Second sensor verification test

The third test replicated exactly the second test, in order to confirm that the sensors react the same way for the same test. As it can be seen in figure 4.3 the DS18b20 records again a reaction time bigger, than the others. The thermistor maintains the offset this time around of 4ºC. All around the test the difference between the DS18b20 and the BME280, when the values are stable is around 1ºC, as it can be seen in the graphics 4.1b, 4.2b and 4.4. So it can be considered that this difference is constant for other tests. In the case of the thermistor the difference to any of the sensors doesn't stay constant, it varies between 2ºC and 4ºC.

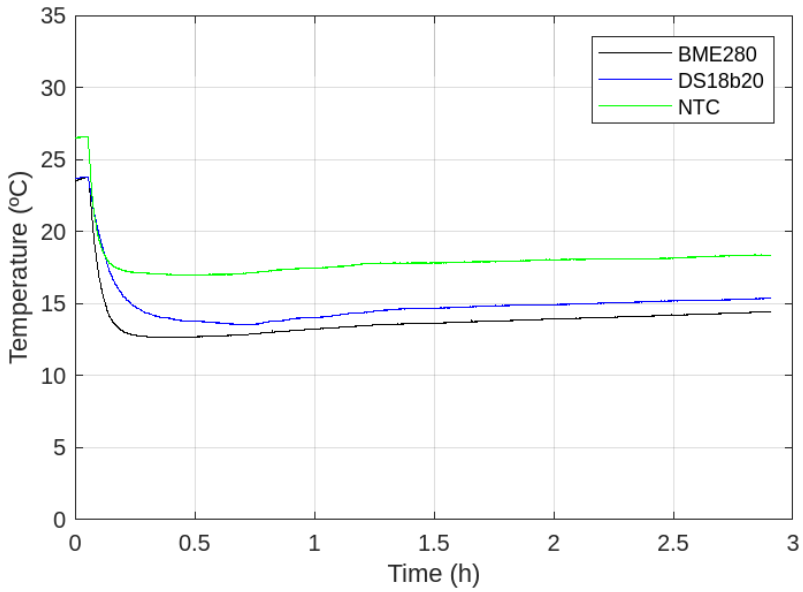


Figure 4.3: Test 3 at room temperature for sensor verification, but with cold water bottles inside the box.

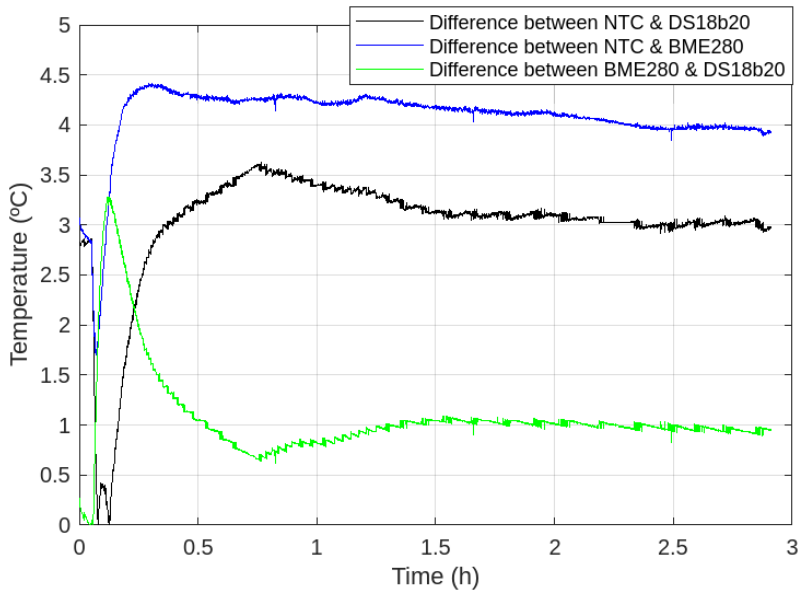


Figure 4.4: Difference on measured temperature by comparing two sensors for test 3.

It can be concluded, when comparing the BME280 and the DS18b20, that both sensors measure with the same precision. The use of the thermistor can be also discarded when analyzing the results since it shows a relative difference to the others and in this way, it can not be regarded as measuring the real temperature. Nevertheless, in the ongoing tests, it was still used, since it can be used to measure the reaction time of the changing dummy blood temperature.

4.1.2 Model Validation

After ending the tests of the sensor, the EPS box tests were done. Since the refrigerator, that was used, was of domestic use, the intended temperature of 4ºC couldn't be achieved. Therefore the first test was done with the initial temperature of 7ºC, which is still within the acceptable temperature range for blood. In this way a challenging situation was created, as the final objective was to compare the tests to the simulation previously elaborated. In order to compare the model to experimental values, the simulation was redone at a starting temperature of 7ºC. As displayed in figure 4.5, there is at first a descent in the temperature, that can be connected with the placement of the bags inside the box. After inserting the box inside the chamber it can be shown a quick step in temperature on the sensor measuring the inside air, the BME 280. And the bags inside the box start slowly getting warmer. As it can be seen after around 4h the temperature of the bags rises to 14.5ºC, making it a total difference of 7.5ºC. We can also fit the points since entering the chamber to the polynomial equation 4.1.2.

$$T(t) = -0.06t^2 + 2.3t + 6.48$$

Since the previous simulations were made for the initial temperature of 4ºC, it was then repeated to compare to the new starting temperature. As it can be seen in figure 4.6 the temperature around the 4h mark in the simulation is higher, finishing at around 18.6ºC.

$$T(t) = -0.189t^2 + 3.659t + 7.01$$

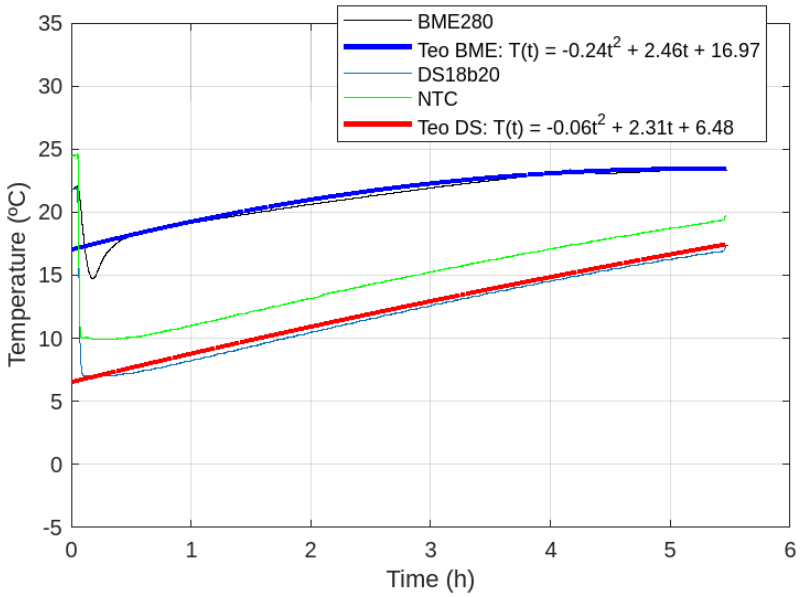


Figure 4.5: First test done in the chamber without PCM.

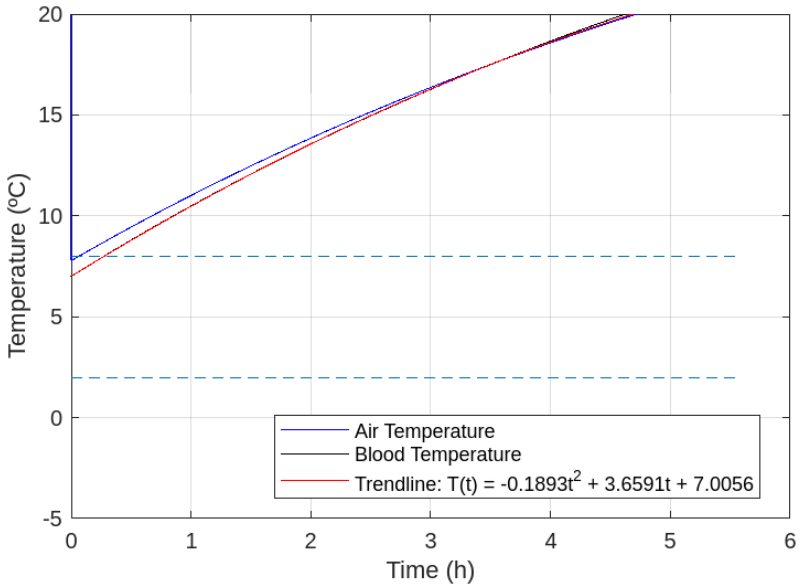


Figure 4.6: Simulation of the model at a start temperature of 7ºC without PCM.

In the second test without PCM, a way to reduce the temperature of the bags to around the desired temperature was tested. Here the bags were frozen during the night and let unfreeze. Before putting the bags inside the box they were still completely unfrozen, even though no block of ice was to be seen. This event showed at later analysis, that the temperature was still below zero. In figure 4.7, it is possible to see a first fall in temperature, where it was checked the temperature, since it still had blocks of ice in it, followed by a waiting time at a lower temperature, that is the time of packing the bags and checking the temperature. Afterward, there is a spike in the temperature, which relates to taking the bags out of the box, with the objective of all the bags having

a similar unfreezing pattern. After the peak of temperature, we can conclude, that the decline in temperature shows the repacking of the blood bags in the box and installing the testing prototype inside of the chamber. The moment it enters the chamber can again be seen because of the growth of temperature in the BME280 temperature values. Since the bag was at temperatures below zero it is to be expected, that the water inside is in the process of phase changing. What makes it need more energy than compared to fluid state to gain 1 ºC. So this process can not be compared to simulations, but it still shows, that during the whole 4h of test in the chamber, it still didn't achieve substantial growth in temperature, it only grew around 3 ºC.

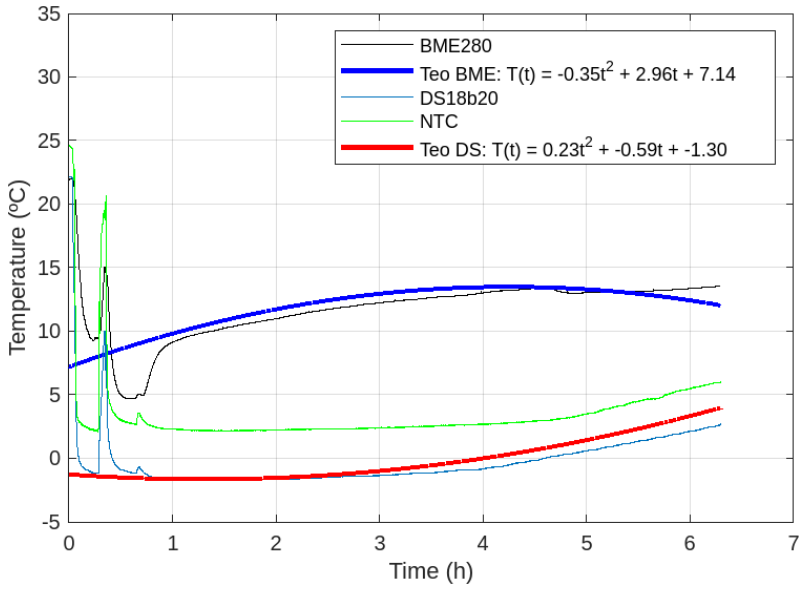


Figure 4.7: Second test done in the chamber without PCM.

The first test of the second round started again with frozen bags, and this time it was attempted to obtain the desired temperature. It was tested the same method of freezing as in the second test without PCM, but using a quick unfreezing method. However, the initial temperature that was achieved was again at 7ºC. During the process of cooling the bags, the PCM had to be frozen in order to use the component of absorbing more heat, while the material changes phase, therefore the PCM had to be placed in the freezer for at least 10h.

Following this step, the bags were placed inside the box. Figure 4.8 once again illustrates a rapid decrease in temperature, followed by a slight temperature increase after the bags are introduced into the chamber. However, in this particular test, a deviation from the typical pattern observed in previous tests becomes apparent. A technical error occurred that led to the malfunctioning of the BME280 and had a possible impact on the whole system. Figure 4.8 represents the measures values of BME280 until 3.5 hours, because after this point the values obtained were not acceptable, as they oscillated between 0 and 100. This oscillation happened until around the 4^{th} hour, when it stopped completely to deliver any values to the ESP32. Comparing the readings of

the BME280 sensor from the point at which it ceased functioning entirely to the point where there is an alteration in the temperature trend observed by the other two sensors, it becomes evident that these events coincide in time. This suggests that the new temperature trend is linked to the sensor issue rather than a natural increase in the heating rate of the environment. These values can also be related to the fact that the PCM completely unfroze and so the intake of heat by the blood bags was higher. The evolution of the temperature of the blood bags can be described by equation 4.1.2.

$$T(t) = -0.01t^2 + 1.00t + 6.54$$

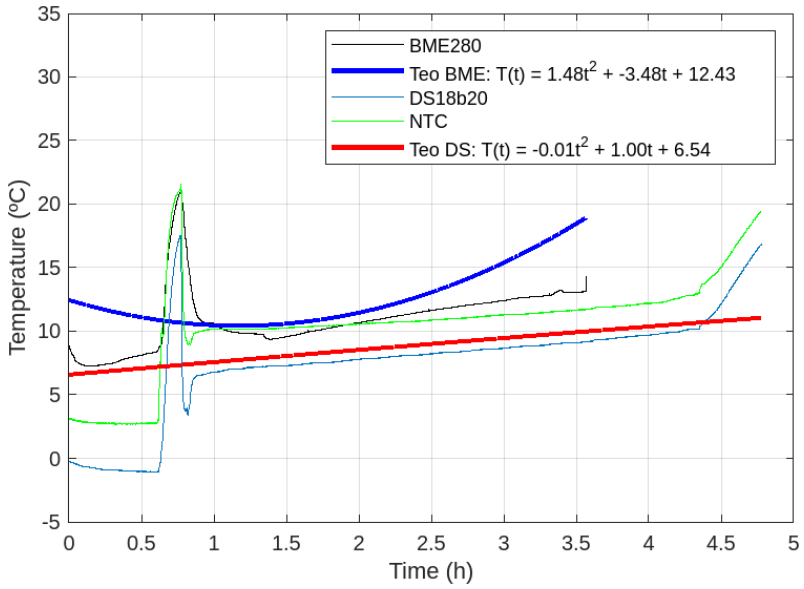


Figure 4.8: First test done in the chamber with PCM.

Although much can't be concluded from this test in light of these unforeseen errors, one thing can be compared to the test without PCM. After 3 hours of the test, during the test without PCM, the bag temperature had grown from an initial temperature of 7ºC to around 13ºC. However, during the test with PCM, it evolves solely from the initial temperature of 7ºC to 10ºC. This can be seen as a significant upgrade since the temperature difference was cut in half.

The fourth and final was again started at a temperature of 7ºC, since the method of freezing was too unreliable for achieving the temperature intended, the bags were left in a refrigerator for more than 24h to achieve again the temperature of 7ºC. At the same time, the PCM was also left in the freezer compute with the specifications written in the container of having to freeze for at least 10h. As it can seen figure 4.9, the start of the test follows the same structure of the others. when it arrives at the lowest temperature of 7ºC it is entered in the climatic chamber for the test. Comparing with the test of 1 PCM, it is possible to assess, that both follow a similar increase of temperature all around the test. As it can be seen the occurrence of an increasing heating rate

doesn't occur during the 4h of test, as it occurred in the first test. At the end of the recorded values, there's a small spike in temperature, however it isn't enough to conclude if that is a change like it occurred in the first test with PCM or it is a small spike more like the one occurring in figure 4.7, when the water inside bag is passing through zero, assuming this is the changing phase temperature even with a saline concentration of 0.9%. When comparing the three curves of the measure tempearature of the DS18b20, it looks like the later theory seem more plausible, since we can also detect a small decrease in the temperature of the air inside the box, referring to be phase change, where heat is extracted from the surroundings to PCM. In this case the blood temperature evolution can be described by:

$$T(t) = -0.11t^2 + 0.13t + 7.07$$

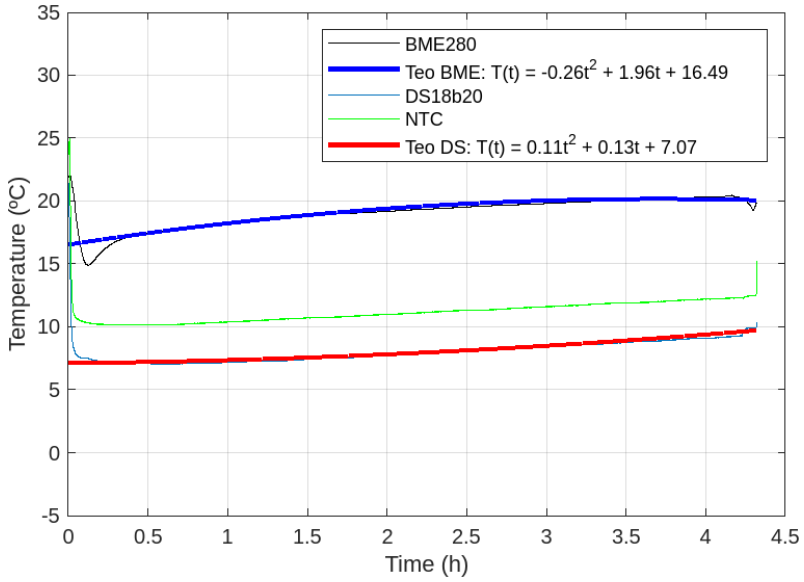


Figure 4.9: Second test done in the chamber with PCM.

After analyzing the results of the temperatures measured we can establish a comparison to the simulations and to what was estimated earlier, since the test couldn't be conducted at expected starting temperature of 4ºC. First it is compared the equations that could be fitted to the curves of the experimental values. Comparing both graphs it can be seen, that the evolution during the two is a bit different. The one thing that can be noted is that after four hours they both have a change on the slope of its blood temperature. In the simulation it can be seen, that this change in the temperature change rate, is due to the fact, that the PCM liquidizes. It is also concluded, that if it can be secured, that the PCM stays frozen until the end of mission, that the blood will be safe within the intended temperature range, when it comes out of the refrigerator at 4ºC. It can be now compared to the simulation a starting temperature at 7ºC. Figure 4.10 shows a similar inclination, that it shown in the experimental tests. In this case the blood follows the subsequent equations

$$T(t) = -0.0121t^2 + 0.1604t + 7.0098$$

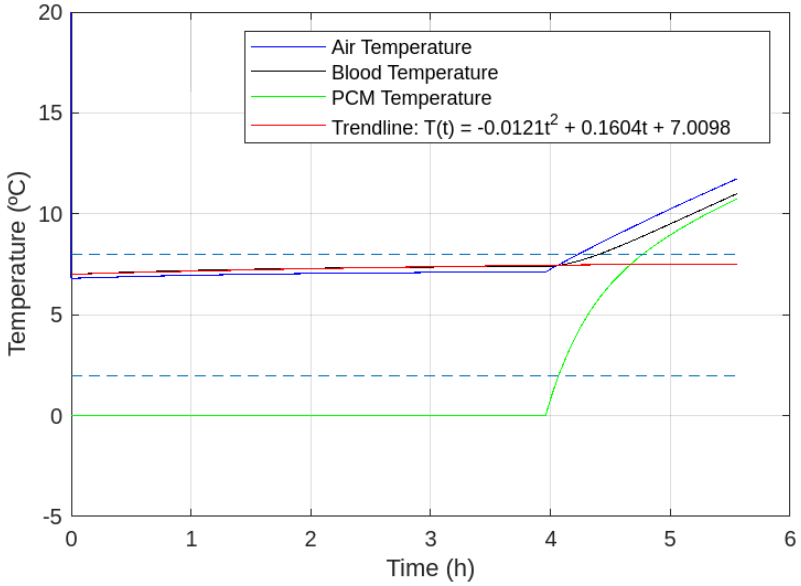


Figure 4.10: Simulation of the model at a start temperature of 7ºC.

In the cases of the tests without PCM it is possible to be concluded, that there is a big disparity between the model and practical test. As for the test with PCM, they have a curve more similar to the model, however, they still don't describe the same curve. Another point to be noted in the comparison of the test results to the simulation is that the air temperature by the simulation, changes directly to the same temperature of the blood, as soon as the later starts. However, during the test, the air temperature measured was always much higher and didn't describe the same pattern as the blood temperature. One possible explanation for the unexpected temperature variations in the box could be its small size, which limits natural airflow. This limitation can result in different temperatures at various points inside the container. Essentially, cold air tends to sink to the bottom, while warmer air stays at the top, creating a layering effect within the box.

Although the humidity doesn't have much influence on the transport of blood, it is important to evaluate during the whole mission since it can cause degradation of material in case of transporting cardboard packages or in cases of very high levels of humidity can even have a negative influence on the electronics.As it is presented in figure 4.11 , it can be shown, that the biggest fluctuations of the humidity levels are when packing the bags inside of the box. It is possible to conclude that the levels of the first test with PCM are elevated, when weighing against the others, on account of being part of the sensor inside of water, when it was opened. In the other tests we can see that they are stable around a humidity of 55%, being that the ones without the PCM are a bit higher, around 60%, and the second test with PCM has a lower humidity, around of 50%. Another point to note in this graph is that the curve of the second test with PCM, red, has a spike on the humidity values at the end, which can be related to the increment of temperature seen before.

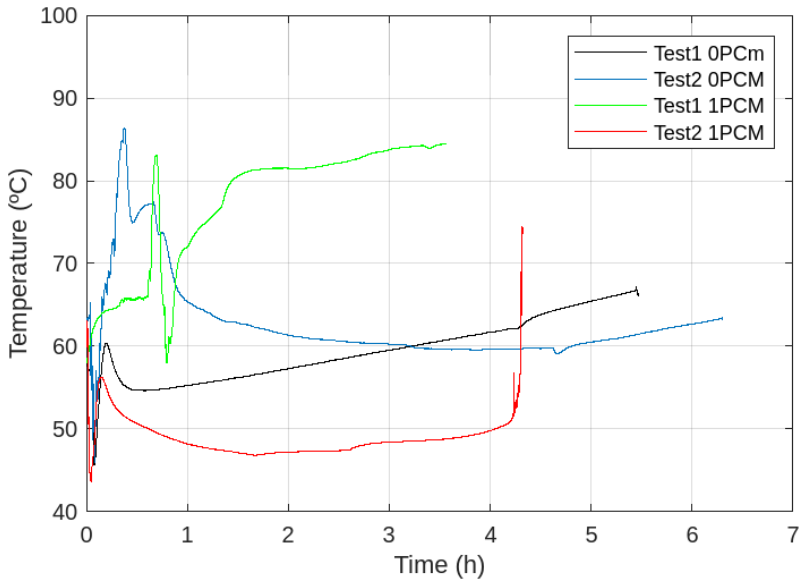


Figure 4.11: Humidity development through the four different tests.

To ensure a balanced interpretation of the results, it is imperative to discuss the study's limitations. One such limitation pertains to the fact, that the dynamic model only takes into consideration the use of convective and conductive heat transfer. When comparing to other studies, it is shown, that the same thought process was implemented[40, 58, 1]. For furthers studies it could be implemented in the dynamic model the use of heat transfer through radiation. Reviewing both the simulation and the test, this contemplation could explain the difference from one to the other. Creating that way a more perfect way to predict the quantity of PCM needed for different applications. It could be considered in the dynamic model the impact of the Kevlar layer on the heat transfer between the box an ambient. It wasn't considered, on account of it primary function being the importance of maintaining the structure in case of an impact. When accessing the model with another layer of insulation due to the fact of the Kevlar, it would be a possibility the need for PCM even lower and so achieving more room to transport blood or other medical necessities.
The use of thermoelectric cooling was discarded , in light of the volume need for the heat sink and the fans to ensure the circulation of the cooled air and at the same time because it is need for a lot of energy. This excess of energy would be need to be supplied by extra batteries, where additional weight would be accounted for. The need for these batteries could be disregarded, if the aircraft would supply this energy. In this case the use of a Peltier module could be considered, however it must be noted that this would also impact the flight range of the UAV.
Another interesting pondering to be made is the use of payload boxes with a bigger volume. This could not only allow the transport of larger temperature sensitive goods as also in a higher quantity. Due to the increase in volume, the intake on heat by the box would also be higher and therefore the heat intake by the blood bags. Creating this way the need the need to firstly use more sensors between the blood bags, so it could be better understood the evolution of the temperature along the mission.

At the same time the use of four boxes, can also be used for transporting goods to more than one final destination, and not as it happens nowadays, where goods are only transported to one final place, due to its short flight range. There's a study, where it is shown, the transport of Biologic Samples with UAVs, between four different institutions. It evaluates how the use of UAvs would show a improvement on time per delivery, if a transport mission had multiple stops, when comparing to ground transport and even to the use of UAVs in a direct model.It is accessed that the daily payload needed of the Oslo University Hospital is planned between approximately 2.2–2.8 kg with estimated volume in drone of 3–3.5 L[45]. The size of the transport box, is accordingly to a selection of four boxes per missions instead of two bigger boxes.

4.2 Payload Box Conceptual Design

After having analyzed the EPS box and the chosen cooling method, it is possible to determine a way to create the payload box, weighing the assumptions made previously and estimating a future process to complete this specialized container.
As it demonstrates in chapter 4, a passive cooling system is more than sufficient to create the planned temperature for maintaining the delivered contents at its preset transport requisites.

The creation of this container isn't only involved with the thermal capacities and monitoring abilities. It must have a sturdy structure as its basis, in order to prevent any damaging events, that could compromise the goods consequently the mission. As seen in chapter 3 the box has already decided to be done with a structure of Kevlar, which give sturdiness and support against impacts and even in a extreme case, if someone is trying to break into it. Continuing with the list of components it is important to implement in order to make this prototype a valid product to be used are a locking system, in order to prevent that any person can access its contents. In light of the box can't be physically supervised at all times, this system must play the role normally executed by the person transporting products. The locking mechanism was thought as being actuate by normally closed solenoid. To open the system it should, be used for a combination code. It should be in a locked position, so in case of a malfunction because of lack of power, the box can't be opened.
To perform this function it is proposed the use of a DC Small electric control lock.[71] This should be connected with a unlocking system. The conceived solution for this purpose is a control reader with the possible unlocking through PIN or RFID.[72]

An other element important to be implemented, is the need for a GPS-module. Although during the mission the location of the payload box, can be associated with the location of the UAV. Nevertheless in cases of a malfunction of aircraft, the box has to be found, with aim of retrieving the precious goods. With this goal in mind, it is planned to implement a GPS-module in the box. The module in question is a Quectel L86-M33, which can be implemented with the micro-controller, ESP32, previously chosen. [73]

Another system that must be implemented with the boxes, is its communication with the ground station. This communication must be integrated, since there should be a surveillance of the situation of the goods, which normally can be instantly evaluated by the transporter. Creating this system is necessary also for cases, where there is a sudden malfunction of the system and it is detected, that the transported contents have been subjected to conditions not acceptable, and a new order can be created and preventing that the package has to arrive to be evaluated. Since the skin of the UAV will be presumably made of a carbon composite, communicating directly from the cargo space to the ground station is almost impossible. Therefore it is planned that the aircraft has antenna outside of the aircraft connected to a micro-controller inside. the micro-controller is then connected to the boxes through a USB cable. Given that the cargo space can have a total of 4 payload boxes, it was assumed that there shouldn't be an antenna for each box, instead the

cable coming from the boxes should be connected to a switch, which afterwards is linked to the micro-controller.

The last component thought to be integrated is a display showing the measured values inside the box, for moments where the box is being transported by a person. Considering that at the time of arrival the person removing, can check directly, how the contents are. The purposed display is a Adafruit 358, this was selected since the team in CEiiA has already been studying for different projects. [74]

With the different component evaluated and projected, it is possible to create a possible configuration of the box. Figure 4.12 show the proposed 3D model. And in figure 4.13 exploded it is shown, how the different components are integrated in the model.

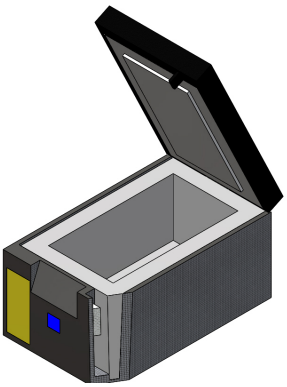


Figure 4.12: Conceptual design of the box with the different components.

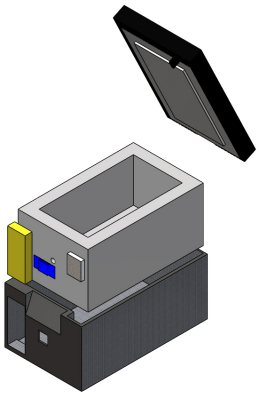


Figure 4.13: Exploded view of 3d model.

Lastly it was made a small prevision of the cost of the box. Firstly the costs that can be directly calculated were listed, seeing that they're related to components and materials that have to be bought. These prices are displayed in table 4.1. Which gives a total 132.70€. In the creation

of the structure should be considered not only the materials, but also the process of creating. The material needed are the fibers, the resin as also the hardener. For the fiber it would be need around 2 m^2, since the area of the box is of 0.328m^2, which would come to a 1 m^2 for 3 layers of fiber and assuming that 50% of the material would be discarded. it means a total of 1.5 m^2 are needed. This would come to a total of 51.74 €.[53]. For the resin and hardener it would be around 1kg, which comes to cost of 27.58€.[75]. The process is a bit more difficult to estimate, since it depends from factory salary and time need. But not assuming the process of constructing the material, it would come to a total of 212.02€

Table 4.1: Cost of the different components

Component	**Cost**
ESP32	9.00 € [76]
BME 280	23.90 € [77]
DS18b20	3.57 € [78]
GPS module	11.28 €[73]
Display	17.96 €[74]
EPS box	8.99 € A
PCM	19.90 € [79]
Control lock	12.79 €[71]
Code panel	25.31 € [72]
Total	132.70€

Chapter 5

Conclusions and Future Works

5.1 Conclusions

The results of this work, distinguished by the creation of a payload box designed for UAV transport, is proof of the ability of creativity to solve pressing logistical problems. The choice to rely on PCMs rather than an active cooling system, given the limitations of smaller-scale missions, reduced weight, while also reducing the amount of space needed in the payload box, thus increasing its efficiency. This payload box was designed with the primary goal of providing a dependable and flexible solution for the safe delivery of temperature-sensitive cargo by UAVs. Recognizing the surging demand for precise, efficient delivery of medical supplies, perishable goods, and scientific instruments, the box was designed to accomplish the mission established by the team in CEiiA.

The study started with an analysis of the state of the art, where it can be checked, that even though some studies have been made, in the search of creating a container to transport medical goods, this boxes functions hasn't as its primary function the delivery of goods by UAVs. Given the constraints of UAVs, like the weight, as also the reduced volume. In the study are presented two possible ways of accomplishing the cooling needs of temperature-sensitive objects.

The first option is the use of an active system, which has the advantage of, having the capability of responding to any changes in temperature, that aren't expected during the mission. For this it was thought of a Peltier module, considering its small and light nature. Although the central technology has this kind of nature, it must be accompanied by other components, in order to respond to the necessities at hand. Firstly a need for a fan to better remove heat through its cold side, since the area of transfer is rather small. The other very important component is the need for large batteries since this method has a very small COP.

The second proposed idea was to opt for a passive PCM system. Seeing that it significantly reduces the weight burden compared to an active cooling system, allowing for more efficient UAV operation and increased payload capacity. This also prevents the use of electricity on board, and

so removing the need for large batteries on any other moving mechanism.

Having presented both of the systems picked as possible solutions for the box being developed. Since testing both systems would be very costly, some simulations were on the before hand to better choose, the route to follow. As seen in chapter 3, the simulations showed, that the use of a simpler system, the passive cooling system, was for the whole trip planned enough and could that way be prevented the use of a more costly and more space-demanding system.

The use of PCMs ensures a reliable and consistent temperature control mechanism throughout the cargo box. These materials undergo phase transitions at precisely defined temperatures, guaranteeing that sensitive cargo remains within the desired temperature range during transit. It was possible to visualize this in chapter 4.

The payload box's design philosophy maintained a central key point as real-time temperature monitoring, cargo modularity, durability, and environmental responsibility. Creating a container to respond to all of these functions was rather challenging, but in the end, it showed its rewards, proving that the use of UAVs can start to be more utilized in healthcare and can also prove to be the first step in supporting the relationship.

In resume, the creation of this temperature-capable payload box for UAVs is a testament to human creativity and potential to find innovative answers to pressing problems. It serves as evidence of how UAV technology is constantly changing and provides a window into the seemingly endless possibilities. We envisage a future when the safe and effective delivery of temperature-sensitive goods becomes a practical reality, transforming businesses and bettering lives on a worldwide scale while improving and expanding the capabilities of this payload box.

5.2 Future Works

From current work it was understood that further research could be undertaken and some directions could be pursued. Working to achieve an efficient payload box to transport by UAV, is what this work was set out to do. Even though it was centralized in the areas of thermal efficiency, it was presented few of the mechanisms need to create such a container.

The first proposed theme that should be worked on is the further development of the communications systems, since this function is rather vital for the transport, and because it certifies a possibility of real-time monitoring the contents of the box. This would give hospital, blood bank and others a higher security in transporting their goods through UAVs.

The other subject selected to be improved, is the choice on material for the skin of the box. In this case the use of aramid composite is a viable solution, however it could be done in a less expensive manner. Since the security of the transported goods, are mostly guaranteed by the payload boxes being transported inside the cargo space, one could even assume, that the use of materials like the aramid composites, could be converted to more accessible material. Another possible improvement that can be looked upon is the the usage of cork, as possible isolation material.

There is a viable channel for communicating the findings of this research in the future. It is possible to consider publishing the collected results in respected publications in the area. Well-known periodicals such as MDPI and the Air Medical Journal are excellent choices. This type of distribution would help the broader academic community comprehend UAV technology in healthcare logistics, perhaps paving the way for additional improvements in this crucial subject.

References

[1] L. Huang and U. Piontek, "Improving Performance of Cold-Chain Insulated Container with Phase Change Material: An Experimental Investigation," *Applied Sciences*, vol. 7, no. 12, 2017. [Online]. Available: https://www.mdpi.com/2076-3417/7/12/1288

[2] M. E. tools, "Overall heat transfer coefficient calculation." [Online]. Available: https://myengineeringtools.com/Thermodynamics/Overall_Heat_Transfer_Coefficient.html

[3] F. P. Incropera, D. P. DeWitt, T. L. Bergman, A. S. Lavine *et al.*, *Fundamentals of heat and mass transfer*. Wiley New York, 1996, vol. 6.

[4] ARANER, "Compression refrigeration cycle, step by step." [Online]. Available: https://www.araner.com/blog/vapor-compression-refrigeration-cycle

[5] I. Banerjee, "Vapor compression refrigeration cycle: What, diagram, efficiency, working, steps." [Online]. Available: https://lambdageeks.com/vapor-compression-refrigeration-cycle/

[6] D. Zhao and G. Tan, "A review of thermoelectric cooling: Materials, modeling and applications," *Applied Thermal Engineering*, vol. 66, no. 1, pp. 15–24, 2014. [Online]. Available: https://www.sciencedirect.com/science/article/pii/S1359431114000854

[7] B. Nie, J. Chen, Z. Du, Y. Li, T. Zhang, L. Cong, B. Zou, and Y. Ding, "Thermal performance enhancement of a phase change material (PCM) based portable box for cold chain applications," *Journal of Energy Storage*, vol. 40, p. 102707, 2021. [Online]. Available: https://www.sciencedirect.com/science/article/pii/S2352152X21004424

[8] J. Clancy, C. Karish, M. Roddy, J. J. Sicilia, and M. T. Bigham, "Temperature-sensitive medications in interfacility transport: The ice pack myth," *Air Medical Journal*, vol. 36, no. 6, pp. 302–306, 2017. [Online]. Available: https://www.sciencedirect.com/science/article/pii/S1067991X17300378

[9] N. B. A. Australia, "Module 1: Managing blood and blood product transfers- implementation." [Online]. Available: https://www.blood.gov.au/inv-mgt-guideline-module-1-implementation

[10] C. K. Gilmore, M. Chaykowsky, and B. Thomas, "Autonomous unmanned aerial vehicles for blood delivery," *RAND Corporation, Santa Monica, California*, 2019. [Online]. Available: https://www.rand.org/content/dam/rand/pubs/research_reports/RR3000/RR3047/RAND_RR3047.pdf

[11] ISO, "Iso 3826-1:2019(en), plastics collapsible containers for human blood and blood components — part 1: Conventional containers," 2019. [Online]. Available: https://infostore.saiglobal.com/preview/557771673254.pdf?sku=861074_SAIG_NSAI_NSAI_2782561

[12] K.-W. Chen, M.-R. Xie, Y.-M. Chen, T.-T. Chu, and Y.-B. Lin, "DroneTalk: An Internet-of-Things-Based Drone System for Last-Mile Drone Delivery," *IEEE Transactions on Intelligent Transportation Systems*, vol. 23, no. 9, pp. 15 204–15 217, 2022. [Online]. Available: https://www.scopus.com/inward/record.uri?eid=2-s2.0-85124244447&doi=10.1109%2fTITS.2021.3138432&partnerID=40&md5=0ac28c3dda3d4ae9332a53179cee5e1c

[13] S. Mohd, K. Gan, and A. Ariffin, "Development of Medical Drone for Blood Product Delivery: A Technical Assessment," *International journal of online and biomedical engineering*, vol. 17, no. 9, pp. 183–196, 2021. [Online]. Available: https://www.scopus.com/inward/record.uri?eid=2-s2.0-85119403652&doi=10.3991%2fijoe.v17i09.24399&partnerID=40&md5=ac03542057a58c584a23072199db17e3

[14] S. M. Adarsh Gangwal, Akshika Jain, "Blood delivery by drones: A case study on zipline," *International Journal of Innovative Research in Science, Engineering and Technology*, vol. 8, no. 1, pp. 8760–8766, 2019. [Online]. Available: http://www.ijirset.com/upload/2019/august/63_Blood.PDF

[15] G. Ling and N. Draghic, "Aerial drones for blood delivery," *Transfusion*, vol. 59, no. S2, pp. 1608–1611, 2019. [Online]. Available: https://onlinelibrary.wiley.com/doi/abs/10.1111/trf.15195

[16] CEiiA, "Ceiia - about us," 2023. [Online]. Available: https://www.ceiia.com/history

[17] ——, "Embraer kc-390," 2023. [Online]. Available: https://www.ceiia.com/aero-embraer

[18] hidrográfico, "Programa/projeto: Troante," 2023. [Online]. Available: https://www.hidrografico.pt/iprojeto/12

[19] CEiiA, "Magellan," 2023. [Online]. Available: https://www.ceiia.com/innovation-magellan

[20] ——, "Adam-automação avançada para manufactura," 2023. [Online]. Available: https://introsys.eu/adam/

[21] IATA, "Dangerous goods regulations," vol. 54, p. 954, 2019. [Online]. Available: https://agashirinov.files.wordpress.com/2015/10/ekp000017565.pdf

[22] K. Yakushiji, F. Yakushiji, T. Yokochi, M. Murata, M. Nakahara, N. Hiroi, and H. Fujita, "Quality control of red blood cell solutions for transfusion transported via drone flight to a remote island," *Drones*, vol. 5, no. 3, 2021, type: Article. [Online]. Available: https://www.scopus.com/inward/record.uri?eid=2-s2.0-85115298770&doi=10.3390%2fdrones5030096&partnerID=40&md5=a9eee7b74f3fa137893631aae49fb91c

[23] T. Wallace, "Transportation of Temperature-sensitive Medications in an Air Medical Setting," *Air Medical Journal*, vol. 38, no. 3, pp. 165–167, 2019. [Online]. Available: https://www.scopus.com/inward/record.uri?eid=2-s2.0-85061127824&doi=10.1016%2fj.amj.2019.01.005&partnerID=40&md5=f35f8a7ec2dd845a41e71954975dc895

[24] J.-J. U. K. U. B. Transfusion and T. T. S. P. A. Committee, "Guidelines for the blood transfusion services in the uk," 2014. [Online]. Available: https://www.transfusionguidelines.org/red-book

[25] N. Teams and T. centres, "Small organ transport boxes – instructions for use." [Online]. Available: https://nhsbtdbe.blob.core.windows.net/umbraco-assets-corp/4382/organ_boxes_instructions_for_use.pdf

[26] J. Scalea, S. Restaino, M. Scassero, G. Blankenship, S. Bartlett, and N. Wereley, "An initial investigation of unmanned aircraft systems (uas) and real-time organ status measurement for transporting human organs," *IEEE Journal of Translational Engineering in Health and Medicine*, vol. PP, pp. 1–1, 11 2018.

[27] D. Amicone, A. Cannas, A. Marci, and G. Tortora, "A smart capsule equipped with artificial intelligence for autonomous delivery of medical material through drones," *Applied Sciences*, vol. 11, no. 17, 2021. [Online]. Available: https://www.mdpi.com/2076-3417/11/17/7976

[28] K. Selleng, M. Baschin, B. Henkel, G. Jenichen, K.-C. Thies, M. Rudolph, F. Reifferscheid, J. Braun, M. Hannich, T. Winter, K. Hahnenkamp, and A. Greinacher, "Blood Product Supply for a Helicopter Emergency Medical Service," *Transfusion Medicine and Hemotherapy*, vol. 48, no. 6, pp. 332–341, 2021. [Online]. Available: https://www.scopus.com/inward/record.uri?eid=2-s2.0-85118145526&doi=10.1159%2f000519825&partnerID=40&md5=db15e81acdbecb707f73eb973a9bbacd

[29] A. Moreno, I. Angulo, H. Landaluce, and A. Perallos, "Easily deployable solution based on wireless technologies for traceability of pharmaceutical drugs," in *IEEE Int. Conf. RFID-Technol. Appl., RFID-TA*, 2011, pp. 252–258, journal Abbreviation: IEEE Int. Conf. RFID-Technol. Appl., RFID-TA. [Online]. Available: https://www.scopus.com/inward/record.uri?eid=2-s2.0-82155188786&doi=10.1109%2fRFID-TA.2011.6068646&partnerID=40&md5=5583aa18528823ad5e3f711ad1c45ea4

[30] J. Taylor, "Recommendations on the control and monitoring of storage and transportation temperatures of medicinal products," p. 11, 2014. [Online]. Available: https://webarchive.nationalarchives.gov.uk/ukgwa/20141205150130/http:/www.mhra.gov.uk/home/groups/comms-ic/documents/publication/con007569.pdf

[31] C. Ng, Y. Lean, S. Yeoh, Q. Lean, K. Lee, A. Suleiman, K. Liew, Y. Kassab, Y. Al-Worafi, and L. Ming, "Cold chain time-and temperature-controlled transport of vaccines: A simulated experimental study," *Clinical and Experimental Vaccine Research*, vol. 9, no. 1, pp. 8–14, 2020. [Online]. Available: https://www.scopus.com/inward/record.uri?eid=2-s2.0-85080142982&doi=10.7774%2fcevr.2020.9.1.8&partnerID=40&md5=bf1079af08532f75a6d35ff2039bf975

[32] V. Pereira, "Falta sangue em lisboa e na região sul. hospitais não têm capacidade de resposta a todas as situações de emergência," 2023. [Online]. Available: https://cnnportugal.iol.pt/videos/falta-sangue-em-lisboa-e-na-regiao-sul-hospitais-nao-tem-capacidade-de-resposta-a-todas-as-situacoes-de-6418adc70cf2dce741b0aa97

[33] S. Sarkar, K. Akshatha, A. Saurabh, B. Samanvitha, and M. Sarwar, "IoT Enabled Cold Supply Chain Monitoring System," in *2022 IEEE 3rd Global Conference for Advancement in Technology, GCAT 2022*, 2022. [Online]. Available: https://www.scopus.com/inward/record.uri?eid=2-s2.0-85145441136&doi=10.1109%2fGCAT55367.2022.9972137&partnerID=40&md5=404b1a129b45d2d6889588d29aa2723f

[34] A. Oakey, T. Waters, W. Zhu, P. G. Royall, T. Cherrett, P. Courtney, D. Majoe, and N. Jelev, "Quantifying the effects of vibration on medicines in transit caused by fixed-wing and multi-copter drones," *Drones*, vol. 5, no. 1, 2021. [Online]. Available: https://www.mdpi.com/2504-446X/5/1/22

[35] K. A. Johannessen, N. K. S. Wear, K. Toska, M. Hansbø, J. P. Berg, and E. Fosse, "Pathologic blood samples tolerate exposure to vibration and high turbulence in simulated drone flights, but plasma samples should be centrifuged after flight," *IEEE Journal of Translational Engineering in Health and Medicine*, vol. 9, pp. 1–10, 2021.

[36] P. MINISTÉRIO DA SAÚDE, "Decreto-lei n.º 267/2007," 2007. [Online]. Available: http://www.ipst.pt/files/IPST/LEGISLACAO/Legislacao_Nacional/Legislacao_Sangue/Decreto_Lei_267_2007.pdf

[37] P. N. A. o. M. Infarmed and H. Products, "Deliberação n.º 77-a/cd/2021." [Online]. Available: https://www.infarmed.pt/documents/15786/17838/11048532.PDF/4bde6495-b33d-4311-8302-784be4a65971

[38] UNICEF Supply Division, "Cold chain support package," 2021. [Online]. Available: https://www.unicef.org/supply/media/6391/file/VaccineCarrierColdBox-guideline-2021.pdf

[39] M. of Health and I. Family Welfare, "Division of blood transfusion services." [Online]. Available: http://nbtc.naco.gov.in/assets/resources/training/8.pdf

[40] L. Damiani, R. Revetria, E. Morra, and P. Giribone, "A Smart Box for Blood Bags Transport : Simulation Model of the Cooling Autonomy Control System," *Advances in Science, Technology and Engineering Systems Journal*, vol. 5, no. 1, pp. 249–255, 2020.

[41] H. Smith, H. Doughty, J. Bishop, M. Herbert, and M. Nash, "Temperature mapping in an air ambulance helicopter: Implications for the delivery of prehospital transfusion," *Transfusion*, vol. 61, no. S1, pp. S206–S213, 2021. [Online]. Available: https://www.scopus.com/inward/record.uri?eid=2-s2.0-85110396499&doi=10.1111%2ftrf.16517&partnerID=40&md5=eff4a5f3109a3a0a28e30e9c3fb75d84

[42] V. Homier, D. Brouard, M. Nolan, M.-A. Roy, P. Pelletier, M. McDonald, F. de Champlain, E. Khalil, F. Grou-Boileau, and R. Fleet, "Drone versus ground delivery of simulated blood products to an urban trauma center: The Montreal Medi-Drone pilot study," *Journal of Trauma and Acute Care Surgery*, vol. 90, no. 3, 2021. [Online]. Available: https://journals.lww.com/jtrauma/Fulltext/2021/03000/Drone_versus_ground_delivery_of_simulated_blood.15.aspx

[43] T. Amukele, P. Ness, A. Tobian, J. Boyd, and J. Street, "Drone transportation of blood products," *Transfusion*, vol. 57, 11 2016.

[44] N. B. Roberts, E. Ager, T. Leith, I. Lott, M. Mason-Maready, T. Nix, A. Gottula, N. Hunt, and C. Brent, "Current summary of the evidence in drone-based emergency medical services care," *Resuscitation Plus*, vol. 13, p. 100347, 2023. [Online]. Available: https://www.sciencedirect.com/science/article/pii/S2666520422001473

[45] K. Johannessen, "A Conceptual Approach to Time Savings and Cost Competitiveness Assessments for Drone Transport of Biologic Samples with Unmanned Aerial Systems (Drones)," *Drones*, vol. 6, no. 3, 2022. [Online]. Available: https://www.scopus.com/inward/record.uri?eid=2-s2.0-85125787314&doi=10.3390%2fdrones6030062&partnerID=40&md5=be743163db80f0a005a43e3cd457bd2e

[46] A. Martin, R. Fharozi, and T. Lesmana, "Development of Portable Blood Carrier Box Employing Thermoelectric Module by Using Oil Palm Empty Fruit

Bunch Composites as Materials of Box," *Journal of Advanced Research in Fluid Mechanics and Thermal Sciences*, vol. 93, no. 2, pp. 50–60, 2022. [Online]. Available: https://www.scopus.com/inward/record.uri?eid=2-s2.0-85128826156&doi=10.37934%2farfmts.93.2.5060&partnerID=40&md5=1ccc3ba6569aef0ca7b1f1745eb4c72c

[47] S. Umchid, P. Samae, S. Sangkarak, and T. Wangkram, "Design and Development of a Temperature Controlled Blood Bank Transport Cooler," in *BMEiCON 2019 - 12th Biomedical Engineering International Conference*, 2019. [Online]. Available: https://www.scopus.com/inward/record.uri?eid=2-s2.0-85080081276&doi=10.1109%2fBMEiCON47515.2019.8990203&partnerID=40&md5=e2165e7c9af0de83832e851fadb3c922

[48] Windpact, "Crash cloud handles repeated impacts better than eps alone," 2021. [Online]. Available: https://windpact.com/crash-cloud-vs-polystyrene/

[49] S. A. Mirdehghan, "1 - fibrous polymeric composites," in *Engineered Polymeric Fibrous Materials*, ser. The Textile Institute Book Series, M. Latifi, Ed. Woodhead Publishing, 2021, pp. 1–58. [Online]. Available: https://www.sciencedirect.com/science/article/pii/B9780128243817000123

[50] D. plate, "What is the difference between carbon fiber and kevlar?" [Online]. Available: https://dragonplate.com/difference-between-kevlar-and-carbon-fiber-dragonplate

[51] dragonplate, "Carbon fiber thermal conductivity and the coefficient of thermal expansion." [Online]. Available: https://dragonplate.com/carbon-fiber-thermal-conductivity-and-the-coefficient-of-thermal-expansion

[52] M. Web, "Dupont™ kevlar® 49 aramid fiber." [Online]. Available: https://www.matweb.com/search/datasheet.aspx?MatGUID=77b5205f0dcc43bb8cbe6fee7d36cbb5&ckck=1

[53] Faservebundwerkstoffe, "Aramid fabric 170 g/m² (twill weave) 100 cm." [Online]. Available: https://www.r-g.de/en/art/190206-AT

[54] ——, "Carbon fabric 160 g/m² (style 442 aero, twill weave) 100 cm." [Online]. Available: https://www.r-g.de/en/art/190225

[55] W. lengths, "Thermistor basics." [Online]. Available: https://www.teamwavelength.com/thermistor-basics/

[56] E. H. Yaxun, "Ds18b20 working principle and temperature measurement principle." [Online]. Available: https://www.ntcsensors.com/Ds18b20_working_principle_and_temperature_measurement_principle/

[57] L. Damiani, R. Revetria, and S. Arecco, "Simulation model of the control system of portable boxes for blood bags transport," 04 2019, p. 1.

[58] P. Fulzele, A. Kumbhare, A. Mangde, A. Gaidhane, P. Palsodkar, A. Narkhede, and G. Mishra, "An iot enabled convenient vaccine cold box for biomedical use," *European Journal of Molecular and Clinical Medicine*, vol. 7, pp. 1615–1624, 09 2020.

[59] . G. G. d'intérêt Economique – Economic Interest Group), "Eps packaging –serving the cold chain." [Online]. Available: https://www.eps.co.uk/pdfs/eps_serving_cold_chain.pdf

[60] W. Fakhira and M. Fadzly, "Smart portable air cooler using thermoelectric peltier," in *AIP Conference Proceedings*, vol. 2129, 2019. [Online]. Available: https://www.scopus.com/inward/record.uri?eid=2-s2.0-85070564917&doi=10.1063%2f1.5118158&partnerID=40&md5=380504f9b3ceb1e5292ebcfe1d468a45

[61] A. Poachaiyapoom, R. Leardkun, J. Mounkong, and S. Wongwises, "Miniature vapor compression refrigeration system for electronics cooling," *Case Studies in Thermal Engineering*, vol. 13, p. 100365, 2019. [Online]. Available: https://www.sciencedirect.com/science/article/pii/S2214157X18303241

[62] D. Workshop, "Peltier effect cooling experiments," 2019. [Online]. Available: https://dronebotworkshop.com/peltier-effect/#:~:text=A%20semiconductor%20Peltier%20cooler%20consists,P%20and%20N%2Dtype%20material

[63] S. H. Zaferani, M. W. Sams, R. Ghomashchi, and Z.-G. Chen, "Thermoelectric coolers as thermal management systems for medical applications: Design, optimization, and advancement," *Nano Energy*, vol. 90, p. 106572, 2021. [Online]. Available: https://www.sciencedirect.com/science/article/pii/S2211285521008247

[64] Z. Abdulghani, "A novel experimental case study on optimization of Peltier air cooler using Taguchi method," *Results in Engineering*, vol. 16, 2022. [Online]. Available: https://www.scopus.com/inward/record.uri?eid=2-s2.0-85137643960&doi=10.1016%2fj.rineng.2022.100627&partnerID=40&md5=4945ef2da94ac2a0cbd664f67d53ce05

[65] A. W. R. HVAC), "Mini refrigerated compressor vapor compression cooling systems." [Online]. Available: https://www.linkedin.com/pulse/mini-refrigerated-compressor-vapor-compression-ann-wee-rigid-hvac-

[66] P. Gear, "Swit mino-s140 140wh pocket v-mount battery pack." [Online]. Available: https://www.productiongear.co.uk/swit-mino-s140-140wh-pocket-v-mount-battery-pack.html

[67] P. Gill, T. T. Moghadam, and B. Ranjbar, "Differential scanning calorimetry techniques: applications in biology and nanoscience." *Journal of biomolecular techniques : JBT*, vol. 21 4, pp. 167–93, 2010. [Online]. Available: https://api.semanticscholar.org/CorpusID:4899427

[68] X. Xiaofeng and Z. Xuelai, "Simulation and experimental investigation of a multi-temperature insulation box with phase change materials for cold storage," *Journal of Food Engineering*, vol. 292, p. 110286, 2021. [Online]. Available: https://www.sciencedirect.com/science/article/pii/S0260877420303745

[69] Botnroll, "Pilha li-ion 18650 3,7v 3350mah." [Online]. Available: https://www.botnroll.com/pt/baterias/3649-bateria-18650-3-7v-3350mah-5a-li-ion-recarreg-vel.html

[70] ——, "Carregador baterias 18650 c/ funÇÃo power bank." [Online]. Available: https://www.botnroll.com/pt/carregadores/3845-carregador-baterias-18650-c-fun-o-power-bank.html

[71] Hogaki, "Dc small electric control lock locker door lock 3v5v12v mini electronic lock unmanned vending machine lock locker electric lock." [Online]. Available: https://hogaki.com/dc-small-electric-control-lock-locker-door-lock-3v5v12v-mini-electronic-lock-unmanned-vending-machine
gclid=CjwKCAjwjOunBhB4EiwA94JWsJOgWdqe749WYSgjjGCzWct0Kop-OX7lr1Dj2Tl83Rh97eNo3IcI
UAQAvD_BwE

[72] M. Electronics, "Leitor de controlo de acesso com pin + rfid 125khz ip20 - orno or-zs-820." [Online]. Available: https://mauser.pt/catalog/product_info.php?cPath=554_2124&products_id=096-9733

[73] ——, "Quectel l86-m33." [Online]. Available: https://pt.mouser.com/ProductDetail/Quectel/L86-M33?qs=GedFDFLaBXFvEvNOo6IDYg%3D%3D&_gl=1*1czwefo*_ga*MTI4NDg5NjQ1Ny4xNjk0MTYyNjQz*_ga_15W4STQT4T*MTY5NDE2MjY0My4xLjAuMTY5NDE2MjY0Ny4wLjAuMA..*_ga_1KQLCYKRX3*MTY5NDE2MjY0My4xLjAuMTY5NDE2MjY0Ny41Ni4wLjA.

[74] ——, "Adafruit 358." [Online]. Available: https://pt.mouser.com/ProductDetail/Adafruit/358?qs=GURawfaeGuA67An5HPa%2FNw%3D%3D

[75] Faservebundwerkstoffe, "Epoxy resin l + hardener l." [Online]. Available: https://www.r-g.de/en/art/100110

[76] M. Electronics, "Espressif systems esp32-devkitc-32e." [Online]. Available: https://pt.mouser.com/ProductDetail/Espressif-Systems/ESP32-DevKitC-32E?qs=GedFDFLaBXFpgD0kAZWDrQ%3D%3D

[77] ——, "Módulo sensor de temperatura, humidade e pressão atmosférica (bme280) - dfrobot sen0236." [Online]. Available: https://mauser.pt/catalog/product_info.php?products_id=095-0287

[78] ——, "Sensor de temperatura - shelly ds18b20." [Online]. Available: https://mauser.pt/catalog/product_info.php?products_id=096-8756&utm_source=google&utm_medium=cpc&utm_campaign=shopping_shelly_pt_012&utm_content=feed_shelly&gclid=CjwKCAjwjOunBhB4EiwA94JWsH3wgNRtwrewdBzBEb-DKXJmajmZE3wl35eG9UuVKvdVgwXbPnm3BwE

[79] DocCheck, "Eutectic accumulator pcm with phase change." [Online]. Available: https://www.doccheckshop.eu/11702/versapak-eutectic-accumulator-pcm-with-phase-change

Appendix A

EPS box

Product page EN

Date rev.: 06/12/2023
Doc. Ref: PDS-1496

GENERAL INFORMATION

Product name : EPS isothermal box

Description : Expanded polystyrene (EPS) packaging, it optimally isolates products and, due to its thermal properties, guarantees the maintenance of the cold chain. High strength and reduced weight. 100% recyclable material. Not foldable

TECHNICAL DATA

reference	capacity	internal dimensions (length x width x height)	external dimensions (length x width x height)	thickness (mm)	pcs/pack
EPSB-035-001	3,5 L	165 x 165 x 130	225 x 225 x 195	30	1
EPSB-047-001	4,7 L	270 x 140 x 125	330 x 200 x 185	30	1
EPSB-073-001	7,3 L	270 x 165 x 165	330 x 225 x 225	30	1

PACKAGING AND LOGISTICS

reference	vol (l)	kg	TARIC	GTIN
EPSB-035-001	9,8719	0,1	39031100	08434868083790
EPSB-047-001	12,21	0,2	39031100	08434868083806
EPSB-073-001	16,7062	0,4	39031100	08434868083813

PRODUCT PHOTO





Appendix B

Sensors

NTC Thermistors, Epoxy PVC Long Leads Sensors



FEATURES

- Accurate over wide temperature range
- High stability
- Excellent price / performance ratio
- High adhesive strength between PVC wire and the encapsulating lacquer
- Material categorization: for definitions of compliance please see www.vishay.com/doc?99912

Pb-free Available

e3

RoHS COMPLIANT

LINKS TO ADDITIONAL RESOURCES

Related Documents

QUICK REFERENCE DATA

PARAMETER	VALUE	UNIT
Resistance value at 25 °C (R_{25})	2.2K to 100K	Ω
Tolerance on R_{25}-value (2)	± 3	%
$B_{25/85}$-value	3977 to 4190	K
Tolerance on $B_{25/85}$-value	± 0.75 to ± 1.5	%
Operating temperature range at zero dissipation	-40 to +85	°C
Maximum power dissipation at 55 °C	250	mW
Min. dielectric withstanding voltage between terminals and sensor body	1500	V_{AC}
Dissipation factor	6.0	mW/K
Response time (1)	≈ 7	s
Weight	≈ 4	g

Notes

(1) Response time in silicone oil MS 200/50. This is the time needed for the sensor to reach 63.2 % of the total temperature difference when subjected to a temperature change from 25 °C in air to 85 °C in oil

(2) Tighter tolerances on R_{25} are available upon request

APPLICATIONS

Temperature measurement, sensing and control in remote locations and for various environmental conditions.

DESCRIPTION

These sensors exist of a small NTC chip reflow soldered between two AWG #24 UL-2468 style wires. They are lacquered and insulated with black epoxy.

MARKING

UL mark on wire, no mark on body.

PACKAGING

The thermistors are packed in cardboard boxes; each box containing 500 pieces.

DESIGN-IN SUPPORT

Other wire length and wire type (UL-2651 style PVC 105 °C), other wire gauge, are available on request.

The products can be provided with a connector on request.

A UL-2651 105 °C multistranded version is available as **NTCLE430**.

For complete curve computation, please visit: www.vishay.com/thermistors/ntc-curve-list/

MOUNTING

Important mounting and handling instructions: see www.vishay.com/doc?29222

By soldering or clamping the wire ends, in any position. Body can be inserted or taped attached. Not intended for fluid immersed applications.

ELECTRICAL DATA AND ORDERING INFORMATION

R_{25} (Ω)	R_{25}-TOL. (± %)	$B_{25/85}$ (K)	$B_{25/85}$-TOL. (± %)	SAP MATERIAL AND ORDERING NUMBER	
				RoHS COMPLIANT WITH EXEMPTION (1)	RoHS COMPLIANT
2200	3	3977	0.75	NTCLE400E3222H	NTCLE400E3222HA
4700	3	3977	0.75	NTCLE400E3472H	NTCLE400E3472HA
5000	3	3977	0.75	NTCLE400E3502H	NTCLE400E3502HA
10 000	3	3977	0.75	NTCLE400E3103H	NTCLE400E3103HA
47 000	3	4090	1.5	NTCLE400E3473H	NTCLE400E3473HA
100 000	3	4190	1.5	NTCLE400E3104H	NTCLE400E3104HA

Notes

Preferred versions for new designs

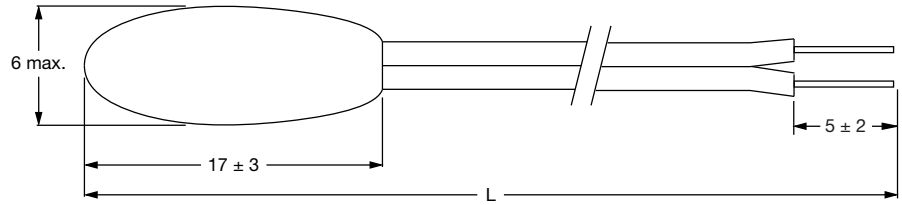
(1) RoHS exemption 7(c)-I: electrical and electronic components containing lead in a glass or ceramic other than dielectric ceramic in capacitors, e.g. piezo-electronic devices, or in a glass or ceramic matrix compound

For technical questions, contact: nlr@vishay.com

THIS DOCUMENT IS SUBJECT TO CHANGE WITHOUT NOTICE. THE PRODUCTS DESCRIBED HEREIN AND THIS DOCUMENT ARE SUBJECT TO SPECIFIC DISCLAIMERS, SET FORTH AT www.vishay.com/doc?91000

DIMENSIONS in millimeters

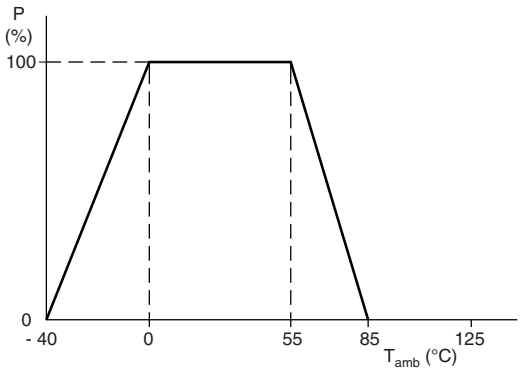
Epoxy-coated type NTCLE400E....



L = 400 mm + 15 / - 0
Other wire lengths or connector attached available on request.

DERATING

Power derating curve.



Note

- Zero power is considered as measuring power max. 1 % of max. power

For technical questions, contact: nlr@vishay.com
THIS DOCUMENT IS SUBJECT TO CHANGE WITHOUT NOTICE. THE PRODUCTS DESCRIBED HEREIN AND THIS DOCUMENT ARE SUBJECT TO SPECIFIC DISCLAIMERS, SET FORTH AT www.vishay.com/doc?91000

RESISTANCE VALUES AT INTERMEDIATE TEMPERATURES WITH R_{25} AT 2.2 kΩ, 4.7 kΩ, 5.0 kΩ , AND 10 kΩ							
T_{OPER} (°C)	PART NR. NTCLE400E3222H(A) R_T (Ω)	PART NR. NTCLE400E3472H(A) R_T (Ω)	PART NR. NTCLE400E3502H(A) R_T (Ω)	PART NR. NTCLE400E3103H(A) R_T (Ω)	*R*-TOL. (± %)	α (%/K)	T-TOL. (± °C)
-40	73 061	156 084	166 047	332 094	5.87	-6.62	0.89
-35	52 778	112 753	119 950	239 900	5.60	-6.39	0.88
-30	38 544	82 344	87 600	175 200	5.33	-6.18	0.86
-25	28 443	60 765	64 643	129 287	5.08	-5.98	0.85
-20	21 199	45 288	48 179	96 358	4.83	-5.78	0.84
-15	15 950	34 075	36 250	72 500	4.60	-5.60	0.82
-10	12 110	25 872	27 523	55 046	4.37	-5.42	0.81
-5	9275	19 814	21 078	42 157	4.15	-5.25	0.79
0	7162	15 300	16 277	32 554	3.94	-5.09	0.77
5	5574	11 909	12 669	25 339	3.74	-4.93	0.76
10	4372	9340	9936	19 872	3.55	-4.79	0.74
15	3454	7378	7849	15 698	3.36	-4.64	0.72
20	2747	5869	6244	12 488	3.18	-4.51	0.70
25	2200	4700	5000	10 000	3.00	-4.38	0.69
30	1773	3788	4030	8059	3.17	-4.25	0.75
35	1438	3071	3267	6535	3.33	-4.13	0.81
40	1173	2505	2665	5330	3.49	-4.02	0.87
45	961.8	2055	2186	4372	3.65	-3.91	0.93
50	793.2	1694	1803	3605	3.80	-3.80	1.00
55	657.5	1405	1494	2989	3.94	-3.70	1.07
60	547.8	1170	1245	2490	4.08	-3.60	1.13
65	458.6	979.7	1042	2084	4.22	-3.51	1.20
70	385.7	823.9	876.5	1753	4.35	-3.42	1.27
75	325.8	696.0	740.5	1481	4.48	-3.33	1.35
80	276.4	590.5	628.2	1256	4.60	-3.25	1.42
85	235.5	503.0	585.2	1070	4.73	-3.17	1.49

For technical questions, contact: nlr@vishay.com
THIS DOCUMENT IS SUBJECT TO CHANGE WITHOUT NOTICE. THE PRODUCTS DESCRIBED HEREIN AND THIS DOCUMENT ARE SUBJECT TO SPECIFIC DISCLAIMERS, SET FORTH AT www.vishay.com/doc?91000

RESISTANCE VALUES AT INTERMEDIATE TEMPERATURES WITH R_{25} AT 47 kΩ				
T_{OPER} (°C)	PART NR. NTCLE400E3473H(A) R_T (Ω)	*R*-TOL. (± %)	α (%/K)	T-TOL. (± °C)
-40	1 589 068	8.91	-6.54	1.36
-35	1 151 627	8.34	-6.34	1.32
-30	842 790	7.79	-6.15	1.27
-25	622 597	7.27	-5.96	1.22
-20	464 110	6.77	-5.79	1.17
-15	348 989	6.28	-5.62	1.12
-10	264 628	5.82	-5.45	1.07
-5	202 280	5.37	-5.30	1.01
0	155 823	4.94	-5.14	0.96
5	120 932	4.52	-5.00	0.91
10	94 528	4.12	-4.86	0.85
15	74 399	3.74	-4.72	0.79
20	58 945	3.36	-4.59	0.73
25	47 000	3.00	-4.47	0.67
30	37 706	3.35	-4.35	0.77
35	30 429	3.69	-4.23	0.87
40	24 696	4.02	-4.12	0.97
45	20 154	4.33	-4.01	1.08
50	16 534	4.64	-3.91	1.19
55	13 633	4.94	-3.81	1.30
60	11 296	5.23	-3.71	1.41
65	9404	5.51	-3.62	1.52
70	7865	5.78	-3.53	1.64
75	6607	6.04	-3.44	1.75
80	5573	6.30	-3.36	1.87
85	4721	6.55	-3.28	2.00

For technical questions, contact: nlr@vishay.com

THIS DOCUMENT IS SUBJECT TO CHANGE WITHOUT NOTICE. THE PRODUCTS DESCRIBED HEREIN AND THIS DOCUMENT ARE SUBJECT TO SPECIFIC DISCLAIMERS, SET FORTH AT www.vishay.com/doc?91000

RESISTANCE VALUES AT INTERMEDIATE TEMPERATURES WITH R_{25} AT 100 kΩ				
T_{OPER} (°C)	PART NR. NTCLE400E3104H(A) R_T (Ω)	*R*-TOL. (± %)	α (%/K)	T-TOL. (± °C)
-40	3 666 299	9.05	-6.69	1.35
-35	2 637 588	8.47	-6.49	1.31
-30	1 916 576	7.91	-6.29	1.26
-25	1 406 111	7.37	-6.10	1.21
-20	1 041 184	6.86	-5.92	1.16
-15	777 846	6.36	-5.75	1.11
-10	586 097	5.89	-5.58	1.06
-5	445 257	5.43	-5.42	1.00
0	340 942	4.99	-5.26	0.95
5	263 054	4.56	-5.11	0.89
10	204 446	4.15	-4.97	0.84
15	160 014	3.75	-4.83	0.78
20	126 087	3.37	-4.70	0.72
25	100 000	3.00	-4.57	0.66
30	79 808	3.36	-4.45	0.75
35	64 077	3.70	-4.33	0.86
40	51 745	4.04	-4.22	0.96
45	42 021	4.36	-4.11	1.06
50	34 308	4.68	-4.00	1.17
55	28 156	4.98	-3.90	1.28
60	23 222	5.28	-3.80	1.39
65	19 246	5.57	-3.71	1.50
70	16 025	5.85	-3.62	1.62
75	13 402	6.12	-3.53	1.73
80	11 258	6.38	-3.45	1.85
85	9496	6.64	-3.36	1.97

TESTS AND REQUIREMENTS

STABILITY TESTS			
IEC	**TEST**	**PROCEDURE**	**DRIFT REQUIREMENT**
60068-2-2	Endurance dry heat	85 °C; 1000 h	$\Delta R/R < 5$ %
60068-2-1	Endurance cold	-40 °C; 1000 h	$\Delta R/R < 5$ %
60539	Endurance max. dissipation	250 mW; 55 °C; 1000 h	$\Delta R/R < 5$ %
60068-2-3	Damp heat, steady state	56 days at 40 °C; 90 % to 95 % RH	$\Delta R/R < 7$ %
60068-20-14	Rapid change of temperature	-40 °C to +85 °C; 50 cycles	$\Delta R/R < 5$ %

For technical questions, contact: nlr@vishay.com
THIS DOCUMENT IS SUBJECT TO CHANGE WITHOUT NOTICE. THE PRODUCTS DESCRIBED HEREIN AND THIS DOCUMENT ARE SUBJECT TO SPECIFIC DISCLAIMERS, SET FORTH AT www.vishay.com/doc?91000

Disclaimer

ALL PRODUCT, PRODUCT SPECIFICATIONS AND DATA ARE SUBJECT TO CHANGE WITHOUT NOTICE TO IMPROVE RELIABILITY, FUNCTION OR DESIGN OR OTHERWISE.

Vishay Intertechnology, Inc., its affiliates, agents, and employees, and all persons acting on its or their behalf (collectively, “Vishay”), disclaim any and all liability for any errors, inaccuracies or incompleteness contained in any datasheet or in any other disclosure relating to any product.

Vishay makes no warranty, representation or guarantee regarding the suitability of the products for any particular purpose or the continuing production of any product. To the maximum extent permitted by applicable law, Vishay disclaims (i) any and all liability arising out of the application or use of any product, (ii) any and all liability, including without limitation special, consequential or incidental damages, and (iii) any and all implied warranties, including warranties of fitness for particular purpose, non-infringement and merchantability.

Statements regarding the suitability of products for certain types of applications are based on Vishay's knowledge of typical requirements that are often placed on Vishay products in generic applications. Such statements are not binding statements about the suitability of products for a particular application. It is the customer's responsibility to validate that a particular product with the properties described in the product specification is suitable for use in a particular application. Parameters provided in datasheets and / or specifications may vary in different applications and performance may vary over time. All operating parameters, including typical parameters, must be validated for each customer application by the customer's technical experts. Product specifications do not expand or otherwise modify Vishay's terms and conditions of purchase, including but not limited to the warranty expressed therein.

Hyperlinks included in this datasheet may direct users to third-party websites. These links are provided as a convenience and for informational purposes only. Inclusion of these hyperlinks does not constitute an endorsement or an approval by Vishay of any of the products, services or opinions of the corporation, organization or individual associated with the third-party website. Vishay disclaims any and all liability and bears no responsibility for the accuracy, legality or content of the third-party website or for that of subsequent links.

Except as expressly indicated in writing, Vishay products are not designed for use in medical, life-saving, or life-sustaining applications or for any other application in which the failure of the Vishay product could result in personal injury or death. Customers using or selling Vishay products not expressly indicated for use in such applications do so at their own risk. Please contact authorized Vishay personnel to obtain written terms and conditions regarding products designed for such applications.

No license, express or implied, by estoppel or otherwise, to any intellectual property rights is granted by this document or by any conduct of Vishay. Product names and markings noted herein may be trademarks of their respective owners.

© 2023 VISHAY INTERTECHNOLOGY, INC. ALL RIGHTS RESERVED

DS18B20 Waterproof Temperature Sensor Cable



Product Description

This Maxim-made item is a digital thermo probe or sensor that employs DALLAS DS18B20. Its unique 1-wire interface makes it easy to communicate with devices. It can converts temperature to a 12-bit digital word in 750ms (max). Besides, it can measures temperatures from -55°C to +125°C (-67F to +257F). In addition, this thermo probe doesn't require any external power supply since it draws power from data line. Last but not least, like other common thermo probe, its stainless steel probe head makes it suitable for any wet or harsh environment.

The datasheet of this DS18B20 Sensor Cable can be found from:
http://www.quick-teck.co.uk/ElectronicElement/eeList.php?typeId=97#title

Feature:

Power supply range:	3.0V to 5.5V
Operating temperature range:	-55°C to +125°C (-67F to +257F)
Storage temperature range:	-55°CC to +125°C (-67F to +257F)
Accuracy over the range of -10°C to +85°C:	±0.5°C
3-pin 2510 Female Header Housing	

Waterproof Stainless steel sheath	
Stainless steel sheath	
Size of Sheath:	6*50mm
Connector:	RJ11/RJ12, 3P-2510, USB.
Pin Definition:	RED: VCC Yellow: DATA Black: GND
Cable length:	1meter, 2m, 3m, 4m are available upon request.

Application:

The DS18B20 Digital Temperature Probe provides 9 to 12 bit (configurable) temperature readings which indicate the temperature of the device. Information is sent to/from the DS18B20 over a 1-Wire interface, so that only one wire (and ground) needs to be connected from a central microprocessor to a DS18B20. Power for reading, writing, and performing temperature conversions can be derived from the data line itself with no need for an external power source.

Because each DS18B20 contains a unique silicon serial number, multiple DS18B20s can exist on the same 1Wire bus. This allows for placing temperature sensors in many different places. Applications where this feature is useful include HVAC environmental controls, sensing temperatures inside buildings, equipment or machinery, and process monitoring and control.

Details:



Figure 1

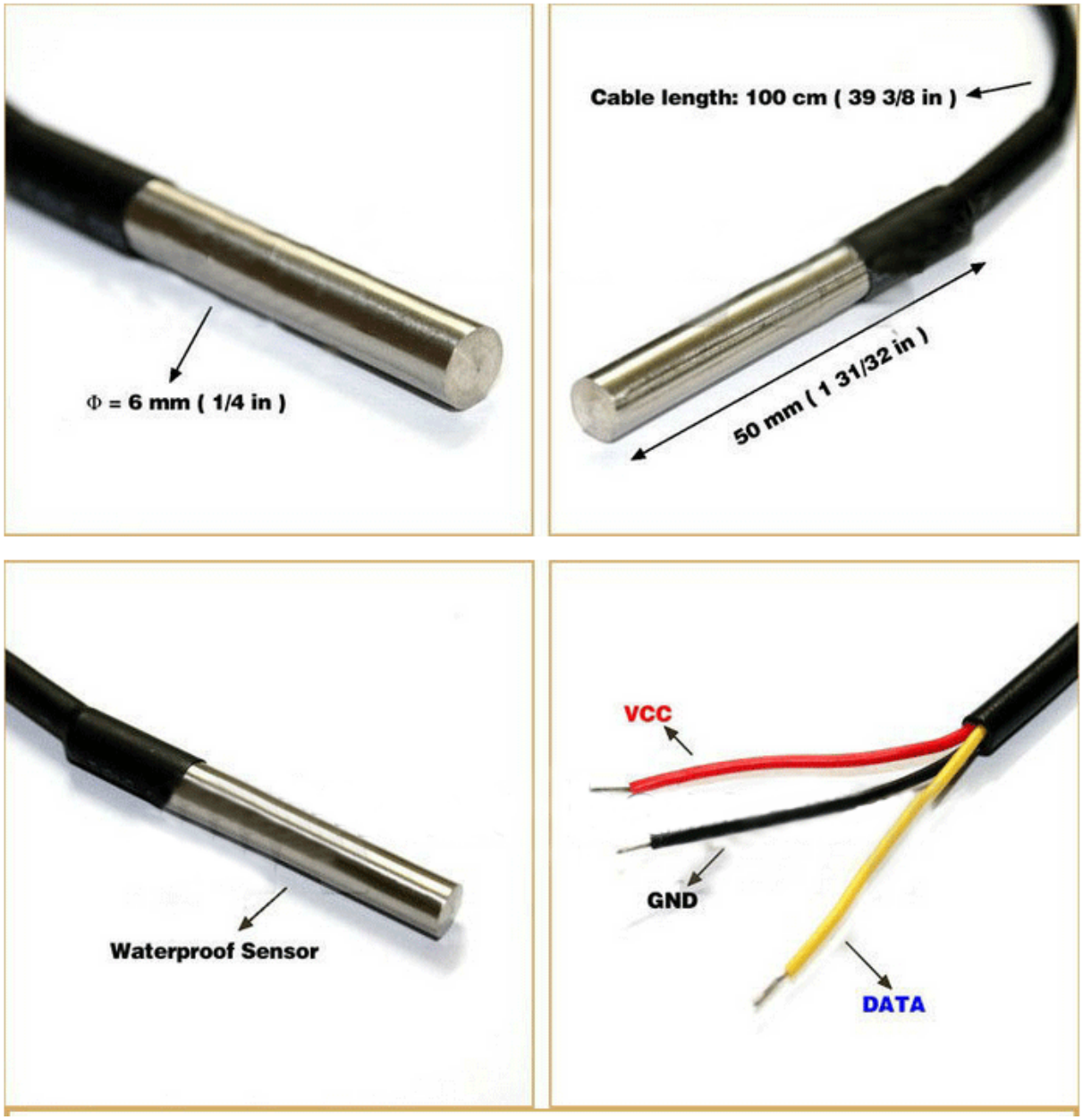
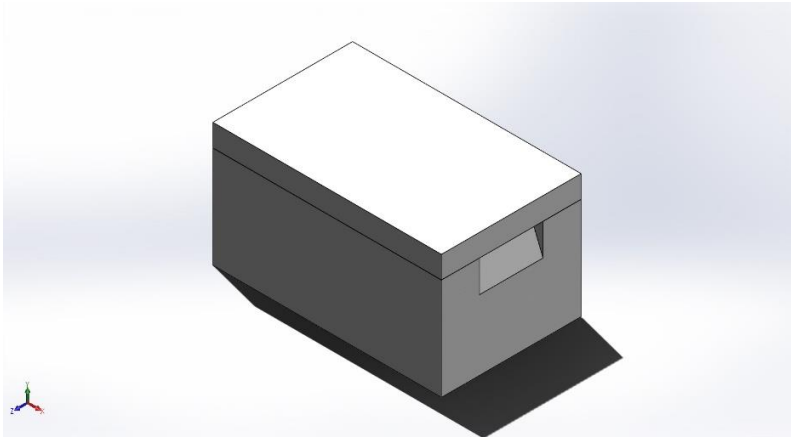

Φ = 6 mm (1/4 in)
Cable length: 100 cm (39 3/8 in)
50 mm (1 31/32 in)
Waterproof Sensor
VCC
GND
DATA

Figure 2

Appendix C

Solidworks simulation

.



Simulation of Assem2 - Copy desenho 3d

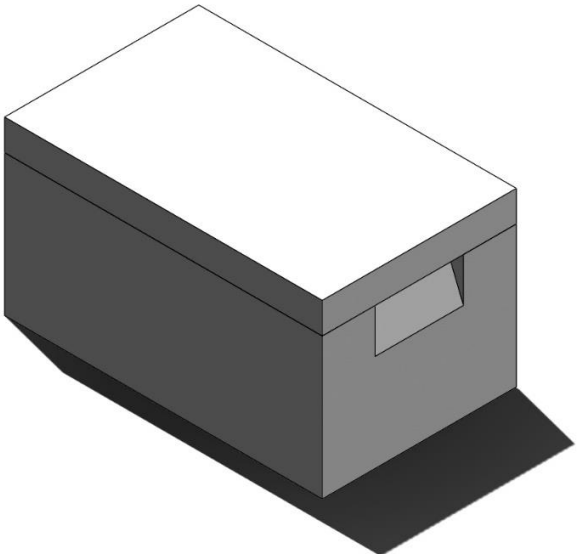
Date: Sunday, 10 September 2023
Designer: Solidworks
Study name: Thermal 2
Analysis type: Thermal(Transient)

Table of Contents

Description 1
Assumptions 2
Model Information 3
Study Properties 5
Units 5
Material Properties 6
Thermal Loads 7
Interaction Information 7
Mesh information 8
Sensor Details 8
Study Results 9
Conclusion 12

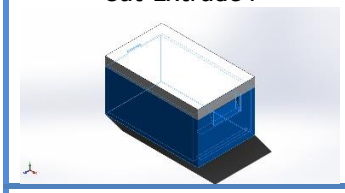
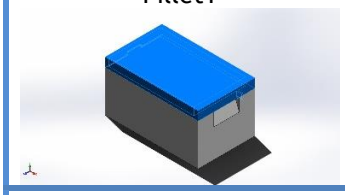
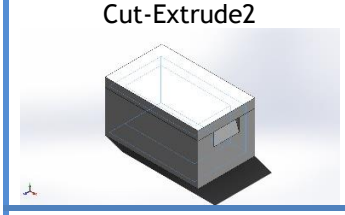
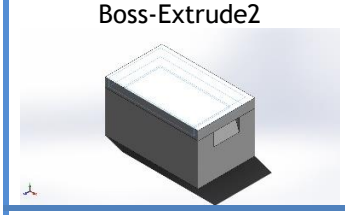
Description

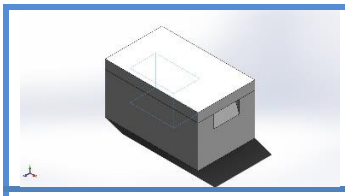
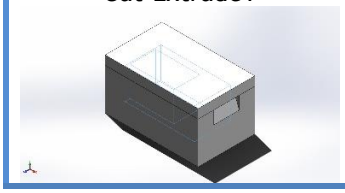
No Data



Model name: Assem2 - Copy desenho 3d
Current Configuration: Default

Solid Bodies

Document Name and Reference	Treated As	Volumetric Properties	Document Path/Date Modified
Cut-Extrude4 	Solid Body	**Mass:2,60788 kg** **Volume:0,00181103 m^3** **Density:1.440 kg/m^3** **Weight:25,5572 N**	**D:\DADOS\Desktop\Manos\Nuno\3d\Carbonbox.SLDPRT** Sep 10 19:28:00 2023
Fillet1 	Solid Body	**Mass:1,14025 kg** **Volume:0,000791839 m^3** **Density:1.440 kg/m^3** **Weight:11,1744 N**	**D:\DADOS\Desktop\Manos\Nuno\3d\Carbontampa.SLDPRT** Sep 4 01:54:09 2023
Cut-Extrude2 	Solid Body	**Mass:0,173301 kg** **Volume:0,00550161 m^3** **Density:31,5 kg/m^3** **Weight:1,69835 N**	**D:\DADOS\Desktop\Manos\Nuno\3d\PSbox.SLDPRT** Sep 4 01:54:09 2023
Boss-Extrude2 	Solid Body	**Mass:0,0683235 kg** **Volume:0,002169 m^3** **Density:31,5 kg/m^3** **Weight:0,66957 N**	**D:\DADOS\Desktop\Manos\Nuno\3d\PStampa.SLDPRT** Sep 4 01:54:09 2023
Boss-Extrude1	Solid Body	**Mass:1,955 kg** **Volume:0,001955 m^3**	**D:\DADOS\Desktop\Manos\Nuno\3d\Part2.SLDPRT**

		**Density:1.000 kg/m^3** **Weight:19,159 N**	Aug 27 20:50:32 2023
Cut-Extrude1 	Solid Body	**Mass:0,0028391 kg** **Volume:0,002581 m^3** **Density:1,1 kg/m^3** **Weight:0,0278232 N**	**D:\DADOS\Desktop\Manos\Nuno\3d\Part3.SLDPRT** Sep 4 01:49:08 2023

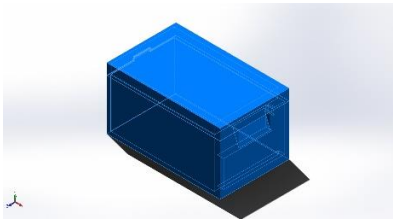
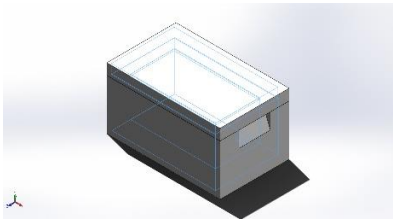
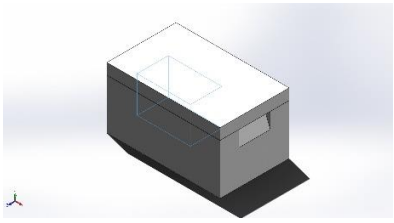
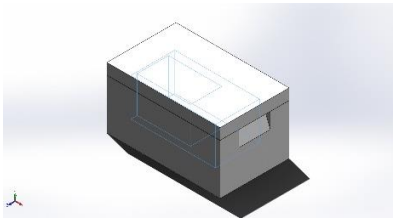
Study Properties

Study name	Thermal 2
Analysis type	Thermal(Transient)
Mesh type	Solid Mesh
Solver type	FFEPlus
Solution type	Transient
Total time	20.000 Seconds
Time increment	60 Seconds
Contact resistance defined?	No
Result folder	SOLIDWORKS document (D:\DADOS\Desktop\Manos\Nuno\3d)

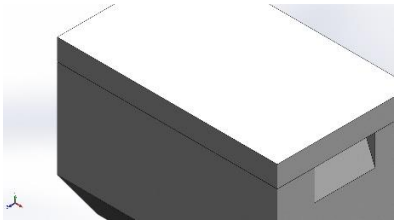
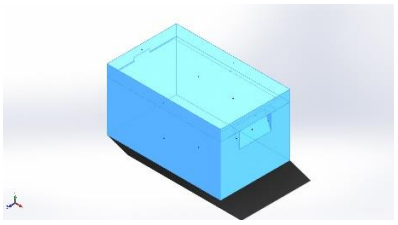
Units

Unit system:	SI (MKS)
Length/Displacement	mm
Temperature	Kelvin
Angular velocity	Rad/sec
Pressure/Stress	N/m^2

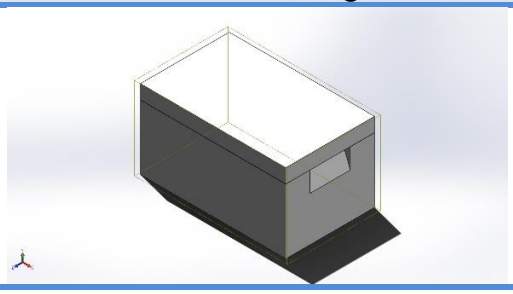
Material Properties

Model Reference	Properties	Components
	**Name:** Kevlar **Model type:** Linear Elastic Isotropic **Default failure criterion:** Max von Mises Stress **Thermal conductivity:** 0,04 W/(m.K) **Specific heat:** 1,42 J/(kg.K) **Mass density:** 1.440 kg/m^3	SolidBody 1(Cut-Extrude4)(Carbonbox-1), SolidBody 1(Fillet1)(Carbontampa-1)
Curve Data:N/A		
	**Name:** eps **Model type:** Linear Elastic Isotropic **Default failure criterion:** Unknown **Thermal conductivity:** 0,036 W/(m.K) **Specific heat:** 1.386 J/(kg.K) **Mass density:** 31,5 kg/m^3	SolidBody 1(Cut-Extrude2)(PSbox-1), SolidBody 1(Boss-Extrude2)(PStampa-1)
Curve Data:N/A		
	**Name:** Water **Model type:** Linear Elastic Isotropic **Default failure criterion:** Unknown **Thermal conductivity:** 0,61 W/(m.K) **Specific heat:** 4.200 J/(kg.K) **Mass density:** 1.000 kg/m^3	SolidBody 1(Boss-Extrude1)(Part2-1)
Curve Data:N/A		
	**Name:** Air **Model type:** Linear Elastic Isotropic **Default failure criterion:** Unknown **Thermal conductivity:** 0,027 W/(m.K) **Specific heat:** 1.000 J/(kg.K) **Mass density:** 1,1 kg/m^3	SolidBody 1(Cut-Extrude1)(Part3-1)
Curve Data:N/A		

Thermal Loads

Load name	Load Image	Load Details
Temperature-1		**Entities:** 1 component(s) **Initial temperature:** 4 Celsius
Convection-1		**Entities:** 14 face(s) **Convection Coefficient:** 20 W/(m^2.K) **Time variation:** Off **Temperature variation:** Off **Bulk Ambient Temperature:** 308,15 Kelvin **Time variation:** Off

Interaction Information

Interaction	Interaction Image	Interaction Properties
Global Interaction		**Type:** Bonded **Components:** 1 component(s) **Options:** Independent mesh

Mesh information

Mesh type	Solid Mesh
Mesher Used:	Blended curvature-based mesh
Jacobian points for High quality mesh	16 Points
Maximum element size	50,9997 mm
Minimum element size	2,54999 mm
Mesh Quality	High
Remesh failed parts independently	Off

Mesh information - Details

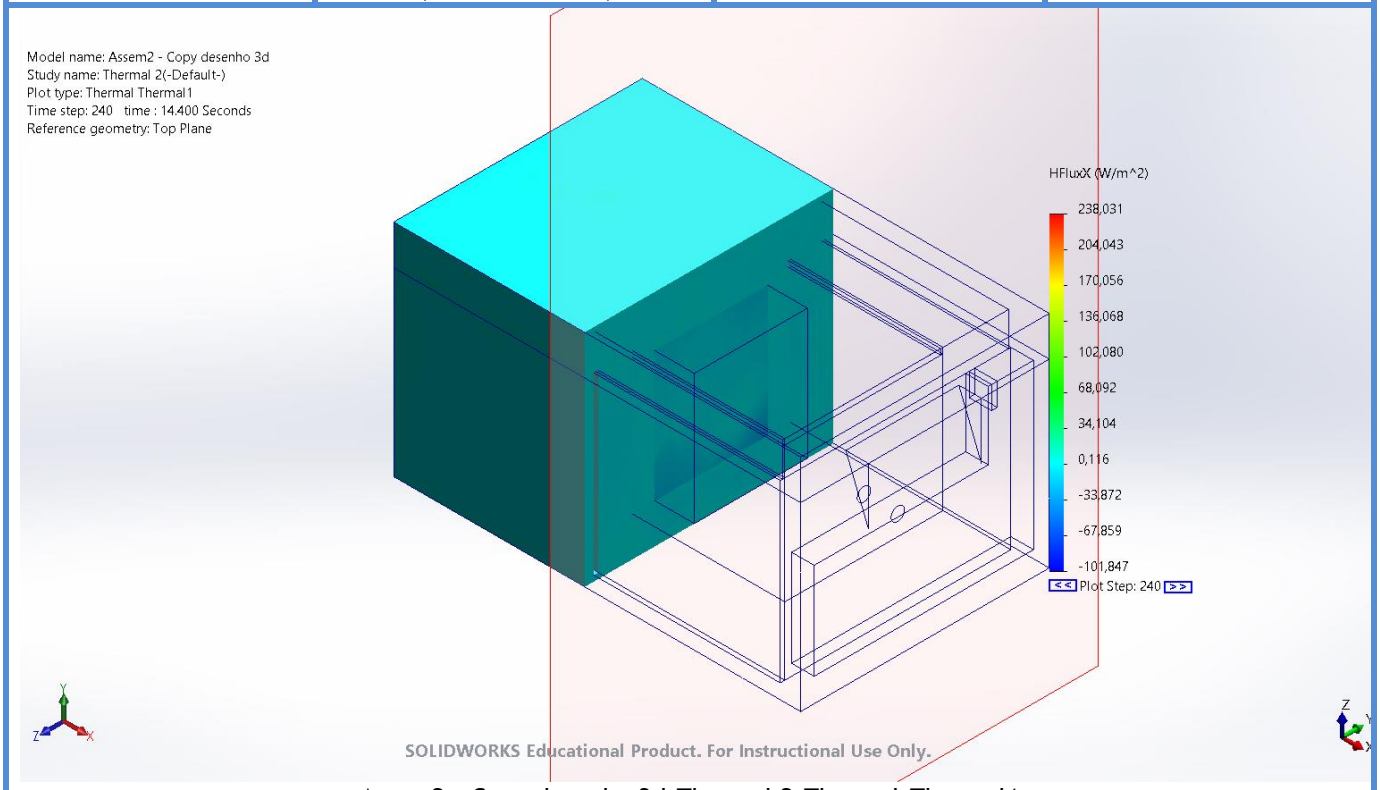
Total Nodes	15568
Total Elements	8054
Maximum Aspect Ratio	16,95
% of elements with Aspect Ratio < 3	78,4
Percentage of elements with Aspect Ratio > 10	1,22
Percentage of distorted elements	0
Time to complete mesh(hh;mm;ss):	00:00:05
Computer name:	

Sensor Details

No Data

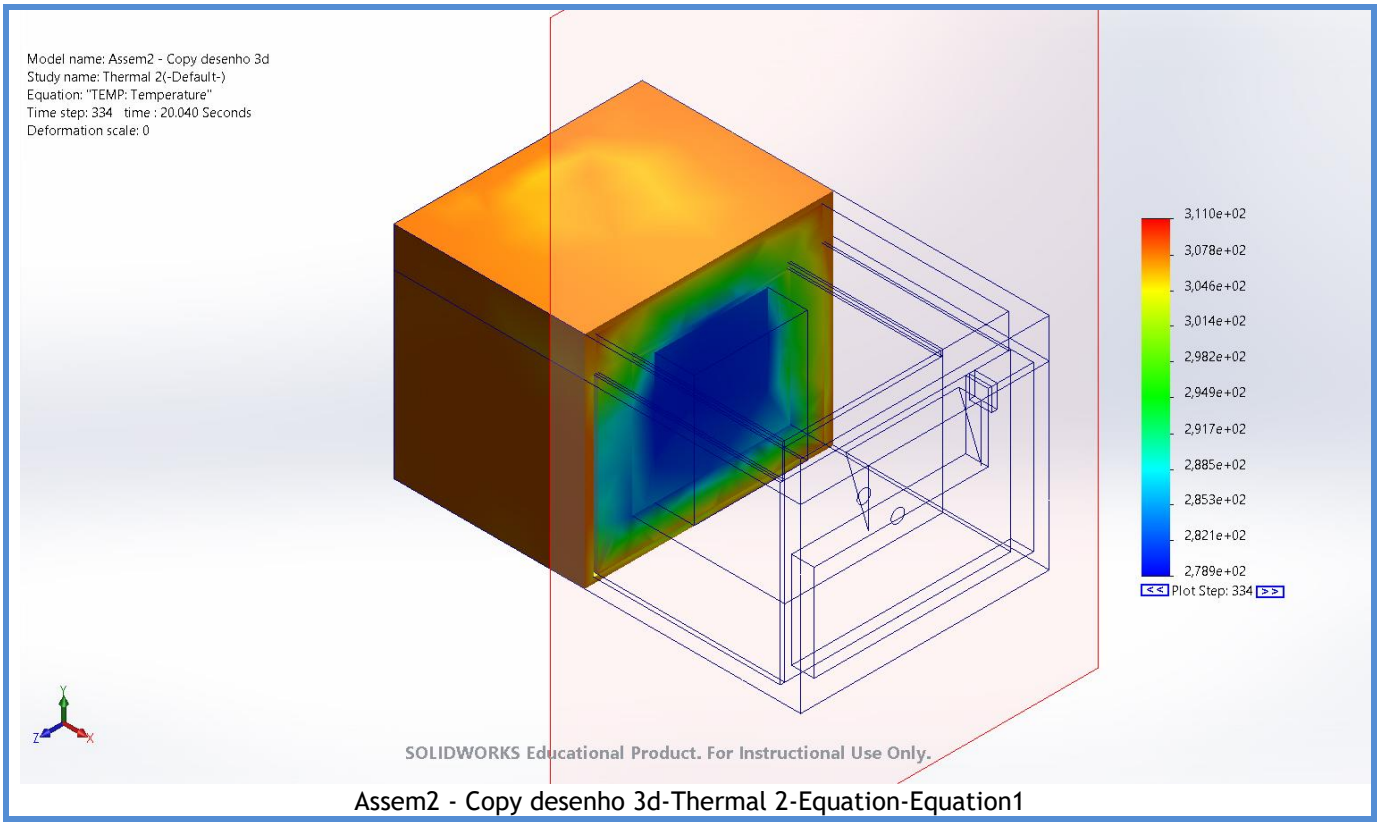
Study Results

Name	Type	Min	Max
Thermal1	HFLUXX: X Heat Flux at Step No: 240(14.400 Seconds)	-101,847W/m^2 Node: 10546	238,031W/m^2 Node: 7932



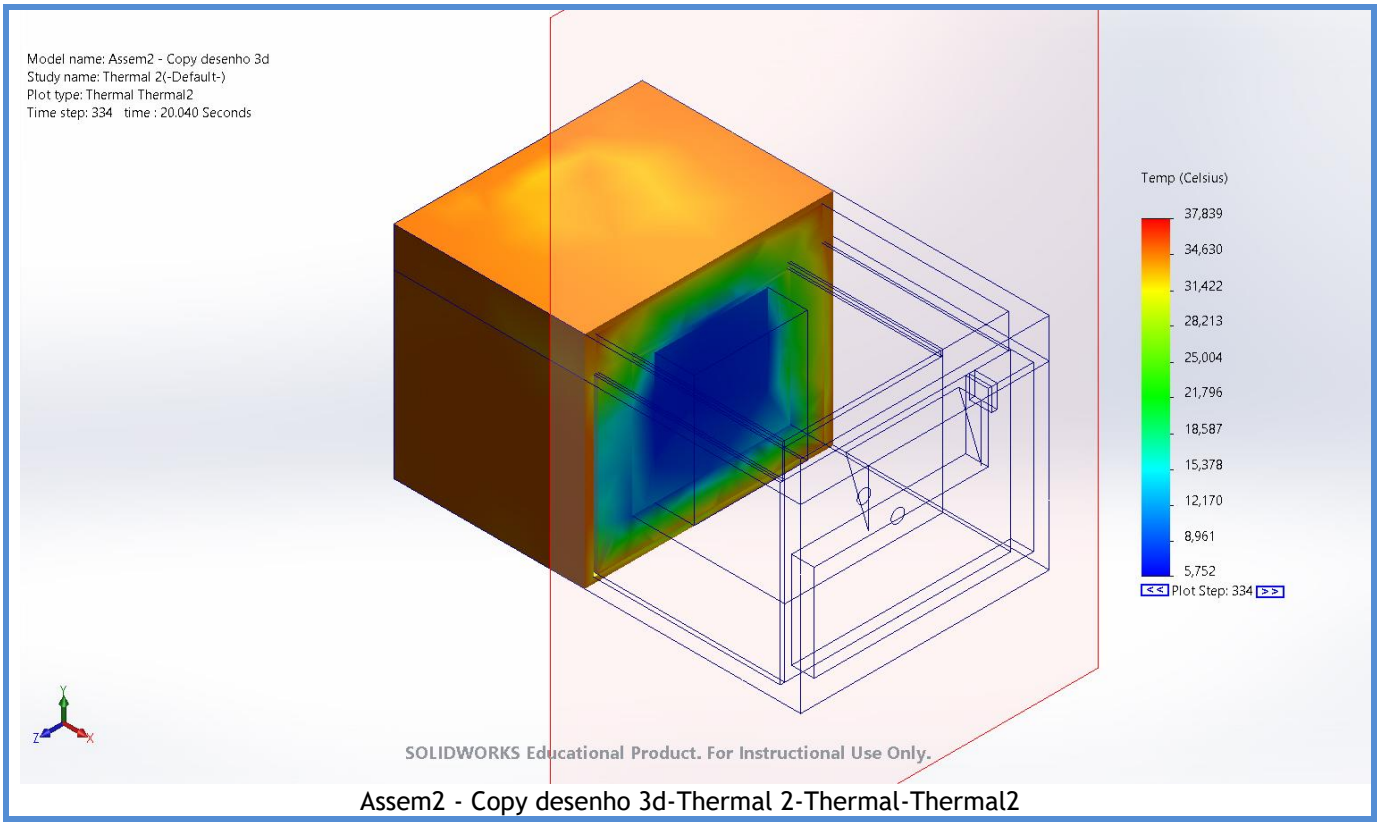
Assem2 - Copy desenho 3d-Thermal 2-Thermal-Thermal1

Name	Type	Min	Max
Equation1	"TEMP: Temperature" at Step No: 334(20.000 Seconds)	2,789e+02SI Node: 15050	3,110e+02SI Node: 10781

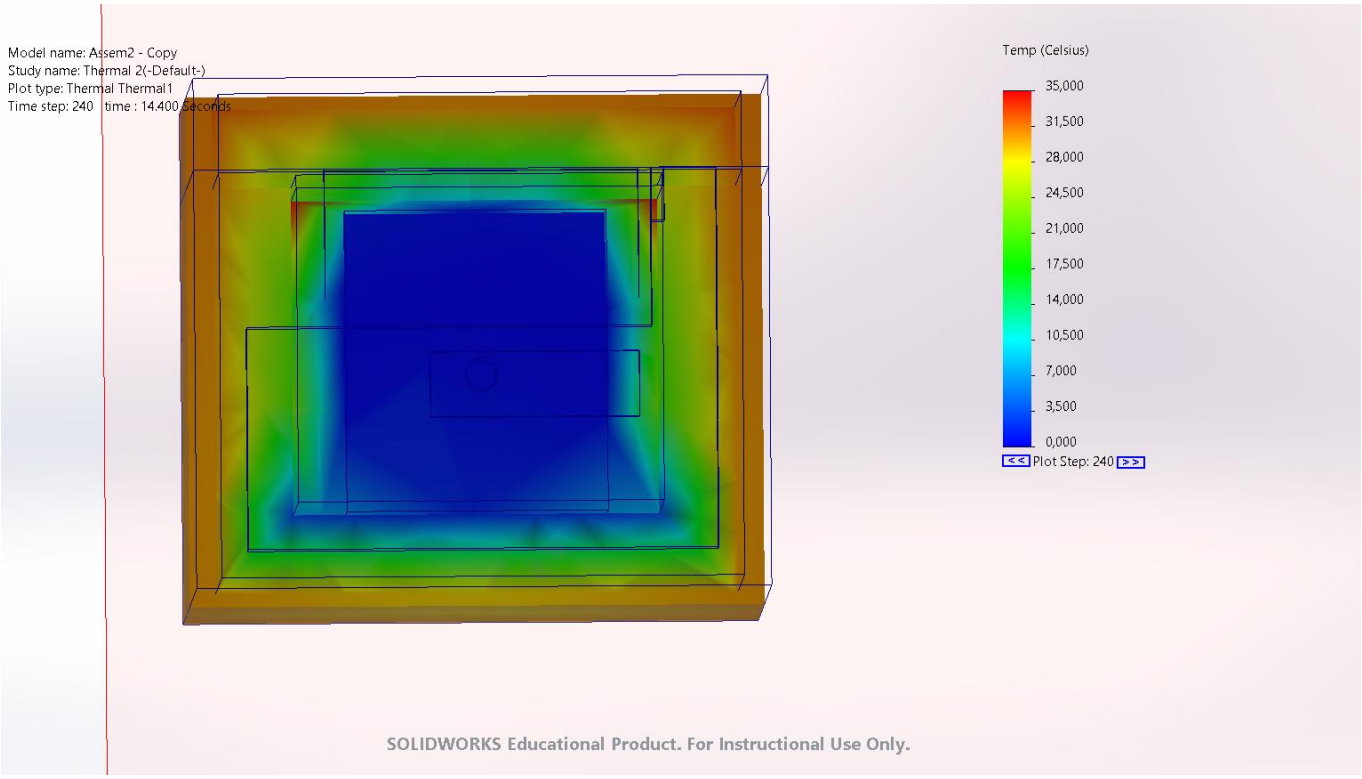


Assem2 - Copy desenho 3d-Thermal 2-Equation-Equation1

Name	Type	Min	Max
Thermal2	TEMP: Temperature at Step No: 334(20.000 Seconds)	5,752Celsius Node: 15050	37,839Celsius Node: 10781



Assem2 - Copy desenho 3d-Thermal 2-Thermal-Thermal2



4h